THE GENERALIZED MAGNETO-TELLURIC METHOD

by

ANTONIO SALDANHA DE SOUSA NEVES

B. Sc., Massachusetts Institute of Technology

1953

SUBMITTED IN PARTIAL FULFILLMENT OF

THE REQUIREMENTS FOR THE DEGREE

OF DOCTOR OF PHILOSOPHY

at the

MASSACHUSETTS INSTITUTE OF TECHNOLOGY

September, 1957

Signature of Author ....
Department of Geology and Geophysics

Certified by ....
Thesis Supervisor

Accepted by ....
Chairman, Department Committee on Graduate Students

TABLE OF CONTENTS

ERRATA

In all maps of the magneto-telluric field the arrows under the horizontal scale are longer than the unit spacing when they should be exactly the length of the unit horizontal spacing.

FIGURES

TABLES

ABSTRACT

The Generalized Magneto-telluric Method

by

Antonio de Sousa Neves

Submitted to the Department of Geology and Geophysics on August 19, 1957, in partial fulfillment of the requirements for the degree of Doctor of Philosophy.

The magneto-telluric method for the determination of earth conductivity at depth has been extended from layered media to arbitrary media, in particular 2 dimensional geometries. By using geographical coverage in the measurements and a semi-quantitative transform to plot the data, the interpretation of sub-surface structure is made possible. A finite difference method has been developed to treat electromagnetic wave propagation in any two dimensional formation. In the particular case of an inclined layer or composite wedge a formal analytic solution was also obtained. Several inclined layer examples were solved by the finite difference method and the geophysical significance of the results considered. These results agreed generally with those of laboratory scale model experiments.

The magneto-telluric method consists in finding the impedance normal to the earth's surface by measuring, at several frequencies, the horizontal components of the electric and magnetic vectors of the magneto-telluric field, a naturally occurring electromagnetic field that

can be described in terms of plane waves incident on the earth. By using geographical coverage in the measurements and a semi-quantitative transform to plot the data the interpretation of sub-surface conductivity is made possible. In the case of inclined layers the semi-quantitative transform possesses characteristics that permiththe identification of the geometry involved. Data obtained theoretically and from the laboratory scale model experiments illustrate these features.

A finite difference method has been developed to treat electromagnetic wave propagation in any two-dimensional geological formations. This method is made possible by the uniformity of the earth's surface of the electromagnetic vector oriented parallel to the strike of an arbitrary 2 dimensional structure and by the relatively strong attenuation of electromagnetic waves within the earth. The solution was carried out by relaxation procedures.

In the particular case of an inclined layer or composite finitely conducting wedge a formal analytic solution was also obtained. It consisted in starting from a general integral solution appropriate for a wedge space and transforming it into a set of singular integral equations by satisfying the boundary conditions on the composite wedge. This system of simultaneous singular integral equations was solved then by inversion through the use of Kontorovich-Lebedev transforms. The final solution is presented in integral form.

A few examples of the response of inclined layers, computed by the finite difference method, are presented. The angle of dip, rather than the conductivity contrast, determines the distance from the strike within which the inclined layer affects the uniform field. Measurements of magnitude and phase angle, taken separately, may lead to confusion with layered media; simultaneous recordings of both quantities avoid the possibility of mistaken interpretation. Sea effects on the magneto-telluric field have also been shown to resemble the response of conductive substrata whenever magnitude alone is measured.

A report on laboratory scale model work has been included. A small one cubic foot tank was used. The model material consisted of brass and brass filings. The plane wave field was simulated by having current fed through two slightly buried horizontal rods, lying at opposite edges of the tank. Data for a vertical layer model and for a buried cylinder model is presented. These results show the same general behavior as those obtained by the finite difference method. Also, frequency response, heating, electromagnetic coupling and other problems associated with the model material are discussed.

ACKNOWLEDGEMENTS

A thesis is never the work of a single person. It is always the result of the atmosphere, personal contact, and opportunities surrounding its author. This is true of the present investigation, and I would like to manifest here my gratitude and indebteness to the following persons and organizations:

Mr. Theodore R. Madden, Lecturer in Geophysics at M. I. T., who supervised most of the work and contributed to it much criticism and ideas. I found him always willing to make possible the execution of ideas and I also owe him much in regards to my closer acquaintance of electromagnetic theory.

Professor Louis Cagniard, of the Faculte des Sciences de l'Universite, Paris, whose paper published in "Geophysics" in 1953 inspired the topic of this thesis. In the fall of 1955 I had the opportunity of meeting Professor Cagniard personally and discuss with him the general features of the method. From this conversation, I derived much encouragement which helped me in making my final decision regarding the thesis subject.

Dr. J. Freeman Gilbert, who called my attention to the work of Dougall on Green's functions.

Professor S. M. Simpson, Jr., Assistant Professor of Geophysics at M. I. T., who suggested the extension of the method of section 3.5 to the general inclined layer problem of section 3.6.

Dr. Manuel V. Cerrillo, of the Research Laboratory of Electronics, who gave much of his time to some mathematical points of the thesis.

Mr. Davis A. Fahlquist, who greatly helped me with many of the problems connected with modelling work.

Mr. Norman F. Ness, with whom I had very helpful discussions regarding the finite difference methods of chapter IV.

Mr. Donald J. Marshall, with whom I discussed many aspects of this thesis.

The faculty of the Department of Geology and Geophysics, which always showed willingness to help in a variety of functions.

The Bear Creek Mining Co., which partially financed the printing of this work.

The U. S. Atomic Energy Commission, Raw Materials Division, from which I received a research assistantship under contract AT(05-1)-718 and which kindly permitted me the use of some of the equipment of the aforementioned project.

Mrs. Joan Grine, who did the drawings on a rather tight schedule.

My family, who has assisted me in many ways, particularly my wife, Joyce, who has helped immensely by taking over the typing and organizing of the thesis.

CHAPTER I

SUMMARY AND HISTORICAL REVIEW

1.1 Summary

The magneto-telluric method is a geophysical procedure for the determination of the sub-surface conductivity, especially at great depths. The name magneto-telluric field was coined by Cagniard (1953) to distinguish the short period variations (about 100 seconds and less) of the earth's electric and magnetic field, which exhibit electromagnetic characteristics, from the long term oscillations which are in the nature of static fields. No restrictions regarding the origin of the radiation are implied; all phenomena having electromagnetic properties are included. The main contributions to the magneto-telluric field seem to arise from electromagnetic waves generated by ionospheric current sheets and by lightning discharges. The first produces a very low frequency spectrum with the most intense components in the 0.01 to 1 cycle range (Cagniard, 1956) the second results in oscillations in the audio range.

Extensive measurements point to the large scale uniformity of the magneto-telluric field (Schlumberger & Kunetz, 1948; Kunetz, 1953, 1954) and calculations by Wait (1954) lead us to expect such behavior.

The uniformity of the magneto-telluric field over large areas permits one to analyse the field by considering plane electromagnetic waves incident on a plane earth. The geometry of the ionospheric layers and the frequencies of interest allow us to neglect the earth's curvature. In other words, we are concerned with rather local effects.

In investigating the behavior of plane wave fields in the earth, the enormous contrast between the magnitudes of the constant of propagation of electromagnetic waves in the air and in the earth materials, plays an important role. Because of this contrast, no matter what the angle at which the wave may incide on the earth, the refracted wave will propagate essentially vertically down. Such property makes feasible the study of the magneto-telluric field without having to track down the radiation sources, which would be an impossibility. As far as the earth is concerned, all the wave may have come at a normal incidence. Further, still by virtue of the contrast in the propagation constants, the current flow across the earth's surface is negligible. Therefore, if we have current flow perpendicular to the strike of a two dimensional geological structure (that is, the magnetic vector polarized parallel to the strike), then the surface magnetic field is constant, even over regions of changing conductivity. If instead the current flow runs parallel to the strike of the two dimensional structure, then it is the electric field that remains constant at the surface. These results may be summarized by stating that when a plane wave incides on a two dimensional geologic structure, the vector component parallel to the strike of the structure is constant at the earth's surface. The importance of these results in mathematical analysis is evident and indeed it contributed to restrict the scope of this work to two dimensional structures. In practical geophysics these properties sound a warning against trying to detect buried structures by measuring the field polarized parallel to it, either electrical or magnetic.

This group of results simplify further the problem of analysis of the magneto-telluric field over one or two dimensional geologic formations. We had seen previously that we could study it by learning about the behavior of plane waves incident on a plane earth. Now we see that we don't even have to consider the field in air. No matter what the geometry of the changes in conductivity, the surface polarized field will be constant and therefore we have to deal only with the propagation of electromagnetic waves within the earth.

At this point, we may introduce the basic ideas of the magneto-telluric method as developped by Cagniard (1953). The magneto-telluric method could be called the impedance method because in fact it consists in obtaining the impedance normal to the earth's surface by measuring the horizontal electric and magnetic fields. This concept of impedance of a region of space, although analogous to that of impedance of an electrical circuit is not as familiar. Usually we define impedance normal to a surface separating two media as the ratio of the tangential electric intensity to the tangential magnetic intensity (Schelkunoff, 483, 1943). For a plane wave on a uniform earth, it is given by

$$\left.\frac{E_z}{H_x}\right|_{y=0} = \sqrt{\frac{\mu\omega}{\sigma}}\; e^{i\pi/4} \qquad (1\text{-}1)$$

where y increases with depth and the earth surface is defined by the plane x-z at $y = 0$. As we see in (1-1), the ratio of E_z/H_x gives us the conductivity σ of the medium because the μ of geologic materials can be considered constant and the radian frequency ω is known.

Plane waves are attenuated exponentially within an uniform earth and in some complicated manner in a non-uniform earth. Since this attenuation becomes stronger for higher frequencies, by measuring E/H at several frequencies we sample the conductivity at different depths. An estimate of the depth measured is afforded by the skin depth p,

$$p = \sqrt{\frac{2}{\mu \omega \sigma}} \tag{1-2}$$

The main contribution to the apparent conductivity measured at the surface comes generally from depths y such that $y \ll p/2$

The generalized magneto-telluric method is the extension to an arbitrary earth of the concept of impedance normal to the earth's surface, employed by Cagniard (1953) in the analysis of a horizontally stratified earth. However, as mentioned earlier, this investigation will be restricted to two dimensional geometries.

While the one dimensional problem treated by Cagniard needed only a spectrum of frequencies at one location, in two dimensional structures we will need coverage along a line perpendicular to the strike of the structure. At each successive points of this line, measurements at a spectrum of frequencies are made, so that the vertical and horizontal changes in conductivity may be detected.

Until some progress is made in the quantitative approach to the interpretation or inverse boundary value problem, we will have to use a mapping device to get a picture of the sub surface. A way in which we may accomplish this is by plotting the apparent resistivities at several frequencies, under the measuring point at a depth equal to the skin depth for the frequency in question. An example of this type of interpretation map is given in fig. 2-6.

The logical starting point for an investigation of two dimensional geological structures is the problem of inclined layers. A diagram of this type of geometry is shown in fig. 3-3. Although the simplest case of two dimensional change in electrical parameters, this problem belongs to a famous class of problems of mathematical physics, known as the finitely conducting wedge problems. These problems have remained not only unsolved, but actually impossible of setting up explicitly. The reason for this situation resides in the nature of the solution of the Helmoltz equation

$$\nabla^2 u + \kappa^2 u = 0 \tag{1-3}$$

in cylindrical coordinates r, ϕ and z. The face of the wedge are planes z - ϕ , so that in an inclined layer problem (which is a composite wedge) the earth's surface is given by $\phi = 0$ and $\phi = \pi$ and the dipping bed is at $\phi = \alpha$. Now the general solution of equations (1-3) is in terms of Hanekl and trigonometric functions, namely

$$u(r, \phi) \longrightarrow H^{(1)}(\kappa R)\left[A(m)\sin m\phi + B(m)\cos m\phi\right] \tag{1-4}$$

The problem is to match u_1 (corresponding to (1-4) in medium of propagation constant k_1) to u_2 along a boundary $\phi = \alpha$, in order to determine the functionals A(m) and B(m). It turns out that the solutions cannot be matched at a constant ϕ boundary, because the Hankel functions have different arguments from one wedge to the other. Or rather, in order to match solutions, A(m) and B(m) would have also to be functions of r which of course cannot be.

These obstacles were managed by starting out with an integral solution for the solution of the Helmoltz equation based on Dougall's (1899) Green's function for a wedge space. This solution consists of an integral over the order of the Bessel functions to account for the fact that the dipping layer may assume any angle,

$$u(r,\phi) = \frac{1}{\pi^2}\int_0^\infty K_{is}(\gamma r)\left[A(s)\cosh s\phi + B(s)\sinh s\phi\right] ds \qquad (1\text{-}5)$$

where $\gamma = -i\kappa$ and K_{is} is the modified Bessel functions of first kind. We will have of course one solution u_1 for one side and a solution u_2 for the other side of the dipping layer geometry. Since we cannot match integrands for the reasons discussed in the previous paragraph, we match integrals and satisfy the conditions,

$u =$ constant at the earth's surface, i.e., $\phi = 0$ and $\phi = \pi$

and

$$\left.\begin{aligned} u_1 &= u_2 \\ \frac{\partial u_1}{\partial \phi} &= \frac{\partial u_2}{\partial \phi} \end{aligned}\right\} \text{at} \quad \phi = \alpha \qquad (1\text{-}6)$$

Introduction of the two integrals like (1-5) (one for u_1 another for u_2) into the above equations, yield a system of 4 singular integral equations in 4 unknowns A(s), B(s), C(s) and D(s).

This system is then solved by the repeated use of Kontorovich Lebedev transforms (N. N. Lebedev, 1946) to invert the system of integral equations into integrals which give explicitly the functionals A(s), B(s), C(s) and D(s). The final solution for the field over an inclined bed is given in equations (3-82) and (3-83) in terms of integrals.

The cumbersomeness of the analytical approach and its downright impossibility when we need to analyse more complicated geometries led to the development in chapter IV, of a finite difference treatment which can be used on any 2 dimensional geological structure. The difficulties arising from the fact that the solution to the Helmoltz equation (1-3) for wave propagation in the earth is a complex number, are taken care of by splitting the Helmoltz equation into a system of two differential equations in two unknowns,

$$\begin{aligned} \nabla^2 A - k'^2 B &= 0 \\ \nabla^2 B + k'^2 A &= 0 \end{aligned} \qquad (1\text{-}6)$$

where $u = A + iB$ and k'^2 is real and equal to $\mu\omega\sigma$. The system (1-6) is then converted to finite differences as

$$\sum_{i=1}^{4} A_i - 4A_o - k'^2 h^2 B_o = 0$$

$$\sum_{i=1}^{4} B_i - 4B_o + k'^2 h^2 A_o = 0$$

and several boundary value problems of interest in connection with plane waves incident on the earth are solved by relaxation techniques (the reader is referred to figs. 4-4 and 4-5 for the mechanism of the relaxation operators).

The use of finite difference methods is feasible on account of the uniformity at the earth's surface of the polarized field as well as on account of the strong attenuation of electromagnetic waves within the earth. In this way we know that the field is constant at the earth's surface, that it behaves in a known manner at a sufficiently far horizontal distance from the region of changing conductivity and also that it becomes "zero" at depth (to the accuracy carried in the finite difference calculation). This gives us a set of homogeneous and inhomogeneous Dirichlet conditions around a closed boundary which make the problem determined.

The finite difference technique was applied to the solution of a set of inclined layer problems. These covered the three dipping angles of 45°, 90°, and 135°, and for each inclination the electrically and magnetically polarized solutions were obtained. The conductivity contrast was 4. Two other examples dealing with vertical beds, one in contact with an infinitely conducting medium, the other in contact with a non-conducting medium, were also solved to give us an idea of the behavior of the field for very high conductivity contrasts.

The inclined layer problems were chosen because their finite difference solution is more general than that of problems involving finite boundaries. Known their reponse at one frequency, we can deduce from it the response at all frequencies (conductivity contrast and angle of dip being constant). In effect, if we plot the apparent resistivities at successive frequencies, at a depth equal to the depth of penetration, all the lines of equal apparent conductivity will go through the strike of the inclined bed. This affords an interpretational procedure for such structures.

Using the solution for the vertical layer in contact with an infinitely conducting medium as the model, a study was made of the effect of the sea coast on the apparent resistivity inland. It was found that increases of the order of 2% on the apparent resistivities occur between $kr = 2.5$ and $kr = 1.5$, k being the propagation constant and r the distance from the measuring station to the sea. When kr becomes smaller than 1.5 the apparent resistivities fall very rapidly. This response may simulate very closely that of a two layered earth with a very conductive substratum.

The results for the inclined layer cases showed that the magneto-telluric field remains unaffected at a kr of 3.5 from the inclined layer contact, either for magnetic or electric polarization. Each polarization showed distinctive features.

As we go across the inclined layer from the resistive to the conductive side, electric polarized waves usually produce just a gradual change from the apparent resistivity of one medium to that of the other medium. However, small effects, towards higher resistivities on the resistive side and lower resistivities on the conductive side preceed and follow, respectively, the gradual transition of apparent resistivity.

For magnetic polarization, as we approach the strike from the resistive side, the first effect felt is usually a lowering of apparent resistivities around kr = 3. This develops in a minimum of apparent resistivity which appears to become stronger for shallower angles (by this we mean that the acute angle is on the resistive side). As we proceed toward the boundary of the media, we run next into a zone of very large apparent conductivities. For 45° and 135° inclined layers the apparent resistivities in this region were about twice that of the resistive medium; for vertical beds the effect is smaller. Finally, as we cross into the conductive medium, the apparent resistivities take values slightly smaller than the resistivity of the conductive medium. These effects disappear at a kr of 3 away from the strike, on the conductive side.

The results from the problems with infinite contrast show that the conductivity contrast does not affect very much the location of these regions of changing conductivity; rather, it is the inclination of the beds that controls them.

In the appendix some modelling results are reported. A scale model of a vertical layer and another of a buried cylinder were run with considerable success. The data obtained confirms, where it is pertinent, the finite difference results .

1.2 Historical notes

This investigation concerns primarily a geophysical method but the main problems pertain to mathematical physics. Consequently, its historical background lies both in geophysics and in mathematical physics.

The basic ideas of the magneto-telluric method are a recent development. They seem to have been motivated (Cagniard, 1956) by the lack of correlation between the predictions of the spherical harmonical analysis of the earth's magnetic field due to Schuster (1889) and Chapman (1919), and the actual measurements at a number of observatories. This fact and the increasing better knowledge of the properties of geologic materials led to the realization of the important role played by local geologic structures. Almost simultaneously while Tikhonov (1950) called attention for the possibilities of the method as a tool for exploration of great depths, Kato and Kikuchi (1950) made some measurements of the phase angle between the electric and the magnetic field and showed that they could arise from electromagnetic propagation on a two layer earth. A year later, in one of his series of papers on the electrical state of the crust, Rikitake (1951) showed that the electrical properties of the earth's crust could be determined by analysing the changes in telluric currents and in the geomagnetic field. The following year saw the publication of another article by Tikhonov and Lipskaia (1952) giving results for a two layer earth with an infinitely conductive bottom layer. Lipskaia (1953) in a later paper elaborated the previous results and showed that they agreed with the data of the observatories at Tucson (Arizona), Toyokhara (Japan), and Zuy (Eastern Siberia). Finally Cagniard (1953) published a very comprehensive paper on the magneto-telluric field over a horizontally layered earth, including methods to deal with the interpretation problem. He also pointed out the possible usefulness of the method as an exploration tool.

Since then there has been considerable activity in the study of the magneto-telluric field. Papers by Bondarenko (1953, 1953) dealt with the electromagnetic nature of the phenomena. In the U. S. work is or has been in progress at the Institute of Geophysics of the University of California, at the California Institute of Technology and at M. I. T. The studies at M. I. T. have already produced preliminary instrumentation for field measurements (Cunningham, 1957)

In this thesis an analytic formal solution was found to the problem of dipping beds and a way of handling arbitrary two dimensional geometries was developped through the use of finite differences. The first problem is related to a whole series of famous problems in the theory of the diffraction, which are sometimes known as wedge problems. A particular case, the diffraction of electromagnetic wave by an infinitely conducting half plate was solved originally in a most ingéneous manner by Sommerfeld (1896). Since then a few different ways of approaching the problem have been developped (Kontorovich and Lebedev, 1939; Clemmow, 1950; Stakgold, 1954; etc.) The more general problem of a diffraction by a perfectly conductive wedge has been solved rather recently by Grinberg (1948), Nomura (1951), Oberhettinger

(1954). At the same time the radio engineers have been trying to analyse the behavior of radio waves as they go over regions of different conductivities. Besides a number of empirical efforts, successful approximate and exact solutions have been obtained by Gunberg (1943), Alpert. and all (1953), Bremmer (1953), and Clemmow (1953). However, in general their work cannot be adapted to our purposes because the high frequency of the radio waves allows them to relax boundary conditions at the contact of two media, a procedure that we cannot follow in our case. The type of solution obtained in this text is different from all mentioned above except for the fact that we start from Dougall's (1899) Green's function which has also been used in an orthodox fashion by Oberhettinger (1954) in his problem.

As to the finite difference approach to electromagnetic propagation in arbitrary two dimensional structures, to the best knowledge of the author it has not been considered in the literature. However, the solution of systems of difference equations by relaxation methods is mentioned by Shaw (1953) and Allen (1954).

CHAPTER II

GENERAL PROPERTIES OF PLANE WAVE FIELDS IN THE EARTH AND THE MAGNETO-TELLURIC METHOD

2.1 The electromagnetic nature of the magneto-telluric field.

It is important to emphasize from the start that the magneto-telluric field is an electromagnetic field. This is just a statement of the scale involved, but it helps in putting the problem in its proper perspective.

Early workers were not aware of this fact and their ideas have not died down completely. Some thought that the variations in the magnetic field were the Biot-Savart field of the telluric (electric) currents in the ground. As such, both the electric and the magnetic fields should be in phase. Another group attributed the telluric currents to a rather simple case of induction by the existing magnetic field. Accordingly, the fields might be expected to be 90° out of phase. As we shall see, theory and experiment do not bear out these ideas.

The old hypothese can only be explained in terms of lack of data regarding the electrical properties of earth materials as well as to the scarcity of simultaneous measurements of the electric and magnetic fields of the earth. The oscillations to which the magneto-telluric method applies have periods of the order of minutes and shorter, up to a few hundred cycles. We know that the conductivities of rocks vary anywhere between 10^{-1} to 10^{-5} mhos/meter. The propagation of an electromagnetic wave of frequency ω in a medium of magnetic permeability μ and conductivity σ can be described by a Helmoltz equation.

$$\nabla^2 u + k^2 u = 0$$

where $k^2 = i\mu\omega\sigma$ (displacement currents neglected). The early ideas of static fields involve the assumption that k, the propagation constant, can be neglected and the field described by Laplace's equation. With the frequencies and conductivities in question, it is clear that we cannot do this without mutilating the problem. This a priori conclusion regarding the electromagnetic character of short period variations of the electric and magnetic field in the earth has been confirmed by an ever increasing amount of data (Schlumberger & Kunetz 1948; Kunetz 1953, 1954). Among the most salient and diagnostic features are (Cagniard, 1956):

a. similarity of simultaneous recordings at places separated by thousands of miles (Madagascar, France, and Venezuela).
b. at the same time and place frequency spectrum of electric and magnetic components is identical
c. uniformity of telluric currents over large areas.
d. the phase angle between the electric field vector and the magnetic field vector, in a given place, are function of period.
e. Correlation of magneto-telluric activity with Sun and auroral activity

On the basis of these characteristics, the origin of the magneto-telluric field is thought to be the motion of large current sheets in the ionosphere. The electromagnetic waves of very large wavelength (as compared with the Earth's size) generated by these planetary currents, upon inciding on the earth are reflected, refracted and diffracted by geologic structures. It is the aim of magneto-telluric method to deduce from the patterns of the surface electromagnetic field the nature of the sub-surface material.

2.2 Uniformity of telluric current sheets.

The question of the uniformity of the magneto-telluric field has been examined critically by Wait (1954). By setting up the field in the form of a spectrum of plane waves due to an aperture distribution, he has shown that if the magneto-telluric field were due to a dipole at about 100 km. high, uniformity might be expected in a range of 35 km., at a frequency of 1 cycle. This is of course, the most unfavorable situation possible. As Cagniard (1953, 1956) has pointed out repeatedly, everything leads us to believe that the magneto-telluric field is not set up by isolated dipoles over our heads, but rather by large current sheets of global scale. And the fields set up by such large ionospheric motions are bound to be uniform and resemble plane wave fields.

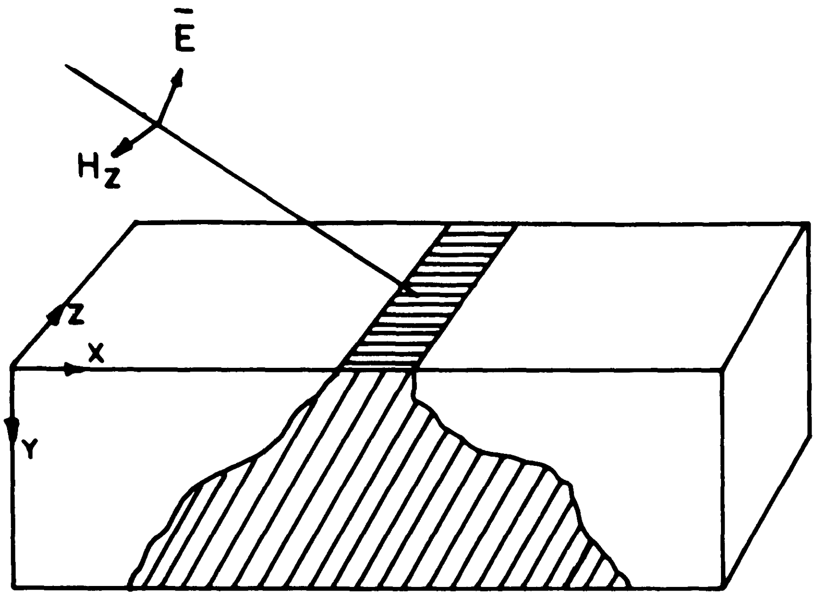

MAGNETICALLY POLARIZED PLANE WAVE INCIDENT
ON A TWO DIMENSIONAL STRUCTURE

FIG. 2-1

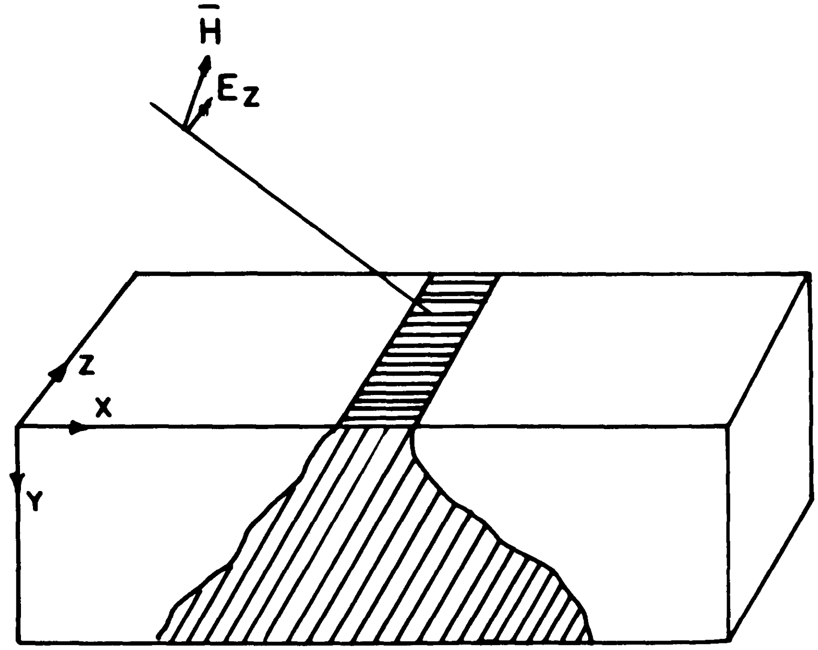

ELECTRICALLY POLARIZED PLANE WAVE INCIDENT
ON A TWO DIMENSIONAL STRUCTURE

FIG. 2-2

2.3 General properties of plane wave fields in the earth

From the previous sections, we have seen that the magneto-telluric field is a plane electromagnetic field. Here we will consider certain general features of such fields in two dimensional geological structures. The results are of great importance not only in simplifying the mathematical analysis, but also in bringing to light some unfavorable conditions for field measurements.

The two dimensional geometries in question are those of interest in geophysics and therefore are always bounded by the earth's surface represented by a plane x-z at $y = o$. All crossections x-y of the structures are identical (see fig 2-1). The impinging plane waves will be arbitrarily oriented. However, for purposes of analysis, we will consider such an arbitrary wave to be the sum of two polarized waves: one, which we will call magnetically polarized, will have the magnetic vector oriented on the z direction, that is along the strike of the structure; the other, which will be called electrically polarized will have the electric vector aligned on the z direction also. By superposition, we may combine these two waves to reconstruct any arbitrarily inciding plane wave. However, for the purposes of this work we will consider separately solutions for magnetic and for electric polarization.

The results to be shown refer to the arbitrariness of the angle of incidence and to the uniformity of the surface polarized electromagnetic field. The first emphasizes the rather well known fact that for the earth and at the low frequencies of interest in geophysics, no matter what the incidence of the plane electromagnetic wave, it will propagate essentially vertically down. The second property is rather surprising, and it consists in the fact that the polarized field (electrical or magnetic) will be constant at the earth's surface, even across regions of changing conductivity.

The importance of these properties is evident. Mathematically it enables one to set up the problems dealing with propagation of plane waves in the earth without reference to air, because instead of continuity conditions at the earth's interface, we have inhomogeneous Dirichlet conditions. The saving in algebra and mathematical difficulties is sizable. Further it makes possible the use of the rather straightforward finite difference method developped in chapter IV. From the practical viewpoint it sounds a warning against electrical measurements over two dimensional structures when dealing with electrical polarization, or magnetic measurements if by any chance magnetic polarization exists; in both cases any sub-surface structure would go undetected.

2.3.1 Arbitrariness of angle of incidence.

If we compare the propagation constants for air and for the earth materials we have respectively

$$k_{air} \approx 10^{-9}$$

$$k_{earth} \approx 10^{-4}$$

Consequently, the phase velocity of an electromagnetic wave in air is much greater than in the earth. If we have an incoming wave at any incidence, in order to have continuity of electromagnetic components across the earth's surface, the refraction at the interface forces the wave in the earth to propagate essentially vertically down. The use, for example, of Snell's law gives a quantitative idea of how close to the normal the angle of refraction is. If ϕ' is the angle of refraction in the earth, ϕ the angle of incidence, and k and k^1 the propagation constants for air and earth, respectively (angles measured from the normal to the surface),

$$\sin\phi' = \frac{K}{k^1} \sin\phi \qquad (2\text{-}1)$$

From equation (2-1) we see that even if ϕ is a grazing incidence (making $\sin\phi \sim 1$), k/k^1 is of the order of 10^{-5}. The angle whose sine is 10^{-5} is around a hundreth of one degree, and this is how far from the vertical the wave propagated in the earth will ever get.

The advantages of this situation are evident. Even if we have waves inciding simultaneously at several incidences, the field inside the earth will never know it. As far as the earth is concerned, all the waves may have incided normally and since previous sections have brought out the uniformity of the magneto-telluric field over large regions, we are free to study the phenomena by considering models with normally incident waves.

2.3.2 The uniformity of the surface magnetic field

Let us assume a magnetically polarized plane wave inciding upon a two dimensional structure (see fig. 2-1). The magnetic vector can be described by one component along the z axis, H_z ; both H_y and H_x are zero. The electrical vector however, will have components E_x and E_y .

As shown in 2.3.1, k (earth) $\gg$ k (air). So we may consider the propagation constant k for air equal to zero in comparison with the propagation constant for the earth. Then, there will be no vertical

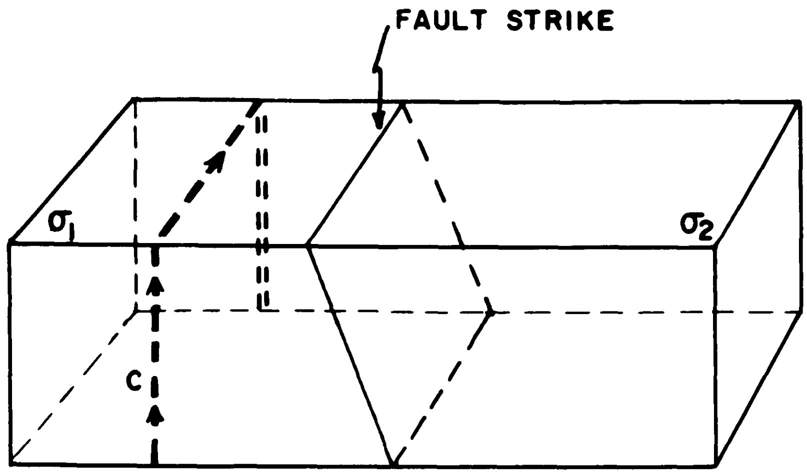

PATH OF INTEGRATION C FOR THE MAGNETIC FIELD

FIG. 2-3

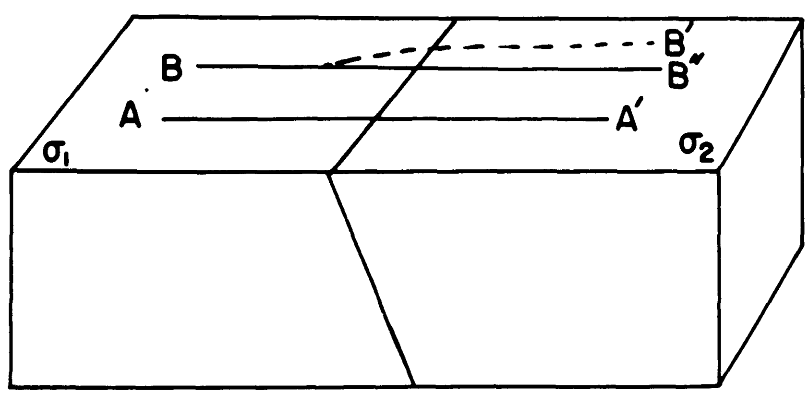

UNIFORMITY OF SURFACE ELECTRIC FIELD

FIG. 2-4

current flow at the surface of separation of air and earth and the normal component of the electric field, E_y , will be zero there.

In order to make the discussion shorter, let us assume we are dealing with a fault, with the understanding that the results are applicable to any two dimensional structure. The fault will separate two regions of different conductivities and propagation constants k_1 and k_2. Now, very far away from the fault boundary the field will behave like over an homogeneous uniform earth. Accordingly, it can be described by

$$\frac{\partial^2 H_z}{\partial y^2} + k^2 H_z = 0$$

or explicitly by

$$H_{z_1} = C_1 e^{ik_1 y} \qquad \text{as} \quad x \longrightarrow -\infty$$

$$H_{z_2} = C_2 e^{ik_2 y} \qquad \text{as} \quad x \longrightarrow +\infty$$

where the subscripts refer to the medium in which the field is being considered. The corresponding total current at these points will be given by

$$I = \int_C \bar{H} \cdot d\bar{s}$$

If we take a unit width of our structure and integrate the far away magnetic fields through a path C as shown in fig. 2-3, we will have at the surface

$$I_1 = \int_0^\infty H_{z_1} dz = C_1$$

$$I_2 = \int_0^\infty H_{z_2}\, dz = C_2$$

Now, since there is no current flow across the air-earth interface, there will be conservation of total current. Therefore the current flow across any crossection y-z is constant and we have

$$I_1 = I_2$$

or

$$C_1 = C_2$$

We may conclude then that the surface magnetic field, in the case of magnetic polarization, is constant, even across regions of changing conductivity. This property is restricted to two dimensional geologic structures. It may be added that the condition of no normal current flow corresponds to the vanishing of the tangential derivative of the magnetic field at the earth's surface. i.e. in cartesian coordinates

$$E_{\text{normal}} = 0$$

$$E = \frac{i\mu\omega}{k^2} \operatorname{curl} \bar{H}$$

$$E_{\text{normal}} = -\frac{i\mu\omega}{k^2} \frac{\partial H_{z_1}}{\partial x} = 0$$

which together with the electromagnetic boundary condition of continuity of tangential H at the boundaries of different media, furnish an alternative proof. If the surface magnetic field is uniform in both sides of the fault and is required to be continuous across it, then the field has to be uniform and equal over all the surface.

2.3.3 The uniformity of the surface electric field

From the invariance of Maxwell's equations to the exchange of E and H vectors in a constant physical setting, we might expect to find for the case of electric polarization a property identical to the one found for magnetic polarization in the previous section.

Considering again for simplicity the same fault geometry of fig. 2-3, we assume an electrically polarized incident wave; that is, the field will be described by E_z , H_y , H_x , all other electromagnetic components being zero. The earth's surface is the plane z-x and the fault plane is hinged on the z axis.

Referring to fig 2-4, consider the E field along the line A A' (on the x direction). Since we are dealing with a.c. phenomena we may consider this line the base line for any measurements of E_z . If we drew another line B, defined by an equal a.c. potential drop from A, this equipotential line could either follow BB' or BB''; in both cases boundary conditions would be matched. However, the hypothesis that we are dealing with an electrically polarized wave, which has no y or x components, would be contradicted if the curved line BB' were the equipotential line because then E would have to have at least y components. Therefore, we conclude that for electrically polarized plane waves, in two dimensional structures, the surface electrical field is constant. Further, since from Maxwell's equations

$$H_x = \frac{1}{i\mu\omega}\frac{\partial E_z}{\partial y}$$

$$H_y = -\frac{1}{i\mu\omega}\frac{\partial E_z}{\partial x}$$

we see that the vertical component of the magnetic field is also zero at the earth's surface.

We note then that the properties of both polarizations are symmetrical as far as the interchange of E and H are concerned. We may summarize 2.3.2 and 2.3.3 in the following table:

	magnetic polarization	electric polarization
field components at the earth's surface	$H_x = 0,\ H_y = 0,\ H_z = \text{const.}$	$H_x = g(x),\ H_y = 0,\ H_z = 0$
	$E_x = f(x),\ E_y = 0,\ E_z = 0$	$E_x = 0,\ E_y = 0,\ E_z = \text{const.}$

2.4 The basic theory of the magneto-telluric method.

The basic concepts of the magneto-telluric method are due to Tikhonov (1952) and Cagniard (1953). Cagniard's paper is a very comprehensive discussion of the magneto-telluric field over a stratified earth.

In order to introduce the main ideas, let us assume that we have a plane wave inciding on a uniform earth. Define a cartesian coordinate system as before, i.e. z into the paper, x horizontal and parallel to the paper, and y vertical and parallel to the paper. From previous considerations, it is clear that if, say, the E field has only a component along z, the electric field is described by

$$\frac{\partial^2 E_z}{\partial y^2} + k^2 E_z = 0 \qquad (2\text{-}2)$$

where $k^2 = i\mu\omega\sigma$ or explicitly by

$$E_z(y) = A e^{iky} \qquad (2\text{-}3)$$

Through Maxwell's equations, we get the corresponding magnetic field

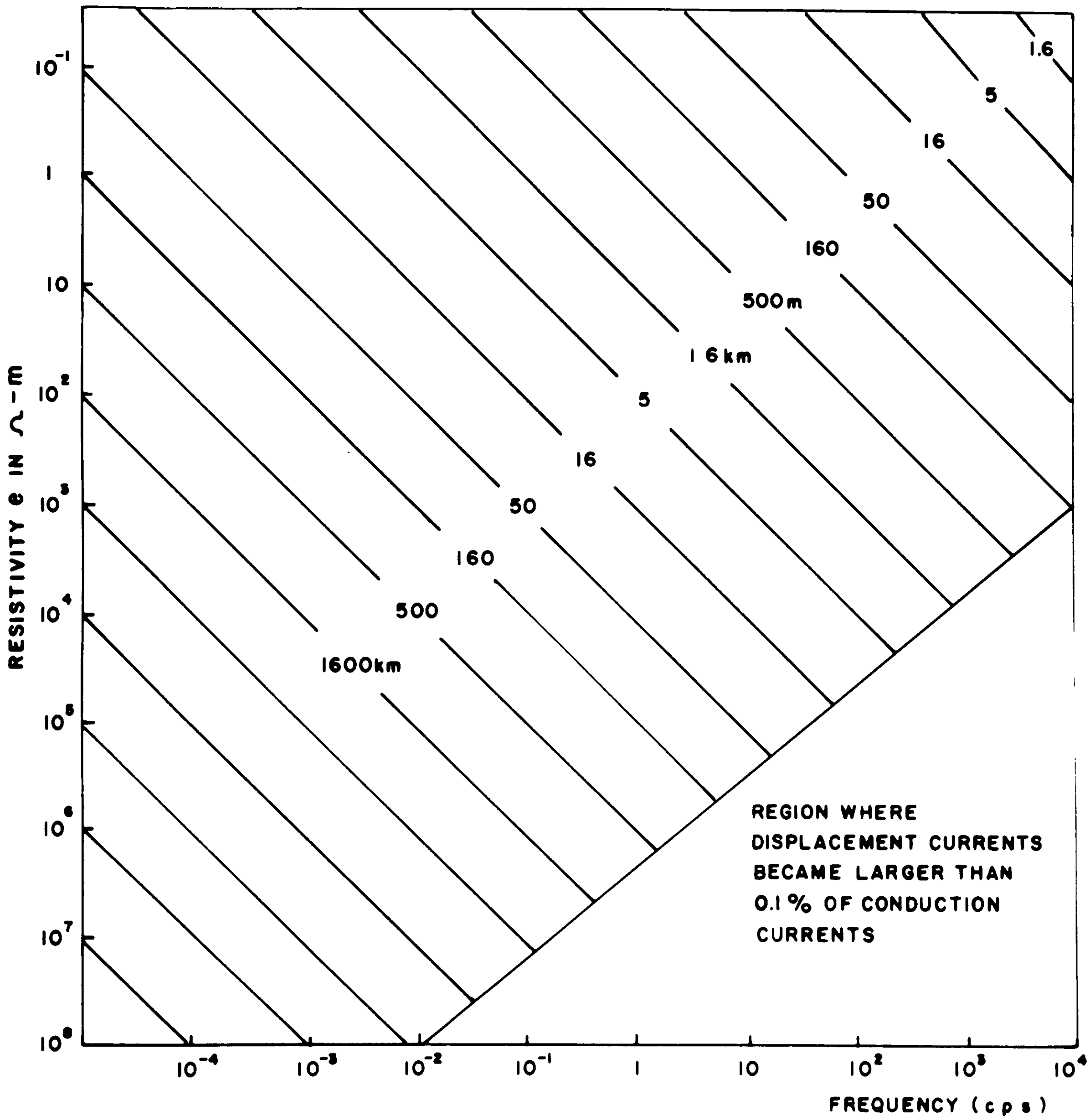

SKIN DEPTHS IN FUNCTION OF RESISTIVITY AND FREQUENCY

FIG 2-5

$$H_x = \frac{1}{i\mu\omega}\frac{\partial E_z}{\partial y} = \frac{k}{\mu\omega} E_z$$

Now, if we consider the ratio

$$\frac{E_z}{H_x} = \sqrt{\frac{\mu\omega}{\sigma}}\, e^{i\pi/4} \tag{2-4}$$

we notice that the measurement of E_z / H_x at surface determines the conductivity of the medium, since we know the frequency and for geologic materials μ can be considered constant. We note further that the electric field increases proportionally to ω and that the magnetic field lags behind the electric field 45°. For a horizontally layered earth the phase lag becomes dependent on frequency (see for example Cagniard, 1953).

The measurement of magnitudes E/H and the associated phase difference at different frequencies are the characteristic feature of the magneto-telluric method.

One of the great advantages of the method is in avoiding the necessity of base points because we are only concerned with a relative measurement. E and H can vary hourly, daily, or in any manner; magnetic storms are welcomed because they enhance the magnitudes of the field; no matter what the conditions, E/H and the phase difference will be constant for a given place at a given frequency.

The added information due to measurements at a spectrum of frequencies is related to the skin depth. As a wave penetrates into a uniform half space, its magnitude is attenuated exponentially as shown in equation (2-3). The skin depth is the depth at which this magnitude becomes 1/e of the surface value and is therefore given by

$$p = \sqrt{\frac{2}{\mu\omega\sigma}}$$

Consequently the E/H measurement, at a frequency ω gives us mostly the sampling of the conductivity above the corresponding skin depth. As we lower the frequency we reach deeper strata. From the work for a layered earth by Cagniard it can be generally stated that in a two layered earth, the conductivity of the bottom layer at a depth h becomes measurably only when $p/h > 1$, the diagnostic values coming in at $p/h \simeq 2$ to 3. The phase difference of E and H is more sensitive and for $p/h \geqslant 0.8$ the measurements are already diagnostic of the conductivity of the lower layer.

To get an idea of the depths that can be investigated with the magneto-telluric method, the reader is referred to fig. 2-5. It can be seen that, at least in principle, for conductivities like those of igneous and metamorphic rocks, depths of the order of 400 km. can be reached at frequencies between 0.1 and 0.01 cycles / second. However, in dealing with such huge vertical scale, we have to pay attention to horizontal changes in conductivity which are bound to occur in comparable horizontal distances. This makes imperative a study of the effect of 2 dimensional changes in conductivity on the magneto-telluric field.

2.5 The generalized magneto-telluric method.

The magneto-telluric method, as developped by Cagniard (Cagniard, 1953), was specifically designed for conditions of horizontal stratification. However, non-horizontal structures are as common, or more common than horizontal ones. In attempting to carry the basic concepts of the magneto-telluric method into the more general geological setting involving horizontal as well as vertical changes of electrical properties, a simple change in the field procedures will be necessary. While over a stratified earth a measurement at one geographical location was sufficient to determine the structure, for complex structures continuous or nearly continuous coverage is needed. Here we will consider only two dimensional structures and as such we will be supposed to have data at the earth's surface along a line perpendicular to the strike of the structure.

In considering any geophysical method of sub-surface investigation, the question of the inverse boundary value problem must be kept in mind. In other words, from the available surface data how do we narrow the deduced structure toward a unique solution? As a general statement, we may say that in the generalized magneto-telluric method, while the successive stations at the surface will show the horizontal changes in conductivity, the different frequencies at every station will afford coverage of depth, the lower frequencies sampling greater depths. In the case of the magneto-telluric field in two space dimensions the inverse boundary value problem consists in solving an integral equation (T. R. Madden, 1956) of the type

$$u(x,0|\omega) = \iint G(x,0|x',y'|\omega)\, f[u(x',y'|\omega)\,\rho(x',y')]\, dA \qquad (2\text{-}6)$$

the two dimensional structure being in plane x, y, and y-o the earth's surface. In the integral equation above $u(x,o|\omega)$ is the measured field at a radian frequency ω, G is the Green's function, $\rho(x',y')$ is the primary source distribution and $f(u,\rho)$ is the overall source distribution which we want to find. If measurements were made at one frequency only, the inverse problem would be generally undetermined, because in effect we would be trying to solve a two dimensional problem with one dimensional data. Considering the analogy between integral equations and systems of algebraic equations we see that the one frequency measurement would produce a situation resembling a system of n equations in n^2 unknowns. By using a spectrum of frequencies we tend to close the gap between the number of equations and unknowns, provided we can account for the frequency behavior of the right hand side of equation (2-6). This can be done in cases involving infinite or semi-infinite boundaries (see section 4.4), but rigorous studies for more general cases are lacking. In the meanwhile, we must tackle the interpretation problem (the inverse boundary value problem) from a purely qualitative point of view. Since the use of a frequency spectrum of waves gives us two dimensional spatial data, we may devise a crossectional mapping device which is related to the inverse transform of the integral equation (2-6) in a manner not exactly known. However the relationship must be close enough so that it provides one with a semi-quantitative picture of the sub-surface situation. Such concept has been employed very successfully by the induced polarization group at M. I. T. (Hallof, Vozoff, 1957; T. R. Madden et. al, 1957) which used the separation between sending and receiving dipoles as a criterium for mapping the properties at depth. In the magneto-telluric field, the sampling of deeper strata is accomplished by lowering frequencies and since this sampling is related to the amount of current at a given depth, we may use the skin depth as a depth parameter in our mapping transform.

An example of this type of crossectional mapping for interpretation purposes is shown in fig. 2-6. The data was obtained on a reduced scale model of a buried cylinder in a homogeneous earth, the conductivity contrast being about 1000. As it will be discussed in detail in the section on modelling, the material was not very homogeneous and the measurements were plagued by many troubles which account for the scatter of values in the homogeneous region as well as for some lack of symmetry. The map was made by plotting the values of apparent resistivity at depths equivalent to the skin depth in the homogeneous material, at the several frequencies used, under the station at which the measurement was made.

Before closing this section we may emphasize again that the transform obtained by the mapping is a purely semi-quantitative guide to interpretation. In the remaining chapters, we will deal with the direct problem. Only when we understand more fully the direct problem can we hope to have some success in solving the inverse problem.

MODEL BURIED CYLINDER

APPARENT CONDUCTIVITIES BY THE MAGNETO-TELLURIC METHOD

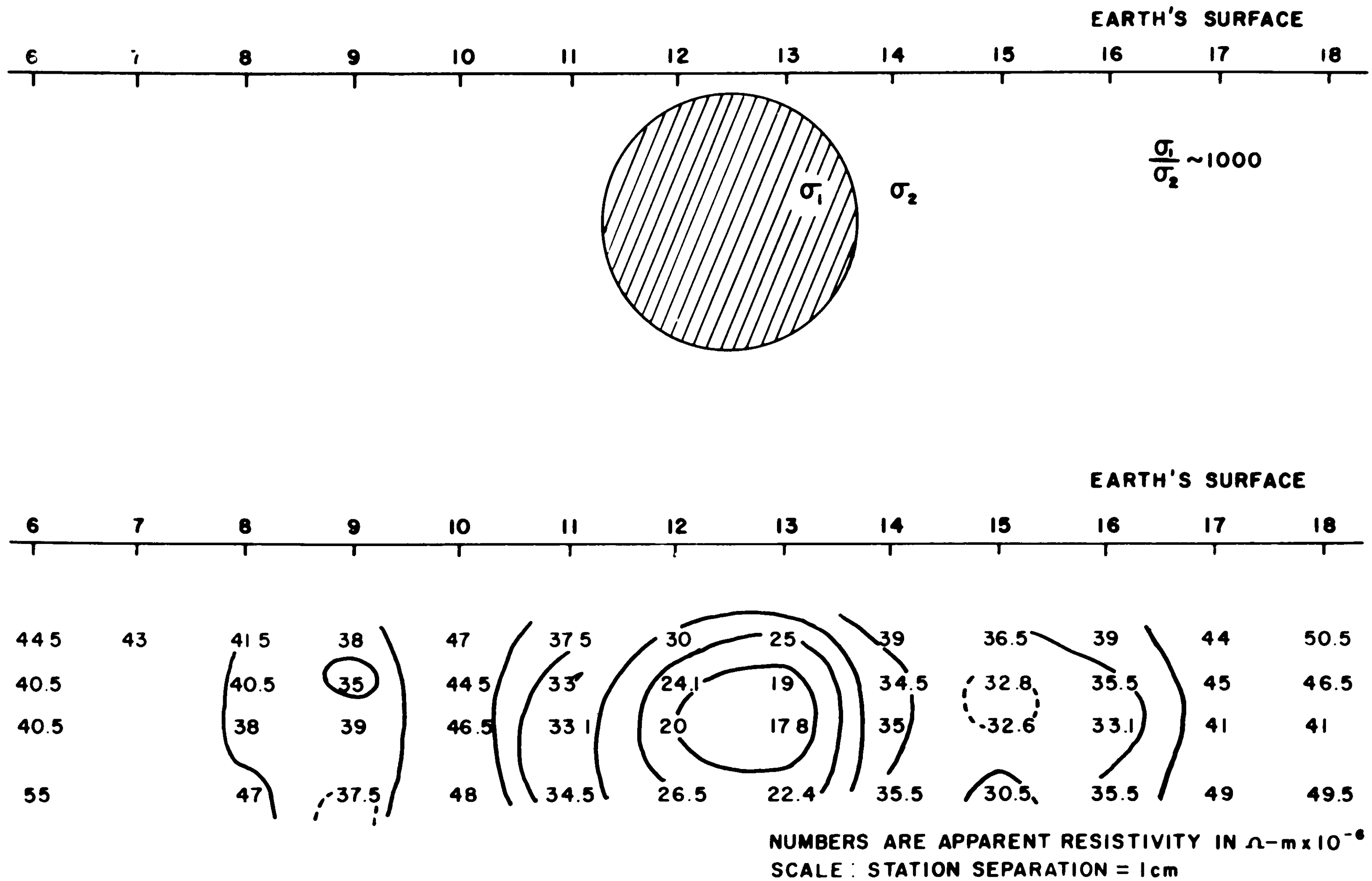

fig. 2-6

CHAPTER III

INCLINED LAYERS

3.1 Introduction

This chapter is devoted to the analytic treatment of the effect of inclined layers on an incident plane electromagnetic wave. The problem is two dimensional, with the earth's surface defined by angles $\phi = 0$ and $\phi = \pi$, and the line of contact between the media of different conductivities at an arbitrary angle $\phi = \alpha$. This type of geometry is an idealization of a rather common and important group of geologic structures. Among them we may cite faults, dipping beds and sea-land contacts.

In the following sections we obtain a formal solution for the general inclined layer problem (i.e. the problem in which both media have finite conductivites). As a step which serves to illustrate the details of the method by which we obtain the solution to the general problem, we solve also the problem of a wedge bounded by a non-conductor on one face and a perfect conductor on the other face. This problem of course, has considerable interest by itself, because it can be used as a model for sea-land contacts and inclined layer problems of large conductivity contrast.

3.2 The electromagnetic field vectors

As explained in 2.3 we will be dealing with an arbitrary incident wave, having x, y, and z components therefore, and in order to make the problem amenable to analysis, we break such a wave into a sum of two electromagnetic waves, one magnetically polarized (i.e polarized parallel to the structure, that is with the magnetic vector parallel to the z axis), the other electrically polarized ($E_x = E_y = 0$, $E_z = 0$) and solve separately for each type of wave. We may afterwards reconstruct the arbitrary wave by superposition of both polarizations.

Although incidentally we deal with electric and with magnetic line sources, our actual solutions will concern plane waves. In other words, we are concerned with the field far away from sources. Because of this and of the fact that much of the structure of the electromagnetic field can be found by physical considerations, we will forego the use of Hertz vectors and we will deal directly with the field vectors E and H. Since according to the polarization we will have either E_z or H_z the rest of the field can be derived from Maxwell's equations. This we proceed to do.

Let us consider first the case of magnetic polarization. The field can be described by the scalar equation

$$\nabla^2 H + K^2 H = 0 \tag{3-1}$$

where $\bar{H} = H a_z$, a_z being a unit vector on the z direction. From Maxwell's equations for periodic time variation

$$E = \frac{i\mu\omega}{K^2} \text{ curl } H a_z \tag{3-2}$$

In cartesian coordinates

$$\mathrm{curl}\ \bar{a}_z H = \bar{a}_x \frac{\partial H}{\partial y} - \bar{a}_y \frac{\partial H}{\partial x}$$

So that the field components are

$$E_x = \frac{i\mu\omega}{k^2} \frac{\partial H}{\partial y} \tag{3-3}$$

$$E_y = -\frac{i\mu\omega}{k^2} \frac{\partial H}{\partial x} \tag{3-4}$$

Therefore continuity of tangential E can be given either by

$$\frac{1}{k_1^2} \frac{\partial H_{z_1}}{\partial y} = \frac{1}{k_2^2} \frac{\partial H_{z_2}}{\partial y} \tag{3-5}$$

$$\frac{1}{k_1^2} \frac{\partial H_{z_1}}{\partial x} = \frac{1}{k_2^2} \frac{\partial H_{z_2}}{\partial x} \tag{3-6}$$

or at the x and y boundaries correspondingly. In cylindrical coordinates we have

$$\mathrm{curl}\ \bar{a}_z H = \bar{a}_r \frac{1}{r} \frac{\partial H}{\partial \phi} - \bar{a}_\phi \frac{\partial H}{\partial r}$$

$$E_\phi = -\frac{i\mu\omega}{k^2} \frac{\partial H}{\partial r} \tag{3-7}$$

$$E_r = \frac{i\mu\omega}{k^2} \frac{1}{r} \frac{\partial H}{\partial \phi} \tag{3-8}$$

giving for the continuity of tangential component of E

$$\frac{1}{k_1^2} \frac{\partial H_1}{\partial \phi} = \frac{1}{k_2^2} \frac{\partial H_2}{\partial \phi} \tag{3-9}$$

Now let us consider the case of electric polarization. The field this time is described by the scalar equation

$$\nabla^2 E + k^2 E = 0$$

where $\bar{E} = E\bar{a}_z$. Again from Maxwell's equation for periodic variation we have

$$H = \frac{1}{i\mu\omega} \text{curl } \bar{a}_z E$$

In cartesian coordinates

$$H_x = \frac{1}{i\mu\omega} \frac{\partial E}{\partial y} \tag{3-10}$$

$$H_y = -\frac{1}{i\mu\omega} \frac{\partial E}{\partial x} \tag{3-11}$$

In cylindrical coordinates

$$H_\phi = -\frac{1}{i\mu\omega} \frac{\partial H}{\partial r} \tag{3-12}$$

$$H_r = \frac{1}{i\mu\omega} \frac{1}{r} \frac{\partial H}{\partial \phi} \tag{3-13}$$

giving for the boundary condition of continuity of H tangential at a boundary

$$\frac{\partial H_1}{\partial \phi} = \frac{\partial H_2}{\partial \phi} \tag{3-14}$$

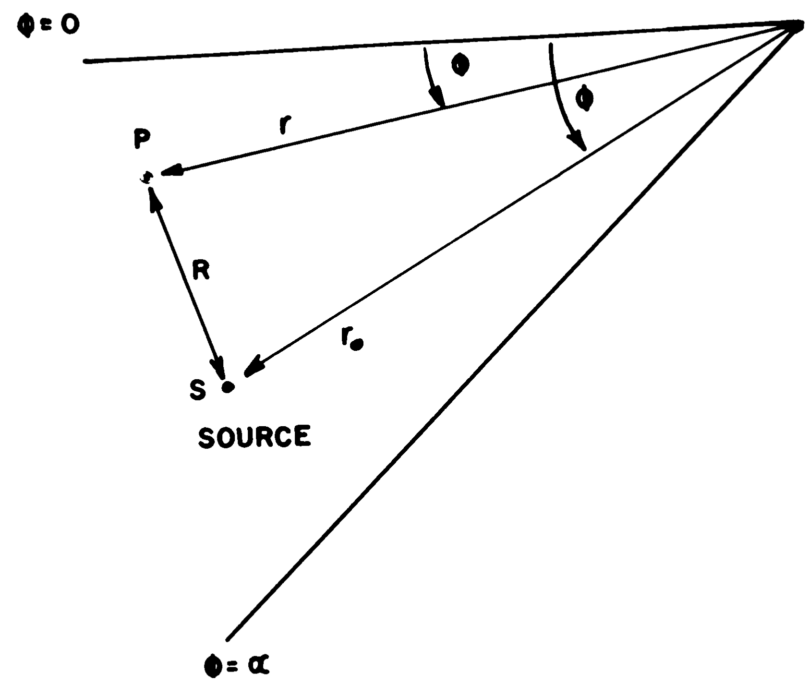

FIG 3-1

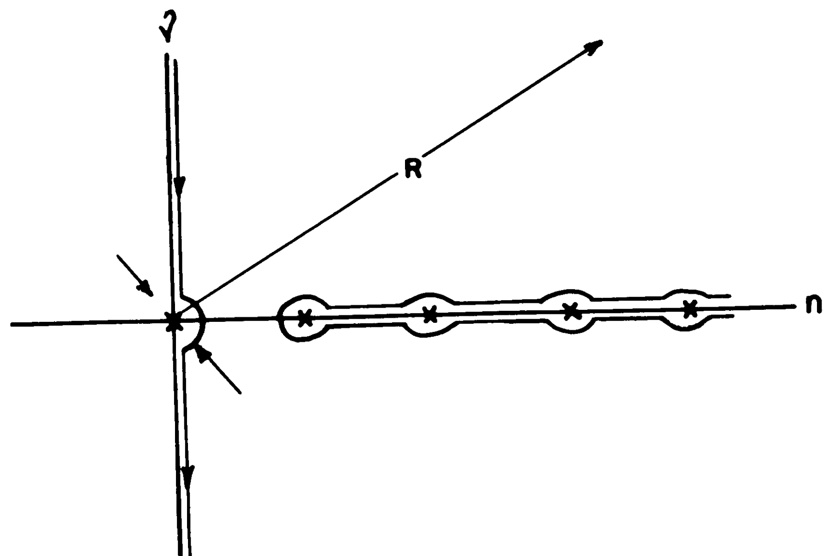

FIG 3-2

3.3 Wave solutions for a wedge space

In order to attack the solution of various types of dipping beds problems, we have to express our wave solutions in a form compatible with geometry under discussion. Before entering into the conditions that force the solution to take special forms we may note that we are using the cylindrical coordinate system, the wedge region being defined by $\phi = 0$ and $\phi = \alpha$, the direction of the angles being counterclockwise; consequently the z axis is perpendicular to the plane of the paper (fig. 3-1). We have seen that either for the magnetic or the electric polarization, the field can be described in terms of an Helmoltz equation.

$$\nabla^2 u + K^2 u = 0 \tag{3-15}$$

where $K^2 = i\mu\omega\sigma$. We write equation (3-15) in cylindrical coordinates

$$\frac{1}{r}\frac{\partial}{\partial r}\left(r\frac{\partial u}{\partial r}\right) + \frac{1}{r^2}\frac{\partial^2 u}{\partial \phi^2} + \frac{\partial^2 u}{\partial z^2} + K^2 u = 0$$

Because no z dependence is involved, the above equation reduces to

$$\frac{\partial^2 u}{\partial r^2} + \frac{1}{r}\frac{\partial u}{\partial r} + \frac{1}{r^2}\frac{\partial^2 u}{\partial \phi^2} + k^2 u = 0 \tag{3-16}$$

Proceeding by the usual method of separation of variables, we assume a solution

$$u(r, \phi) = R(r)\,\Phi(\phi)$$

which substituted back into (3-16) gives

$$\frac{r}{R}\frac{\partial}{\partial r}\left(r\frac{\partial R}{\partial r}\right) + \frac{1}{\Phi}\frac{\partial^2 \Phi}{\partial \phi^2} + K^2 r^2 = 0$$

allowing us to set

$$\frac{r}{R}\frac{\partial}{\partial r}\left(\frac{1}{r}\frac{\partial R}{\partial r}\right) + K^2 r^2 = -\frac{1}{\Phi}\frac{\partial^2 \Phi}{\partial \phi^2} = m^2$$

and separate the R and Φ dependent equations

$$r\frac{\partial}{\partial r}\left(r\frac{\partial R}{\partial r}\right) + (K^2 r^2 - m^2)R = 0 \tag{3-17}$$

$$\frac{\partial^2 \Phi}{\partial \phi^2} + m^2 \Phi = 0 \tag{3-18}$$

The R equation is satisfied by linear combinations of the Hankel functions of first and second kind. Since we will be dealing with divergent, outgoing waves, and do not desire solutions concerning incoming convergent waves, which would produce singularities in places where none exist, we will use only Hankel functions of the first kind. As for the solutions of the Φ equation, they are easily seen to be formed by combinations of cos $m\phi$ and sin $m\phi$. That is

$$R(r) \longrightarrow H^{(1)}(KR)$$

$$\Phi(\phi) \longrightarrow e^{\pm im\phi}$$

or

$$u(r,\phi) \longrightarrow e^{\pm im\phi}\, H^{(1)}(KR) \tag{3-19}$$

In order to obtain a representation of the two dimensional Green's function appropriate to a wedge space (Dougall, 1899), we consider the field of cylindrical waves produced by a line source (eventually by removing the line source to infinity we produce plane waves). This field can be represented by (Morse and Feshbach, 1323, 1953)

$$H_0^{(1)}(KR) = \frac{2}{\pi i}\, K_0(\gamma R) \tag{3-20}$$

where $-\gamma = iK$ and $R = r + r_o - 2rr_o\cos(\phi - \phi_o)$. By using an addition theorem for Bessel functions (Gray & Mathews, 103, 1922) we write (3-20) as

$$H_o^{(1)}(KR) = \frac{2}{\pi i}\sum_{m=0}^{\infty}(2-\epsilon_m)\,K_m(\gamma r)\,I(\gamma r_o)\cos m(\phi-\phi_o) \qquad (3\text{-}21)$$

where r real and $0 < r_o < r$. $K_m(\gamma r)$ and $I(\gamma r_o)$ are the modified Bessel functions of first and second kind respectively and

$$\epsilon_m = \begin{cases} 1 & m = 0 \\ 0 & m \neq 0 \end{cases}$$

The necessary integral representation of $H_o^{(1)}(k\,r)$ has to allow for the fact that the angle of the wedge is arbitrary. Therefore, the integral in question will have to be over the m variable. Expression (3-21) shows clearly the potentiality of being transformed into such an integral, having further the advantage of containing the needed discontinuity. If we call S the integrand of the integral representation of the Green's functions that we are looking for, from Cauchy's residue theorem we know that

$$\oint S\,dA = 2\pi i\sum_{0}^{\infty}\text{RESIDUES} = \sum_{m=0}^{\infty}(2-\epsilon_m)\,K_m(\gamma r)\,I_m(\gamma r_o)\cos m(\phi-\phi_o) \qquad (3\text{-}22)$$

Equality (3-22) requires function S to have poles at $m = 0, 1, 2, \ldots$ One such function is $f(m)/\sin m\pi$ which has a m^{th} residue $(-1)^m f(m)$ and where $f(m)$ does not posess any singularities in the complex plane. Since our integral has to be equal to (3-21), we may suspect that the numerator of S is

$$f(m) = (-1)^m\cos m(\phi-\phi_o)\,K_m(\gamma r)\,I_m(\gamma r_o)$$

$$= \cos m(\pi-\phi+\phi_o)\,K_m(\gamma r)\,I_m(\gamma r_o)$$

By integrating S through the appropriate path, we will achieve the double purpose of obtaining the needed integral representation and also of checking that inded it yields the series of the addition theorem. The integration in the complex plane can be written fully

$$-\int_{\rho}^{-i\infty} S\,d\nu - \int_{-i\infty}^{-\rho} S\,d\nu + \oint_R S\,dm + \oint_{\rho} S\,dm = 0 \qquad (3\text{-}23)$$

with the convention that the positive direction is clockwise. The The path of integration is shown in fig. 3-2.

As $\rho \to 0$

$$\oint_{\rho} S\,dm = \oint \frac{\cos m(\pi - \phi + \phi_0) K_m(\gamma r) I_m(\gamma r_0)}{\sin m\pi}\,dm = i K_0(\gamma r) I_0(\gamma r_0)$$

As $R \to \infty$, the integral along the large circle R vanishes and the only contribution comes from the poles along the real axis η

$$\oint_R S\,dm = 2\pi i \sum_{m=1}^{\infty} \frac{1}{\pi} \cos m(\phi - \phi_0)\, K_m(\gamma r)\, I_m(\gamma r_0)$$

Therefore (3-23) reduces to

$$\oint_{-i\infty}^{i\infty} S\,d\nu = i \sum_{\eta=0}^{\infty} (2 - \epsilon_m) K_n(\gamma r)\, I_n(\gamma r_0) \cos \eta(\phi - \phi_0) = K_0(\gamma r)$$

Where

$$S = \frac{\cos m(\pi - \phi + \phi_0) K_m(\gamma r) I_m(\gamma r_0)}{\sin m\pi} \qquad (3\text{-}24)$$

Now if we let in the left hand side of equation (3-24) $\nu = is$ we get

$$K_0(\gamma R) = \int_{-\infty}^{\infty} \frac{\cosh s(\pi - \phi + \phi_0)}{\sinh s\pi} K_{is}(\gamma r)\, I_{is}(\gamma r_0)\,ds$$

Using the equalities

$$K_{is}(\gamma r) = \frac{\pi}{2} \frac{1}{\sinh s\pi} \left[I_{-is}(\gamma r) - I_{is}(\gamma r) \right]$$

$$K_{is}(\gamma r) = K_{-is}(\gamma r)$$

We get the final form for the integral representation of a line source of cylindrical waves

$$K_o(\gamma R) = \frac{2}{\pi}\int_0^\infty \cosh s(\pi - \phi + \phi_o)\, K_{is}(\gamma r)\, K_{is}(\gamma r_o)\, ds$$

Now that we have obtained the Green's function expression for a wedge space, we may write the general solution to the unhomogeneous wave equation in such a geometry as a sum of the source term plus the homogeneous solution (3-19),

$$u = u\,(\text{source}) + u\,(\text{reflected})$$

$$= \frac{1}{4} H_o^{(1)}(KR) + \left[H_m^{(1)}\, e^{\pm im\phi} \right]$$

$$= \frac{1}{\pi^2}\int_0^\infty K_{is}(\gamma r)\, K_{is}(\gamma r_o) \left[\cosh s\left(\pi - |\phi - \phi_o|\right) + Ae^{s\phi} + Be^{-s\phi}\right] ds$$

In dealing with a problem consisting of several wedges, the solution in the wedges without sources can be written

$$u = \frac{1}{\pi^2}\int_0^\infty K_{is}(\gamma r)\left[Ae^{s\phi} + Be^{-s\phi}\right] ds \qquad (3\text{-}25)$$

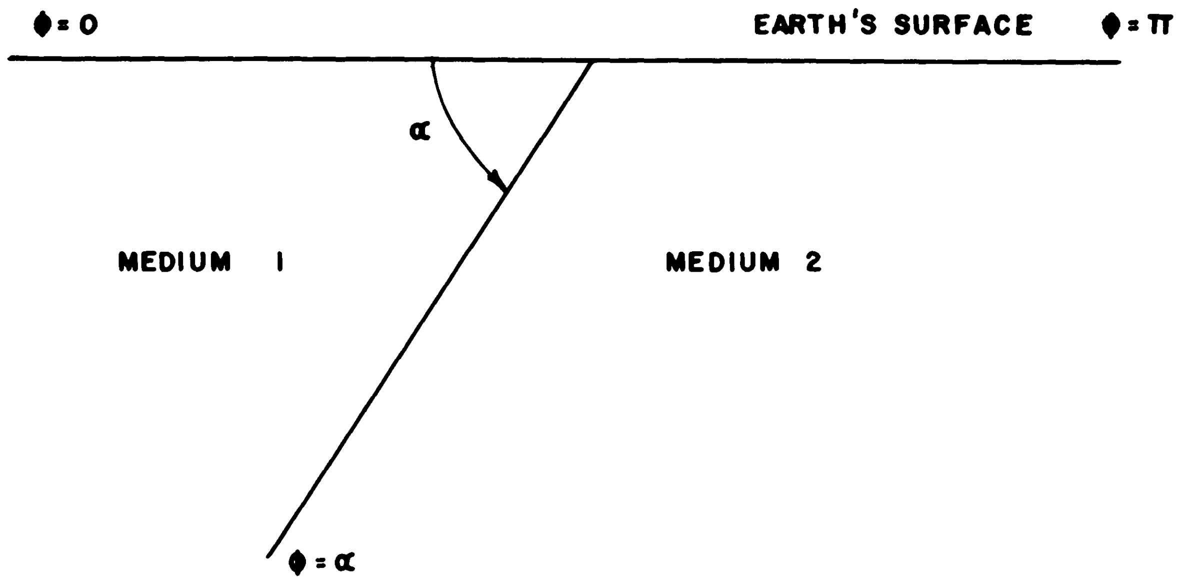

INCLINED LAYER PROBLEM
FIG 3-3

3.4 Difficulties in formulating the wedge problem

In most boundary value problems once the appropriate general solution is found, the only difficulty usually arises on evaluating the integrals obtained after the matching of boundary conditions. For the wedge problem, besides the possible obstacles to the integration of the result, we must add difficulties in matching boundary conditions. This may account for the fact that the problem had not yet been formulated exactly. Let us illustrate these difficulties. Suppose we are dealing with the general inclined layer problem. Since our sources are in air and we can describe the field completely in terms of the field in the earth (due to the general properties of plane wave fields in the earth discussed in section 2.3) we would have (see also fig. 3-3)

$$u_1 = \frac{1}{\pi^2}\int_0^\infty K_{is}(\gamma_1 r)\left[A(s)\cosh s\phi + B(s)\sinh s\phi\right] ds \tag{3-26}$$

$$u_2 = \frac{1}{\pi^2}\int_0^\infty K_{is}(\gamma_2 r)\left[C(s)\cosh s\phi + D(s)\sinh s\phi\right] ds \tag{3-27}$$

subject to boundary conditions

$$u_1 = u_0 = \text{constant} \qquad \text{at } \phi = 0,\ \phi = \pi$$

$$\left.\begin{aligned} u_1 &= u_2 \\ \frac{1}{K_1^2}\frac{\partial u_1}{\partial \phi} &= \frac{1}{K_2^2}\frac{\partial u_2}{\partial \phi} \end{aligned}\right\} \quad \text{at } \phi = \alpha \tag{3-28}$$

The difficulty becomes immediately apparent. As we try to match the integrands of (3-26) and (3-27) along boundary $\phi = \alpha$ we see that this is impossible because the factor in the integrand connected with the radial dependence consists of Bessel functions which have different arguments from one side to the other of the boundary. Since the Bessel functions don't match at the boundary and we cannot introduce any further radial dependence on the solution, the integrands cannot ever match at a ϕ constant boundary.

The same happens even for the simpler conditions at $\phi=0$ and where u_1 and u_2 cannot be constant due to the r dependence. Indeed it turns out that for the above formulation only homogeneous Dirichlet or Neuman conditions will enable us to use the simple procedure of finding the functionals A and B from algebraic equations involving the integrands.

The impossibility of matching the boundary conditions in a simple way is basically the result of the form assumed by the two dimensional Helmoltz equation combined with the use of the method of separation of variables. No trouble would arise, for example, if the term containing k^2 in the Helmoltz equation could be lumped together with the ϕ dependent equation and the solution for the R equation contained only the separation variable m. A very interesting attempt at bypassing this obstacle was carried by Kontorovich and Lebedev (1939), who developped a transform pair which enabled one to transform the Helmoltz equation in cylindrical coordinates into a one dimensional unhomogeneous equation in ϕ . Unfortunately, restrictions placed on the behavior of the solution at zero and infinity as well as the dependence of the transform on the propagation constant k do not permit the use of this approach in our problem.

In face of the failure to develop means to avoid the problems connected with the behavior of the radial solution, we are forced to tackle the wedge problem head on. That is, since we cannot match integrands, we will have to match integrals. The result is that we are drawn into the attempt of solution of systems of singular integral equations with several unknowns. This comprises the following sections.

3.5 Inclined layers with infinite contrast

We begin by considering the case of inclined layers where one of the media posesses an infinite conductivity. This is an appropriate model for cases of large contrasts between dipping beds in the earth or for the case of the effects of the sea on the magneto-telluric field.

From equation (3-25) we know that the solution is given by

$$u(r,\phi) = \frac{1}{\pi^2}\int_0^\infty K_{is}(\gamma r)\left[A(s)\cosh s\phi + B(s)\sinh s\phi\right] ds \qquad (3\text{-}29)$$

Since one of the media is infinitely conductive the electromagnetic field is zero at its boundary. So the boundary conditions are,

$$\begin{aligned} u &= h = \text{constant} \quad \text{at } \phi = 0 \\ u &= 0 \qquad\qquad\quad\;\; \text{at } \phi = \alpha \end{aligned} \qquad (3\text{-}30)$$

In order for (3-29) to satisfy (3-30), A(s) and B(s) have to satisfy the following pair of simultaneous singular integral equations

$$h = \frac{1}{\pi^2}\int_0^\infty K_{is}(\gamma r)\, A(s)\, ds \qquad (3\text{-}31)$$

$$0 = \frac{1}{\pi^2}\int_0^\infty K_{is}(\gamma r)\left[A(s)\cosh s\alpha + B(s)\sinh s\alpha\right] ds \qquad (3\text{-}32)$$

Very little is known presently about the solution of systems of singular integral equations. Therefore, rather than attempt a direct solution of (3-31) and (3-32) we try to find an integral transform that will convert our integral equations into integrals. One transform that is appropriate for this end is the Lebedev transform (N. N. Lebedev, 1946). The transform pair can be written as

$$F(s) = \int_0^\infty f(x)\, K_{is}(x)\, dx \tag{3-33}$$

$$x\, f(x) = \frac{2}{\pi^2} \int_0^\infty K_{is}(x)\, s \sinh s\pi \; F(s)\, ds \tag{3-34}$$

provided that Lesbesque integrals of first class for $x^2 f(x)$ and $x f'(x)$ exist.

In order to identify (3-31) with (3-34) we let

$$x = \gamma r \quad , \quad f(x) = \frac{h}{\gamma r} \quad , \quad F(s) = \frac{A(s)}{2 s \sinh s\pi} \tag{3-35}$$

Then A(s) is given by the following integral

$$A(s) = h s \sinh s\pi \int_0^\infty \frac{K_{is}(\gamma r)}{r}\, dr \tag{3-36}$$

To evaluate (3-36) we begin by expressing it in terms of Bessel functions of the first kind. Using the equalities (H. T. F. II, 1953, 4 and 5)

$$K_\nu(z) = \frac{\pi i}{2}\, e^{\frac{\nu\pi i}{2}}\, H_\nu^{(1)}(iz) \tag{3-37}$$

$$H_\nu^{(1)}(z) = \frac{1}{i \sin \nu\pi} \left[J_{-\nu}(z) - J_\nu(z)\, e^{-i\nu\pi} \right] \tag{3-38}$$

and also recalling that $-i\kappa = \gamma$ or $\gamma = e^{-i\pi/2}\kappa$ we get

$$K_{is}(\gamma r) = \frac{\pi i}{2} e^{-\frac{\pi s}{2}} \frac{1}{\sinh s\pi} \left[J_{is}(\kappa r) - J_{-is}(\kappa r) e^{\pi s} \right] \qquad (3\text{-}39)$$

and therefore integral (3-36) becomes

$$A(s) = i\pi h s \int_0^\infty \left[\frac{e^{-\frac{\pi s}{2}} J_{is}(\kappa r)}{r} - \frac{e^{\frac{\pi s}{2}} J_{-is}(\kappa r)}{r} \right] dr \qquad (3\text{-}40)$$

Equation (3-40) has the form of an Hankel integral transform whose inverse is known (T. I. T., II, 1953, 7), so we can write directly

$$A(s) = 2h\pi \cosh \frac{\pi}{2} s \qquad (3\text{-}41)$$

B(s) still remains to be found. However u vanishes identically at and from (3-32) we see that B(s) has to satisfy

$$A(s) \cosh s\alpha + B(s) \sinh s\alpha = 0 \qquad (3\text{-}42)$$

from which

$$B(s) = -\frac{2h\pi \cosh \pi/2\, s}{\sinh s\alpha} \cosh s\alpha \qquad (3\text{-}43)$$

Therefore the solution to the problem of dipping layers with infinite conductivity can be written

$$u(r,\phi) = \frac{2h}{\pi} \int_0^\infty \left[K_{is}(\gamma r) \cosh \frac{\pi}{2} s \cosh s\phi - K_{is}(\gamma r) \frac{\cosh \pi/2\, s}{\sinh s\alpha} \cosh s\alpha \sinh s\phi \right] ds \qquad (3\text{-}44)$$

Integrals of the type of the first term of (3-44) were studied by Ramanujan and his results quoted by several authors (H. T. F. II, 54)

$$u(r,\phi) = u_1 + u_2 \qquad (3\text{-}45)$$

$$u_1 = \frac{h}{2\pi} \int_0^\infty K_{is}(\gamma r) \cosh s\frac{\pi}{2} \cosh s\phi \, ds = h \cos(\kappa r \sin\phi)$$

Equation (3-45) describes a downgoing plane wave as well as a upgoing wave. This last wave cannot of course exist because it would be a violation of the conditions at infinity; next we will show how the second term of the integral contains the factor that cancels this exponentially increasing wave.

The second term of (3-44) is

$$u_2 = -\frac{2h}{\pi}\int_0^\infty \left[K_{is}(\gamma r)\frac{\cosh \frac{\pi}{2}s}{\sinh s\alpha}\cosh s\alpha \sinh s\phi\right] ds \tag{3-46}$$

Expanding $\cosh s\alpha \cosh \frac{\pi}{2}s$, (3-46) becomes

$$u_2 = -\frac{2h}{\pi}\int_0^\infty K_{is}(\gamma r)\left[\frac{\cosh s(\frac{\pi}{2}-\alpha)}{\sinh s\alpha}\sinh s\phi + \sinh s\tfrac{\pi}{2}\sinh s\phi\right] ds \tag{3-47}$$

The second term of (3-47) is again one of the integrals of the type studied by Ramanujan (H. T. F. II, 53) and we may write

$$u_2 = -\frac{h}{i}\sin(\kappa r\sin\phi) - \frac{2h}{\pi}\int_0^\infty K_{is}(\gamma r)\frac{\cosh s(\frac{\pi}{2}-\alpha)}{\sinh s\alpha}\sinh s\phi \, ds$$

which makes the solution

$$u(r,\phi) = he^{i\kappa r\sin\phi} - \frac{2h}{\pi}\int_0^\infty K_{is}(\gamma r)\frac{\cosh s(\frac{\pi}{2}-\alpha)}{\sinh s\alpha}\sinh s\phi \, ds \tag{3-48}$$

Equation (3-48) gives then the polarized field in terms of an incident vertically propagating plane wave minus the field which will arise from reflection and refraction effects.

If we consider the fact that the Lebedev transform of $\cosh s(\frac{\pi}{2}-\alpha)$ is given by $\frac{\pi}{2}e^{i\kappa r\sin\alpha}$ we see that equation (3-48) satisfies the boundary conditions reducing the h at the surface and to zero at

We will be satisfied here to leave the solution in integral form, showing thus that the problem can be solved by the application of fairly simple procedures. The evaluation of the integral in (3-48) is another problem in itself, which we choose not to deal with. We might add that if we tried to reduce the integral of (3-48) to an infinite series by use of Cauchy's theorem, this series would be divergent. The possibility of evaluating the integral by numerical methods is exceedingly laborious because there are no tables of modified Bessel functions of imaginary order, and further, because usually the numerical integration of complex functions requires an enormous amount of computation. However, the cases of interest connected with equation (3-48) have been solved by the numerical method of chapter IV and the results presented in section 4.6.

3.6 The general inclined layer problem.

By the general inclined layer problem we understand the problem of finding the field associated with plane electromagnetic waves inciding normally to the earth's surface, when the earth is composed of two regions of different but finite conductivity. These two regions meet at a semi-infinite planar contact i.e. a fault or a bedding plane (see fig. 3-3)

The general inclined layer structure is a special case of the problem known in mathematical physics as the composite wedge problem. This problem, to the best knowledge of the author, had not been solved yet either in physics or in geophysics. I would like to mention that I am indebted to professor S. M. Simpson, Jr. for the suggestion of extending the methods of section 3.5 to the general problem.

In the following, we will treat specifically the case of electrical polarization, but the case of magnetic polarization is identical with the exception of the constants in the derivative boundary conditions. Referring back to equation (3-24) and fig. 3-3, we see that the problem consists in solving

$$u_1(r,\phi) = \frac{1}{\pi^2}\int_0^\infty K_{is}(\gamma_1 r)\left[A(s)\cosh s\phi + B(s)\sinh s\phi\right] ds \tag{3-50}$$

$$u_2(r,\phi) = \frac{1}{\pi^2}\int_0^\infty K_{is}(\gamma_2 r)\left[C(s)\cosh s\phi + D(s)\sinh s\phi\right] ds \tag{3-51}$$

subject to the boundary conditions

$$\begin{aligned} u_1 &= u_0 = \text{constant}, \ \text{at } \phi = 0 \\ u_2 &= u_0 = \text{constant}, \ \text{at } \phi = \pi \end{aligned} \tag{3-52}$$

and

$$\left.\begin{aligned} u_1 &= u_2 \\ \frac{\partial u_1}{\partial \phi} &= \frac{\partial u_2}{\partial \phi} \end{aligned}\right\} \text{at } \phi = \alpha \tag{3-53}$$

where u_1 is the electrical field in medium 1, u_2 the electrical field in medium 2, $\phi = 0$ and $\phi = \pi$ is the earth's surface and $\phi = \alpha$ is the fault or inclined layer plane. Introducing (3-50) and (3-51) into (3-53), (3-52) we get a system of 4 simultaneous integral equations in 4 unknowns A(s), B(s), C(s) and D(s)

$$\phi = 0 \qquad u_0 = \frac{1}{\pi^2}\int_0^\infty A(s)\, K_{is}(\gamma_1 r)\, ds \tag{3-56}$$

$$\phi = \pi \qquad u_0 = \frac{1}{\pi^2}\int_0^\infty K_{is}(\gamma_2 r)\left[C(s)\cosh s\pi + D(s)\sinh s\pi\right] ds \tag{3-57}$$

$$\phi = \alpha \quad \begin{cases} 0 = \dfrac{1}{\pi^2}\displaystyle\int_0^\infty \Big\{\cosh s\alpha\left[K_{is}(\gamma_1 r)\,A(s) - K_{is}(\gamma_2 r)\,C(s)\right] + \\ \qquad + \sinh s\alpha\left[K_{is}(\gamma_1 r)\,B(s) - K_{is}(\gamma_2 r)\,D(s)\right]\Big\}\, ds & \text{(3-58)} \\[2ex] 0 = \dfrac{1}{\pi^2}\displaystyle\int_0^\infty s\Big\{\sinh s\alpha\left[K_{is}(\gamma_1 r)\,A(s) - K_{is}(\gamma_2 r)\,B(s)\right] + \\ \qquad + \cosh s\alpha\left[K_{is}(\gamma_1 r)\,B(s) - K_{is}(\gamma_2 r)\,D(s)\right]\Big\}\, ds & \text{(3-59)} \end{cases}$$

Now if we define $\quad E(s) = C(s)\cosh s\pi + D(s)\sinh s\pi$

(3-60)

equation (3-57) becomes

$$u_0 = \frac{1}{\pi^2}\int_0^\infty K_{is}(\gamma_2 r)\; E(s)\, ds \tag{3-61}$$

which is similar to equation (3-56)

But back in 3.5 we solved an integral equation of the type of (3-56) and (3-57) by using the Lebedev transform (see equation (3-33) and (3-34))and therefore we know immediately that the solution to (3-56) and (3-57) is

$$\left.\begin{matrix} A(s) \\ \\ E(s) \end{matrix}\right\} = u_0 \pi \cosh s\pi/2 \tag{3-62}$$

Introducing (3-62) in (3-60)we obtain

$$D(s) = \frac{A(s) - C(s)\cosh s\pi}{\sinh s\pi} \tag{3-63}$$

Therefore we have reduced the number of integral equations and unknowns from 4 to 2; A(s) and D(s) are known now. So the system of integral equations becomes,

$$\int_0^\infty \left\{ K_{is}(\gamma_2 r)\left[\cosh s\alpha - \frac{\cosh s\pi}{\sinh s\pi}\sinh s\alpha\right] C(s) - K_{is}(\gamma_1 r)\sinh s\alpha\; B(s)\right\} ds = \tag{3-64}$$

$$= \int_0^\infty \left[K_{is}(\gamma_1 r)\cosh s\alpha - K_{is}(\gamma_2 r)\frac{\sinh s\alpha}{\sinh s\pi}\right] A(s)\, ds = W(\gamma_1, \gamma_2, r)$$

$$\int_0^\infty s\left\{K_{is}(\gamma_2 r)\left[\sinh s\alpha - \frac{\cosh s\pi}{\sinh s\pi}\cosh s\alpha\right] C(s) - K_{is}(\gamma_1 r)\cosh s\alpha\; B(s)\right\} ds =$$

$$= \int_0^\infty s\left\{K_{is}(\gamma_1 r)\sinh s\alpha - K_{is}(\gamma_2 r)\frac{\cosh s\alpha}{\sinh s\pi}\right\} A(s)\, ds = V(\gamma_1, \gamma_2, r) \tag{3-65}$$

which can be written

$$W(\gamma_1,\gamma_2,\tau) = \int_0^\infty \left[K_{is}(\gamma_2\tau)\, g(s)\, C(s) - K_{is}(\gamma_1\tau) \sinh s\alpha \; B(s)\right] ds \tag{3-66}$$

$$V(\gamma_1,\gamma_2,\tau) = \int_0^\infty s\left[K_{is}(\gamma_2\tau)\, f(s)\, C(s) - K_{is}(\gamma_1\tau) \cosh s\alpha \; B(s)\right] ds \tag{3-67}$$

where

$$g(s) = \cosh s\alpha - \frac{\cosh s\pi}{\sinh s\pi} \sinh s\alpha \tag{3-68}$$

$$f(s) = \sinh s\alpha - \frac{\cosh s\pi}{\sinh s\pi} \cosh s\alpha \tag{3-69}$$

Now the Lebedev transform pair can be written

$$F(s) = \frac{2}{\pi^2}\int_0^\infty \frac{K_{is}(x)}{x} dx \int_0^\infty K_{is}(x)\, s \sinh s\pi \; F(s)\, ds$$

So that if we multiply (3-66) and (3-67) by $\frac{K_{is}(\gamma_1\tau)}{\tau}$ and integrate between o and ∞, we get

$$\int_0^\infty \frac{K_{is}(\gamma_1\tau)}{\tau} d\tau \int_0^\infty K_{is}(\gamma_2\tau)\, g(s) C(s)\, ds - \frac{\pi^2}{2}\frac{\sinh s\alpha}{s \sinh s\pi} B(s) = \int_0^\infty W(\gamma_1,\gamma_2,\tau)\frac{K_{is}(\gamma_1\tau)}{\tau} d\tau \tag{3-70}$$

$$\int_0^\infty \frac{K_{is}(\gamma_1\tau)}{\tau} d\tau \int_0^\infty s\, K_{is}(\gamma_2\tau)\, f(s)\, C(s)\, ds - \frac{\pi^2}{2}\frac{\cosh s\alpha}{\sinh s\pi} B(s) = \int_0^\infty V(\gamma_1,\gamma_2,\tau)\frac{K_{is}(\gamma_1\tau)}{\tau} d\tau \tag{3-71}$$

We are now in position of eliminating the functional B(s) between (3-70) and (3-71)

$$\int_0^\infty \frac{K_{is}(\gamma_1\tau)}{\tau}\,d\tau \int_0^\infty \left[s'\cosh s'\alpha\; g(s) - s\sinh s'\alpha\; f(s)\right] K_{is}(\gamma_2\tau)\, C(s)\, ds = \tag{3-72}$$

$$= \int_0^\infty \left[s'\cosh s'\alpha\; W(\gamma_1,\gamma_2,\tau) - \sinh s'\alpha\; V(\gamma_1,\gamma_2,\tau)\right] \frac{K_{is}(\gamma_1\tau)}{\tau}\,d\tau$$

Defining

$$h(s',s) = s'\cosh s'\alpha\; g(s) - s\sinh s'\alpha\; f(s) \tag{3-73}$$

$$l(s',s) = s'\cosh s'\alpha\; W(\gamma_1,\gamma_2,\tau) - \sinh s'\alpha\; V(\gamma_1,\gamma_2,\tau) \tag{3-74}$$

we write (3-72) as

$$\int_0^\infty \frac{K_{is}(\gamma_1\tau)}{\tau}\,d\tau \int_0^\infty h(s,s')\, K_{is}(\gamma_2\tau)\, C(s)\, ds = \int_0^\infty l(s';\gamma_1,\gamma_2,\tau)\,\frac{K_{is}(\gamma_1\tau)}{\tau}\,d\tau \tag{3-75}$$

The above integral equation will then be satisfied if

$$l(s';\gamma_1,\gamma_2,\tau) = \int_0^\infty h(s,s')\; K_{is}(\gamma_2\tau)\; C(s)\, ds \tag{3-76}$$

Using again the Lebedev transform pair (equation (3-33) and (3-34)) we solve integral equation (3-75) obtaining

$$C(s) = \frac{2}{\pi^2}\;\frac{s\sinh s\pi}{h(s)} \int_0^\infty \frac{l(s,\gamma_1,\gamma_2,\tau)}{\tau}\; K_{is}(\gamma_2\tau)\, d\tau \tag{3-77}$$

where we have dropped the subscripts of s' because now there is no need to distinguish one s from the other.

Following the same procedure as above, we may eliminate C(s) from equation (3-66) and (3-77) and get

$$B(s) = \frac{2}{\pi^2} \frac{s \sinh s\pi}{h^*(s)} \int_0^\infty \frac{l^*(s,\gamma_1,\gamma_2,r)}{r} K_{is}(\gamma_1 r)\, dr \tag{3-78}$$

with

$$h^*(s) = s \cosh s\alpha \; g(s') - s' f(s) \sinh s\alpha \tag{3-79}$$

$$l^*(s,\gamma_1,\gamma_2,r) = s' f(s')\, W(\gamma_1,\gamma_2,r) - g(s')\, V(\gamma_1,\gamma_2,r) \tag{3-80}$$

By substituting (3-62), (3-77) and (3-78) into (3-50) and (3-51) we obtain the solution to the problem of inclined layers in an explicit form,

$$u_1(r,\phi) = \frac{1}{\pi^2}\int_0^\infty K_{is}(\gamma_1 r)\left[u_0 \pi \cosh s\tfrac{\pi}{2} \cosh s\phi + \frac{2}{\pi^2} \frac{s \sinh s\phi \sinh s\pi}{h^*(s)} \int_0^\infty \frac{l^*(s,\gamma_1,\gamma_2,r)}{r} K_{is}(\gamma_1 r)\, dr\right] ds \tag{3-81}$$

$$u_2(r,\phi) = \frac{1}{\pi^2}\int_0^\infty K_{is}(\gamma_2 r)\left\{\left[\frac{2}{\pi^2}\left(\cosh s\phi - \frac{\cosh s\pi}{\sinh s\pi}\sinh s\phi\right)\frac{s \sinh s\pi}{h(s)} \int_0^\infty \frac{l(s,\gamma_1,\gamma_2,r)}{r} K_{is}(\gamma_2 r)\, dr \right. + \right.$$
$$\left.\left. + \left[\frac{u_0 \pi \cosh s\frac{\pi}{2} \sinh s\phi}{\sinh s\pi}\right]\right\} ds \tag{3-82}$$

The full expressions abbreviated by h*, l*, h and l are given respectively by (3-80), (3-81), (3-73) and (3-74).

Since in the next chapter we will study by a finite difference technique the response of arbitrary structures, including inclined layers, we will leave the solution of the general inclined layer problem in the integral form of equations (3-81) and (3-82).

CHAPTER IV

ARBITRARY TWO DIMENSIONAL GEOMETRIES

4.1 A finite difference approach

The difficulties associated with the inclined layer problem--the simplest problem with conductivity variation in two dimensions--give us an idea of the enormous mathematical obstacles which arise as soon as we depart from one dimensional variation of the electrical parameters. Further, as soon as we go beyond geometries which happen to coincide with coordinates systems in which the wave equation is separable, purely analytic solutions are generally impossible.

However, such complex phenomena are the rule in geophysics. This immediately suggests the use of something more versatile than analytic expressions, namely, finite differences. Plane wave problems in two dimensions are emminently suitable to treatment by such methods for several reasons. First, plane wave fields can be described by a scalar in two dimensions. Second, from the discussion in chapter 2.3, we know that this scalar is constant at the surface of the ground, enabling us to discuss the field in terms only of its behavior inside the earth. Since the electromagnetic field damps rather rapidly within the earth, attenuating quickly reflection and diffraction effects, a short distance from the disturbing region we find ourselves in a region where the waves behave like on a homogeneous medium (or like on a stratified medium or any sort of structure for which we know the analytic solution). These characteristics allow us to use finite difference nets which cover a relatively small space dimension.

In this manner, we can approximate the problem having boundaries at infinity by a perfectly determined boundary value problem with finite boundaries. The boundary values are that the field is constant at the earth's surface, zero at a finite depth and that it behaves in a known manner (like over a homogeneous or stratified earth) far away from the region of changing conductivity. Dirichlet inhomogeneous and homogeneous conditions are then given on a closed boundary, while across the boundaries of changing conductivity electromagnetic continuity conditions are to be upheld.

It is clear that with such a model, simple progression procedures cannot work properly. Rather, this is the type of finite difference problem for which relaxation methods are suited. The following sections develop a technique to handle by finite differences the Helmoltz equation with the application of the relaxation method to the resulting equation.

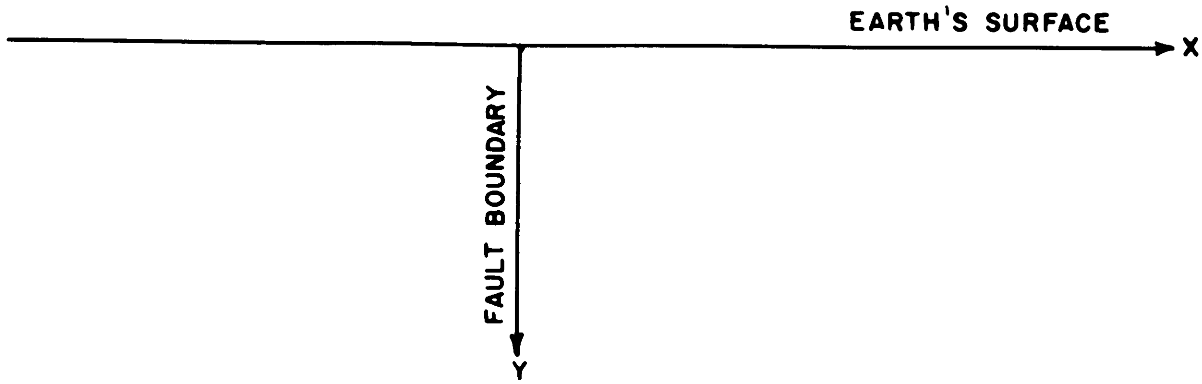

AN INFINITE BOUNDARY PROBLEM

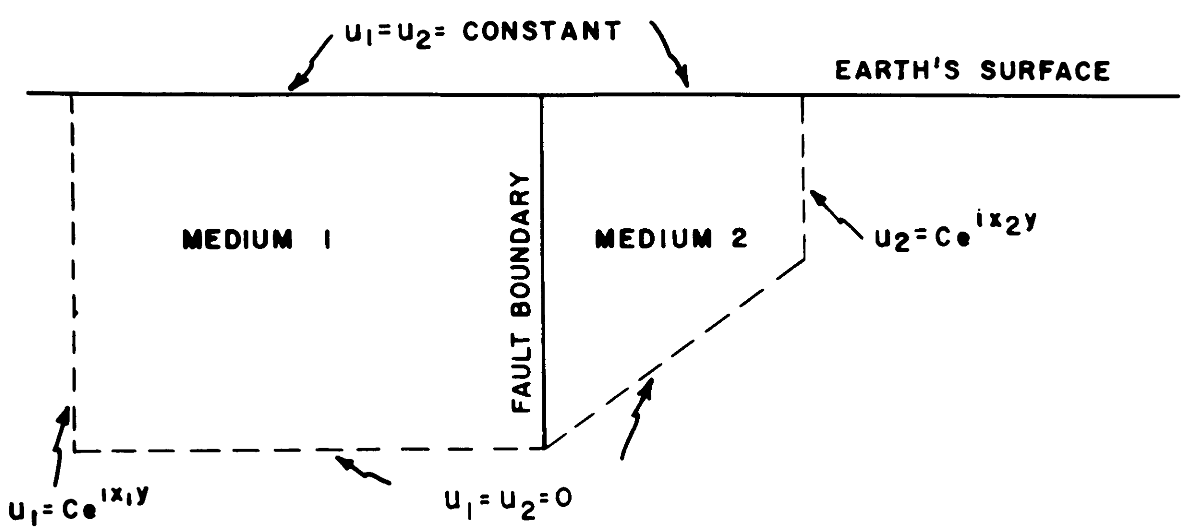

APPROXIMATION OF THE INFINITE BOUNDARY PROBLEM
BY A FINITE REGION WITH APPROPRIATE BOUNDARY VALUES

FIG. 4-1

4.2 The method of solution

The reduction of a problem involving infinite boundaries to a problem dealing with finite boundaries, involves certain approximations. In the present section, we will proceed to specify and justify these approximations.

We may start by recalling two characteristics of plane waves in the earth, discussed in section 2.3. First, in the case of a uniform earth, it was found that the electromagnetic waves propagated essentially vertically downward, no matter what the angle of incidence was. Second, for an earth having arbitrary two dimensional changes of conductivity, it was found that the electromagnetic field vector polarized along the strike of the structures would have a constant surface value. This polarized electromagnetic field vector is exactly the same vector which will be used to describe the field in finite differences, because its polarization allows it to be treated as a scalar. To these two properties of plane waves in the earth, we may add a third that results from the fact that the earth is a dissipative medium; namely, that the electromagnetic field will be attenuated exponentially with depth in a uniform earth. This is an extremely important characteristic because it guarantees the rather rapid damping in the earth of electromagnetic waves, which as we will see makes possible our method. (As referred previously the far away picture does not have to be that of a uniform earth. We adopt it here for simplicity of discussion, and because we are interested mostly in solving inclined layer problems. However, this is just a device to allow the specification of Dirichlet conditions necessary to make the problem definite. Any other appropriate set up could be used for the far away field).

Let us examine how we use the above properties to convert the infinite boundary problem into a finite boundary problem amenable therefore to finite difference techniques. The top boundary will be the earth's surface where we know that the polarized field assumes a constant value. The bottom boundary will be the depth for which the polarized field becomes exponentially "zero", to the order of significant figures carried in the computation. This bottom boundary does not have to be parallel to the earth's surface. It certainly won't be in cases of quarter spaces of different conductivities in contact, i.e. for faults and inclined beds. For such cases the lower boundary, which is characterized by the vanishing of the polarized field, may be assumed to be as pictured in fig. 4-1. The validity of this procedure is based on the fact, to be discussed in detail in section 4.5.3, that the near surface field (which is the one in which we are interested) is negligibly affected by the depth at which we assume it to "become zero", as long as at this depth $Kr \geq 4$. Finally as we go far away along the earth's surface from the region where the changes in conductivity occur, the field will tend to that of a uniform earth; in other words, the diffracted field is attenuated geometrically and by absorption away from the diffracting region and very soon becomes negligible compared with the incident field. The incident field will behave like

$$u = C e^{iKy} \tag{4-1}$$

at a point of the earth's surface infi·itely far away from the region of diffraction. Actually, the total field becomes essentially described by equation (4-1) at distances of only a few kr from the region of changing conductivity.

In this manner we have changed the infinite boundary problem into a finite boundary problem. The space under consideration is now the closed region bounded by the earth's surface, by the depth at which the field goes to zero within the accuracy of the calculation, and by the horizontal distance from the diffracting region at which the field becomes essentially described by a vertically propagating plane wave. At the top and lateral boundaries we have unhomogeneous Dirichlet conditions, at the bottom homogeneous Dirichlet conditions and across the bodies of different conductivities contained within the bounded region we will have to satisfy electromagnetic continuity conditions.

In order to obtain an idea of the distances along the surface for which the diffracted field becomes negligible, we will consider, say, a vertical fault separating regions of different conductivities. The argument could be carried for any two dimensional structure, but to make the exposition brief, we assume the geometric simplicity of a vertical fault. Now we know that the solution far away from the boundary is

$$\begin{aligned} u_1 &= C e^{iK_1 y} \qquad & x \longrightarrow -\infty \\ u_2 &= C e^{iK_2 y} \qquad & x \longrightarrow +\infty \end{aligned} \tag{4-2}$$

As we approach the fault boundary from $\pm\infty$ we come under the influence of diffraction effects. Diffraction effects behave very much like induced sources disposed along the fault boundary. These sources distort the simple uni-directional field of equation (4-2) and the field near the boundary becomes dependent on both x and y coordinates. Mathematically, this arises from the necessity of satisfying continuity conditions for E and H tangential at the boundary. The field in the diffraction region will have the general form

$$u(x,y) = M(x,y)\, e^{iw(x,y)}$$

Our concern therefore is to determine at what distance from the fault boundary equation (4-3) becomes equal to equation (4-2) within a specified order of accuracy. A way of obtaining a conservative estimate of such a distance is to consider the attenuation of a one dimensional wave, under the assumption that such wave is due to "sources" at the fault boundary. Referring to table I we note that for a distance x, such that $Re[Kx]=5$ the plane wave attenuates to 0.7% of the initial value; for another distance x, such that $Re[Kx]=7$ the plane wave amplitude reduces to 0.09% of the initial magnitude, and so on. Now, if the "sources" at the fault boundary produced a field of magnitude equal to that of the incident (primary) field, at this distance where $Re[Kx]=5$ the diffracted field would contribute slightly less than 0.7% of the total field; if we want farther away to x such that $Re[Kx]=7$, the contribution would be less than 0.09%. (We may note that the wave length of an electromagnetic wave corresponds to a distance for which $Re[Kx]$ is slightly larger than 6) All these estimates are conservative because in our problem the "sources" at the boundary will never create fields equal to the incident field. Further the "strength" of these "sources" is very likely to decrease in an approximately exponential manner with depth.

Using the criteria described above, we can safely choose a distance x, away from the fault boundary, where the diffraction field becomes zero to the order of accuracy carried; from such a distance out the field will behave uni-directionally as on a uniform, homogeneous earth. This will be the situation existing previous to the application of relaxation procedures to the problem. If indeed the choice is conservative after the solution by relaxation methods, the unidirectional behavior of the field will be extended some more towards the fault boundary, past the initial estimate.

Summarizing, the problem becomes that of finding the electromagnetic field throughout media 1 and 2, given

1) $u_1 = u_2 =$ constant for all x, at $y = 0$

2) $u_1 = u_2 = 0$ for all x, at a certain depth $y = y_1$

3) $u_1 = u_2$

$$\frac{1}{K_1^2}\frac{\partial u_1}{\partial x} = \frac{1}{K_2^2}\frac{\partial u_2}{\partial x} \qquad \frac{\partial u_1}{\partial x} = \frac{\partial u_2}{\partial x} \quad \text{at } x = 0$$

4) $u_1 = Ce^{iK_1 y}$ at $x = -x_1$ for all $y = 0$

5) $u_2 = Ce^{iK_2 y}$ at $x = x_2$ for all $y = 0$

This is the situation for a vertical fault at $x = 0$. For any other geometry the treatment is similarly straightforward

4.3 The Helmoltz equation in finite differences

4.3.1 The Helmoltz equation in homogeneous media

We will be dealing with phenomena obeying the Helmoltz equation

$$\nabla^2 u + \kappa^2 u = 0 \qquad (4\text{-}4)$$

where $\kappa^2 = i\mu\omega\sigma$, μ the magnetic permittivity, ω the radian frequency of the electromagnetic wave and σ the conductivity of the media. As usually we neglect displacement currents and sinusoidal time dependence $e^{-i\omega t}$ has been assumed.

In order to be able to treat the complex scalar u by finite differences, we obtain from (4-4) two equations dealing with real variables in the following way. Let $u = A + iB$

$$\nabla^2 (A + iB) + i\mu\omega\sigma\,(A + iB) = 0 \qquad (4\text{-}5)$$

from which we get by separating real and imaginary parts

$$\begin{aligned} \nabla^2 A - \mu\omega\sigma B &= 0 \\ \nabla^2 B + \mu\omega\sigma A &= 0 \end{aligned} \qquad (4\text{-}6)$$

These two coupled equations can be written in cartesian coordinates

$$\begin{aligned} \frac{\partial^2 A}{\partial x^2} + \frac{\partial^2 A}{\partial y} - \sigma\mu\omega B &= 0 \\ \frac{\partial^2 B}{\partial x^2} + \frac{\partial^2 B}{\partial y^2} + \mu\omega\sigma A &= 0 \end{aligned} \qquad (4\text{-}7)$$

To obtain the finite difference representation of these differential equations, we consider the representation of a function in a Taylor series about a point

$$f(\xi) = f(a) + \frac{(\xi - a) f'(a)}{1!} + \frac{(\xi - a)^2 f''(a)}{2!} + \cdots \tag{4-8}$$

Then for $f(a+h)$ and $f(a-h)$ (see diagram 4.2) we get, neglecting 4th and higher order terms

$$f''(a) = \frac{f(a+h) - 2f(a) + f(a-h)}{h^2} \tag{4-9}$$

Similarly, neglecting third order terms and higher, we obtain for the first derivative the expression

$$f'(a) = \frac{f(a+h) - f(a-h)}{2h} \tag{4-10}$$

Writing for the successive points in the x direction f_{m-1}, f_m and f_{m+1} instead of $f(a-h)$, $f(a)$ and $f(a+h)$, and for the points on the y direction f_{n-1}, f_n, f_{n+1} we can express (4-7) as

$$\frac{A_{m+1,n} - 2A_{m,n} + A_{m-1,n}}{h_x^2} + \frac{A_{m,n+1} - 2A_{m,n} + A_{m,n-1}}{h_y^2} - \mu\omega\sigma B_{m,n} = 0$$

$$\frac{B_{m+1,n} - 2B_{m,n} + B_{m-1,n}}{h_x^2} + \frac{B_{m,n+1} - 2B_{m,n} + B_{m,n-1}}{h_y^2} + \mu\omega\sigma A_{m,n} = 0 \tag{4-11}$$

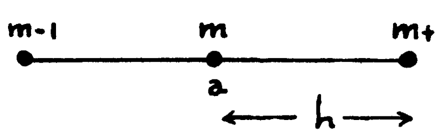

FIG. 4-2

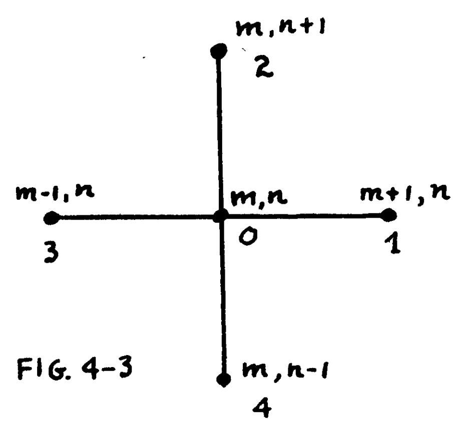

FIG. 4-3

If we let $h_x = h_y$, we can simplify the above equation to

$$A_{m+1,n} + A_{m-1,n} + A_{m,n+1} + A_{m,n-1} - 4A_{m,n} - \mu\omega\sigma h^2 B_{m,n} = 0$$
$$B_{m+1,n} + B_{m-1,n} + B_{m,n+1} + B_{m,n-1} - 4B_{m,n} + \mu\omega\sigma h^2 A_{m,n} = 0 \qquad (4\text{-}12)$$

If for easier reading we use subscripts 0, 1, 2, 3 and 4 instead of (m, n), (m+1, n), (m, n+1), (m-1, n) and (m, n-1) (see fig. 4-3) we rewrite equations (4-11) and (4-12) as

$$A_1 + A_2 + A_3 + A_4 - 4A_0 - \mu\omega\sigma h^2 B_0 = 0 \qquad (4\text{-}13)$$

$$B_1 + B_2 + B_3 + B_4 - 4B_0 + \mu\omega\sigma h^2 A_0 = 0 \qquad (4\text{-}14)$$

where the 5 first terms in each equation can be recognized as the Laplacian operator in finite differences. We see from (4-13) and (4-14) that at every point of the region under consideration, we have to satisfy a system of two finite difference equations in two unknowns. Consequently at every point of the finite difference net, we will have two solutions, one for A another for B.

The solution of the system of equations in A and B is not going to give us directly the quantities in which we are interested, that is, the components of the electromagnetic field. However, there is a simple relationship which we will show presently.

If we attempted to solve the problem analytically, we would express it in terms of the field component, E or H, which would be aligned parallel to the z axis (and parallel therefore to the generatrix of the geologic structure). This component would satisfy $\nabla^2 u + K^2 u = 0$ where k is complex, and the solution of this differential equation would be

$$u(x,y) = M(x,y)\, e^{iW(x,y)}$$

where M is the magnitude and W the phase angle of the field component.

In the finite difference set of equations we have an A and a B at every point of the net so that the solution is given by

$$u_{m,n} = A_{m,n} + i\, B_{m,n} \tag{4-16}$$

In order to relate the solution of the finite difference equations to that of the differential equation, it is sufficient to expand (4-15) and equate it to (4-16), from which we get

$$\begin{aligned} A_{m,n} &= M_{m,n} \cos W_{m,n} \\ B_{m,n} &= M_{m,n} \sin W_{m,n} \end{aligned} \tag{4-17}$$

We may note that the equality sign is not very rigorous insofar as the finite difference solution will always be slightly different from the differential solution, but we use it with this understanding. Therefore the magnitude and phase of the field component (E or H) at every point of the finite difference net will be given by

$$\begin{aligned} M_{m,n} &= \sqrt{A^2_{m,n} + B^2_{m,n}} \\ W_{m,n} &= \arctan \frac{B_{m,n}}{A_{m,n}} \end{aligned} \tag{4-18}$$

The other field component can be deduced from Maxwell's curl equations. As we have shown in 2.3 and 3.1, at the earth's surface the curl reduces, for both magnetic and electric polarizations, to the vertical derivative of the polarized field. Since our interest is basically in obtaining the non-polarized field at the surface, we will have to make sure that the finite difference solution pesesses a reliable vertical derivative, at least near the surface; this subject will be discussed further in an appropriate place.

4.3.2 Relaxation operators in homogeneous media

The unit relaxation operators corresponding to the Helmoltz equation are readily derived from equations (4-13) and (4-15) and are shown in fig. 4-4. As fig. 4-5 illustrates, each equation and operator possses one term in the plane of the variable not included in the Laplacian operator. Therefore a change in one of the variables, besides affecting its own Laplacian, is transmitted to the equation with the Laplacian in the other variable. Convergence in such a system can be delicate. From equation (4-13) and (4-14) we may note that this "feed-back" effect depends solely on $k^2 h^2$, a quantity which is the measure of fineness of the net. In general the convergence of the relaxation is slower the finer the net size. This is because, with decreasing net sizes, changes in one of the variables affects the equation with the Laplacian on the other variable increasingly less. It should not be thought though, that for differential intervals the coupling between the equation disappears completely; this is not so. Whatever the interval, as long as the relaxation process is far from the solution, although $k^2 h^2$ may be very small, the necessary change in the variable will be perforce large, cancelling thus the effect of weak coupling. The slowing down of convergence only comes in when we approach the solution and then there may be some tendency for oscillatory convergence.

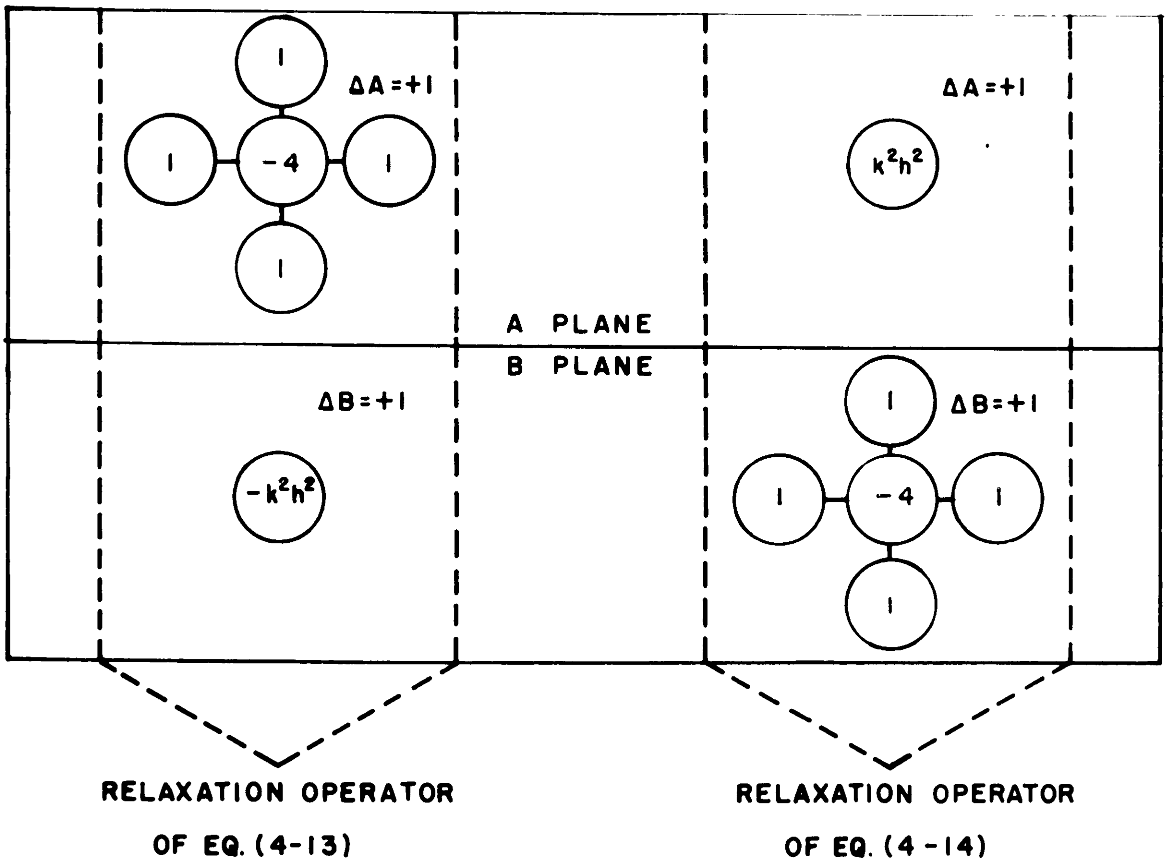

ΔA=+1
1
1
-4
1
1
ΔA=+1
k²h²
A PLANE
B PLANE
ΔB=+1
-k²h²
ΔB=+1
1
1
-4
1
1
RELAXATION OPERATOR
OF EQ. (4-13)
RELAXATION OPERATOR
OF EQ. (4-14)

FIG.4-4

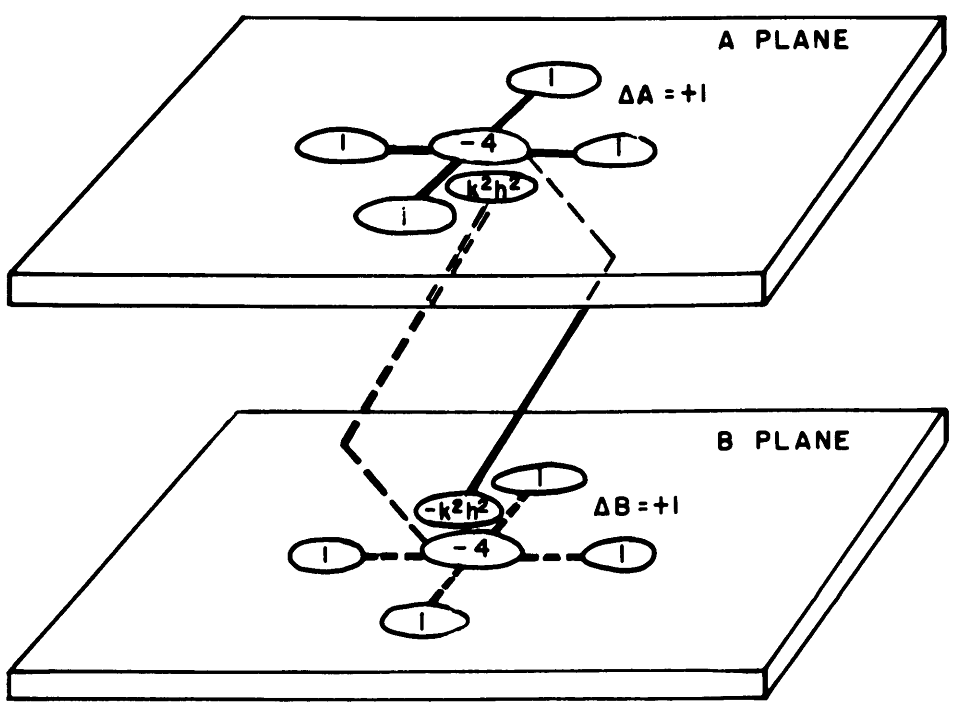

A PLANE
ΔA=+1
1
1
-4
1
1
k²h²
B PLANE
ΔB=+1
-k²h²
1
1
-4
1
1

FIG. 4-5

For large net sizes $(K^2h^2 \geqslant 2)$ the convergence is very fast because relaxation can be effected in a manner such that by the change of one variable we achieve liquidation of the residuals of both the A and B equations.

Up to this point we have been speaking of the simultaneous convergence of both equations. Yet we have also to consider the convergence of each equation per se, which becomes important as the coupling weakens, that is, as the net size becomes smaller. This type of convergence can be speeded up by the use of relaxation operators which operate mainly at the node, little affecting the neighboring points. Such procedure is sometimes called "block relaxation" and any block relaxation operator can be formed by superposition of the simple operators described by equation (4-13) and (4-14), and fig. 4-4. A rather convenient operator of this type is despicted in fig. 4-6. Generally, block relaxation is useful only when dealing with fine grids or media of low conductivity (in contrast with another of higher conductivity). Otherwise its cumbersomeness does not make up for the added speed.

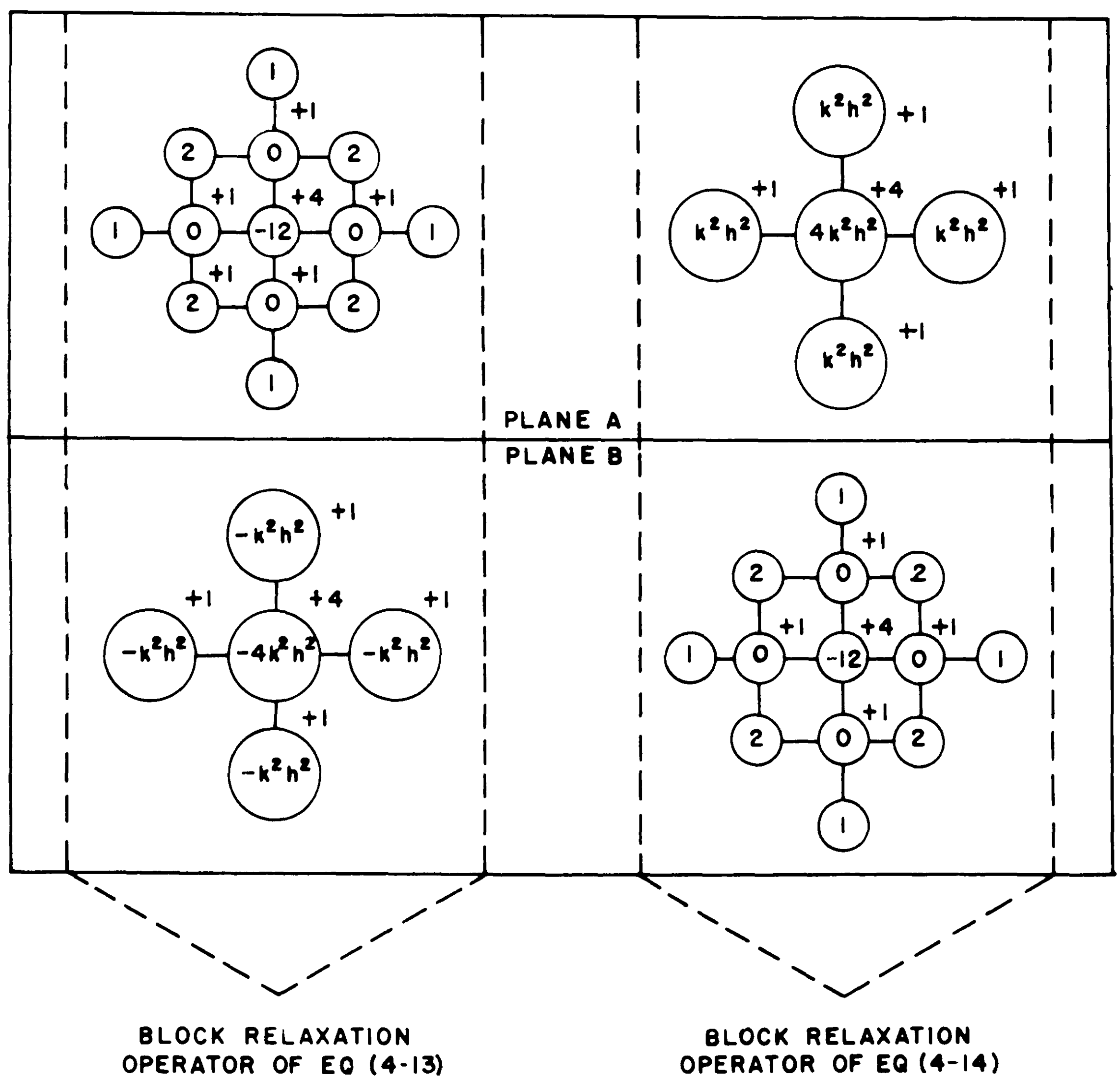

PLANE A
PLANE B
1
+1
2
0
2
+1
+4
+1
1
0
-12
0
1
+1
+1
2
0
2
1
k^2h^2
+1
+1
+4
+1
k^2h^2
$4k^2h^2$
k^2h^2
k^2h^2
+1
$-k^2h^2$
+1
+1
+4
+1
$-k^2h^2$
$-4k^2h^2$
$-k^2h^2$
+1
$-k^2h^2$
BLOCK RELAXATION
OPERATOR OF EQ (4-13)
BLOCK RELAXATION
OPERATOR OF EQ (4-14)

FIG 4-6

4.3.3 Relaxation operators for boundary conditions.

All the previous relaxation operators were developped for a homogeneous mediu. As such they cannot be used at boundaries of media of different electrical properties, where continuity of normal derivaties or of some multiple of the derivatives are required. This impossibility arises of course from the need to compute residuals at the boundary points, which would lead to the inclusion of a point beyond the region where the operator used is valid.

The problems in which we are interested deal with more than one medium. Since continuity of E and H tangential have to be satisfied at the boundaries of the media, and since in our formulation E or H can be obtained as derivatives of H or E, every problem to be considered will involve continuity of derivative conditions. In order to exemplify the procedure used to find the relaxation operators valid at boundaries, we will present the development of two important types of boundary operators: operators for straight boundaries (coinciding with nodes) and operators for boundaries in the shape of a corner.

a. relaxation operator for the straight boundaries

As an illustration of the changes undergone by the operators of equation (4-13) and (4-14) at a straight boundary coinciding with the nodes, we will consider a vertical boundary between two media. Let us say that the electromagnetic field is magnetically polarized, so our scalar component is the magnetic field. We may notice that this is the type of boundary operator for the problem of vertical layers or fault. As seen previously in that problem we need not consider the boundary the earth's surface. There, the specification of a constant polarized field, implies no vertical component of the non-polarized field vector, so that one boundary value actually satisfied both electric and magnetic boundary conditions. The continuity conditions are to be used at the interval boundaries of the bounded region, namely at the vertical interface.

The conditions, in the case of magnetic polarization are

$$u_1 = u_2$$

$$\frac{1}{K_1^2}\frac{\partial u_1}{\partial x} = \frac{1}{K_2^2}\frac{\partial u_2}{\partial x}$$

where $K_j^2 = i\mu\omega\sigma_j$ (for electric polarization simple equality of normal derivatives is required)

Let us first consider the continuity of multiples of the normal derivatives

$$i\mu\omega\sigma_{(2)}\left[\frac{\partial A^{(1)}}{\partial x} + i\frac{\partial B^{(1)}}{\partial x}\right] = i\mu\omega\sigma_{(1)}\left[\frac{\partial A^{(2)}}{\partial x} + i\frac{\partial B^{(2)}}{\partial x}\right]$$

or

$$K_{(2)}^2\frac{\partial A^{(1)}}{\partial x} = K_{(1)}^2\frac{\partial A^{(2)}}{\partial x} \qquad K_{(2)}^2\frac{\partial B^{(1)}}{\partial x} = K_{(1)}^2\frac{\partial B^{(2)}}{\partial x}$$

where $K^2 = \mu\omega\sigma$, and also where the superscripts or subscripts in parentheses indicate the medium in which the function is defined. In finite differences, we write the above equations as

$$K_{(2)}^2\left(A_1^{(1)} - A_3^{(1)}\right) = K_{(1)}^2\left(A_1^{(2)} - A_3^{(2)}\right) \tag{4-19}$$

$$K_{(2)}^2\left(B_1^{(1)} - B_3^{(1)}\right) = K_{(1)}^2\left(B_1^{(2)} - B_3^{(2)}\right) \tag{4-20}$$

Fig. 4-7 shows the position in the finite difference and indicated by the subscripts 1, 2, 3, 4. Clearly then $A_1^{(1)}$, $B_1^{(1)}$ and $A_3^{(2)}$ and $B_3^{(2)}$ are ficticious points, that is, they are not in the region where the functions $u^{(1)}$ and $u^{(2)}$ are defined, respectively.

Recalling the expression for the Helmoltz equation in homogeneous media

$$\begin{aligned} &A_1^{(1)}+A_2^{(1)}+A_3^{(1)}+A_4^{(1)}-4A_0^{(1)}-K_{(1)}^2h^2B_0^{(1)}=0 \\ &B_1^{(1)}+B_2^{(1)}+B_3^{(1)}+B_4^{(1)}-4B_0^{(1)}+K_{(1)}^2h^2A_0^{(1)}=0 \end{aligned} \qquad \text{medium 1} \qquad (4\text{-}21)$$

$$\begin{aligned} &A_1^{(2)}+A_2^{(2)}+A_3^{(2)}+A_4^{(2)}-4A_0^{(2)}-K_{(2)}^2h^2B_0^{(2)}=0 \\ &B_1^{(2)}+B_2^{(2)}+B_3^{(2)}+B_4^{(2)}-4B_0^{(2)}+K_{(2)}^2h^2A_0^{(2)}=0 \end{aligned} \qquad \text{Medium 2} \qquad (4\text{-}22)$$

we elliminate between equations (4-19), (4-20) and (4-21), (4-22) the ficticious points $A_1^{(1)}$, $B_1^{(1)}$, $A_3^{(2)}$ and $B_3^{(2)}$ (Southwell, 1946; Allen, 1954) obtaining

$$\begin{aligned} &K_{(2)}^2\left(4A_0^{(1)}+K_{(1)}^2h^2B_0^{(1)}-A_2^{(1)}-A_4^{(1)}-2A_3^{(1)}\right)=K_{(1)}^2\left(2A_1^{(2)}+A_2^{(2)}+A_4^{(2)}-4A_0^{(2)}-K_{(2)}^2h^2B_0^{(2)}\right) \\ &K_{(2)}^2\left(4B_0^{(1)}-K_{(1)}^2h^2A_0-B_2^{(1)}-B_4^{(1)}-2B_3^{(1)}\right)=K_{(1)}^2\left(2B_1^{(2)}+B_2^{(2)}+B_4^{(2)}-4B_0^{(2)}+K_{(2)}^2h^2A_0^{(2)}\right) \end{aligned} \qquad (4\text{-}23)$$

The additional conditions specifying the continuity of tangential H require

$$\begin{aligned} A_0^{(1)} &= A_0^{(2)} & \qquad B_0^{(1)} &= B_0^{(2)} \\ A_2^{(1)} &= A_2^{(2)} & \qquad B_2^{(1)} &= B_2^{(2)} \\ A_4^{(1)} &= A_4^{(2)} & \qquad B_4^{(1)} &= B_4^{(2)} \end{aligned} \qquad (4\text{-}24)$$

at the boundary. This reduces equati n (4-23) to

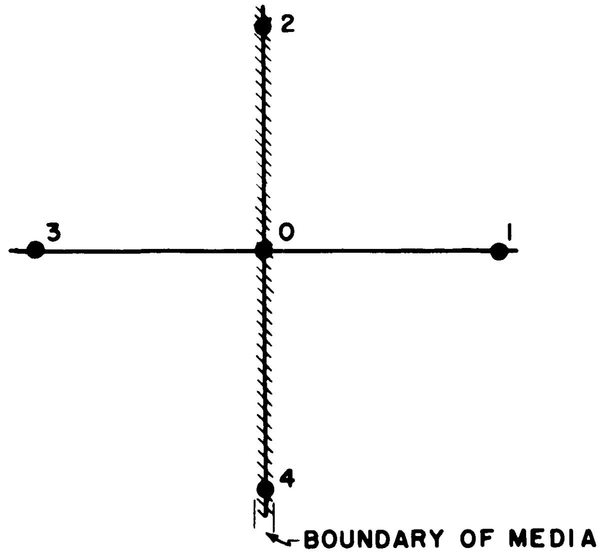

STRAIGHT BOUNDARY

FIG. 4-7

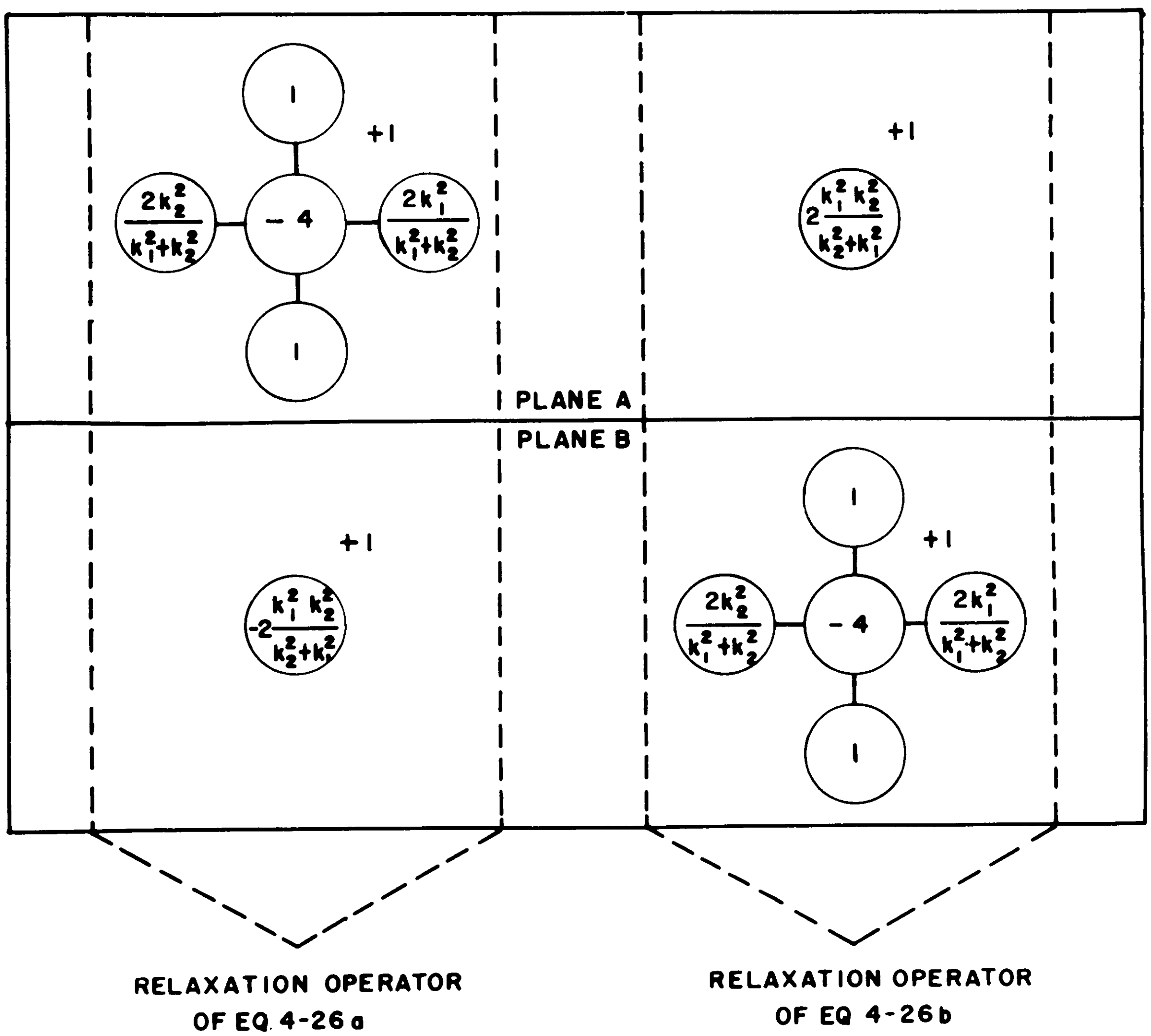

FIG. 4-8

$$4A_0(K_{(2)}^2+K_{(1)}^2)+2K_{(2)}^2K_{(1)}^2h^2B_0-(K_{(1)}^2+K_{(2)}^2)A_2-(K_{(1)}^2+K_{(2)}^2)A_4-2K_{(2)}^2A_3^{(1)}-2K_{(1)}^2A_1^{(2)}=0$$

(4-25)

$$4B_0(K_{(2)}^2+K_{(1)}^2)-2K_{(2)}^2K_{(1)}^2h^2A_0-(K_{(1)}^2+K_{(2)}^2)B_2-(K_{(1)}^2+K_{(2)}^2)B_4-2K_{(2)}^2B_3^{(1)}-2K_{(1)}^2B_1^2=0$$

where the components without supercripts (or subscripts) in parentheses are understood to be at the boundary of the medium. We may write equations (4-25) in a more familiar form

$$\frac{2K_{(1)}^2}{K_{(2)}^2+K_{(1)}^2}A_1^{(2)}+A_2+\frac{2K_{(2)}^2}{K_{(2)}^2+K_{(1)}^2}A_3^{(1)}+A_4-4A_0-\frac{2K_{(1)}^2K_{(2)}^2h^2}{K_{(1)}^2+K_{(2)}^2}B_0=0$$

(4-26)

$$\frac{2K_{(1)}^2}{K_{(2)}^2+K_{(1)}^2}B_1^{(2)}+B_2+\frac{2K_{(2)}^2}{K_{(2)}^2+K_{(1)}^2}B_3^{(1)}+B_4-4B_0+\frac{2K_{(1)}^2K_{(2)}^2h^2}{K_{(1)}^2+K_{(2)}^2}A_0=0$$

Considering equation (4-26) we see that the first row of nodes adjacent to the boundaries is affected by the weighing factor of the normal components of the Laplacian. Therefore, in order to keep the operators of this transitional nodes consistents we must also weigh one of the components of their Laplacian. From (4-26) and (4-21), (4-22) it is easily deduced that the operator for the row of adjacent nodes will be in medium 1

$$\sum_{i=2}^{4}A_i^{(1)}+\frac{2K_{(2)}^2}{K_{(1)}^2+K_{(2)}^2}A_1^{(1)}-4A_0^{(1)}-K_{(1)}^2h^2B_0^{(1)}=0$$

(4-29)

$$\sum_{i=2}^{4}B_i^{(1)}+\frac{2K_{(2)}^2}{K_{(1)}^2+K_{(2)}^2}B_1^{(1)}-4B_0+K_{(1)}^2h^2A_0^{(1)}=0$$

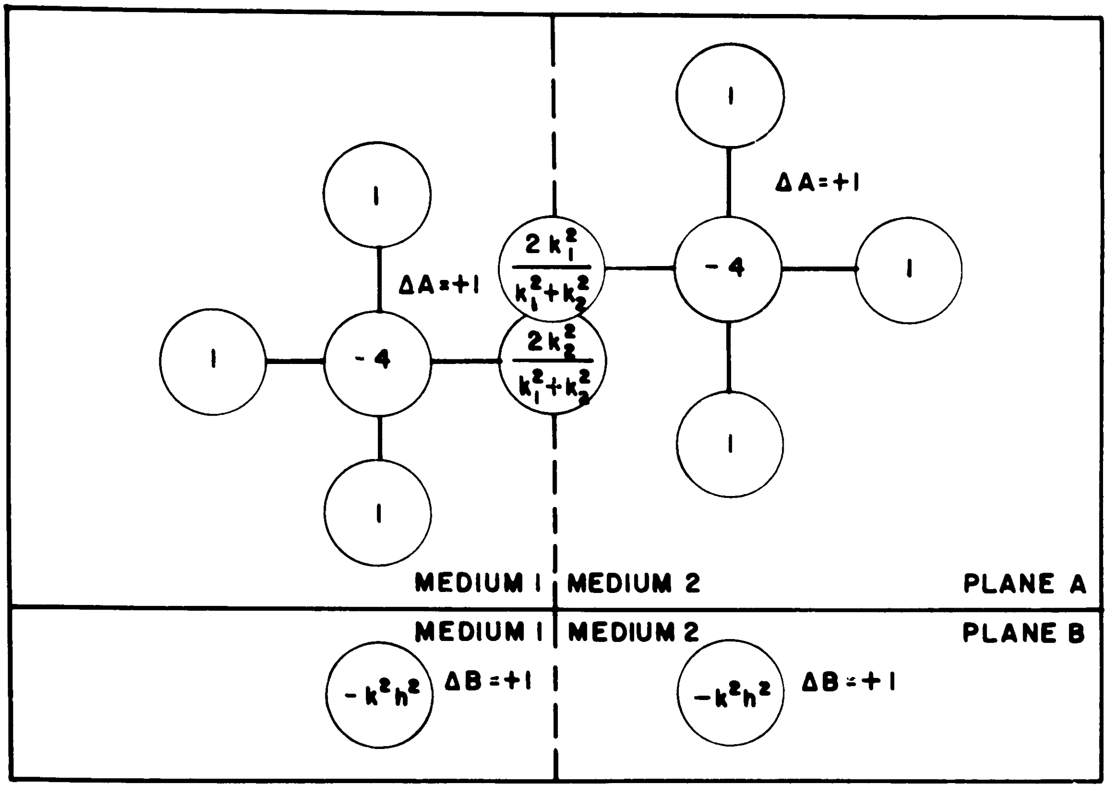

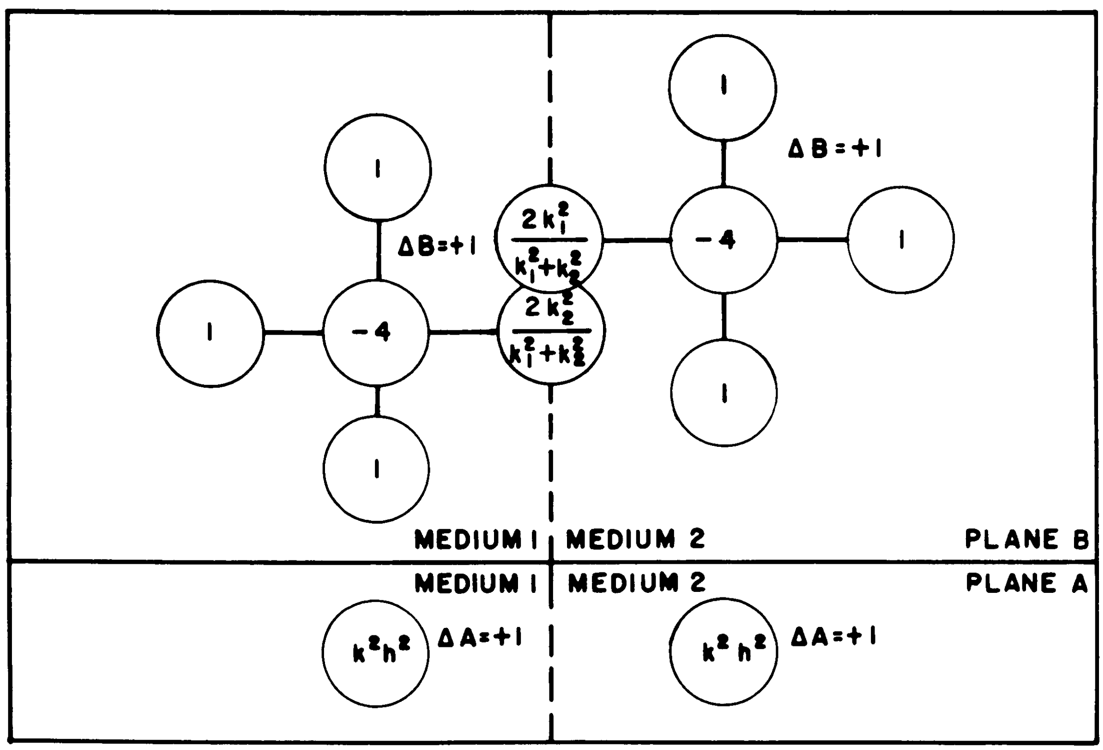

RELAXATION OPERATORS AT NODES ADJACENT TO BOUNDARIES

EQ (4-27) AND (4-28)

FIG. 4-9

and for medium 2

$$A_1^{(2)} + A_2^{(2)} + A_4^{(2)} + \frac{2K_{(1)}^2}{K_{(1)}^2 + K_{(2)}^2} A_3 - 4A_o - K_{(2)}^2 h^2 = 0$$

$$B_1^{(2)} + B_2^{(2)} + B_4^{(2)} + \frac{2K_{(1)}^2}{K_{(1)}^2 + K_{(2)}^2} B_3 - 4B_o + K_{(2)}^2 h^2 = 0 \qquad (4\text{-}28)$$

The graphical pattern of these operators is despicted in fig. 4-9.

b. relaxation operators at right angle wedge shaped boundaries

The right angle wedge shaped boundary is very useful in the idealization of buried structures, i.e. finite bodies of rectangular shape, dikes, step like structures (which could be used to study the effects of roots of mountains or the effect of abrupt change in depth from an oceanic to a continental crust), etc. We will show presently that a possible type of operator for such "corner" points is one that probably could be written down intuitively from the results for the straight line boundary.

If we assume again that we are dealing with magnetic polarization and considering now fig. 4-10, we see that at point 0 we have to satisfy

$$K'^2 \frac{\partial A}{\partial \eta} = K^2 \frac{\partial A'}{\partial \eta}$$

$$K'^2 \frac{\partial B}{\partial \eta} = K^2 \frac{\partial B'}{\partial \eta}$$

as well as continuity of A and B. But from the chain rule for partial derivatives and from the type of symmetry under consideration, we also have

$$\frac{\partial u}{\partial \eta} = \frac{\partial u}{\partial x}\frac{\partial x}{\partial \eta} + \frac{\partial u}{\partial y}\frac{\partial y}{\partial \eta} = \frac{\partial u}{\partial x} - \frac{\partial u}{\partial y}$$

where u stands for any of the field components A, A$'$, B, or B$'$; then we can express the boundary condition in finite differences as

$$\begin{aligned} K'^2\left[A_1 - A_3 - A_2 + A_4\right] &= K^2\left[A_1' - A_3' - A_2' + A_4'\right] \\ K'^2\left[B_1 - B_3 - B_2 + B_4\right] &= K^2\left[B_1' - B_3' - B_2' + B_4'\right] \end{aligned} \tag{4-29}$$

From the Helmoltz equation for homogeneous media

$$\begin{cases} HA - K^2 h^2 B_0 = 0 \\ HB + K^2 h^2 A_0 = 0 \end{cases} \qquad \begin{cases} HA' - K'^2 h^2 B_0 = 0 \\ HB' + K'^2 h^2 A_0 = 0 \end{cases}$$

we have that

$$\begin{aligned} -(A_3' + A_2') &= A_1' + A_4' - 4A_0 - K'^2 h^2 B_0 \\ (A_1 + A_4) &= -A_2 - A_3 + 4A_0 + K^2 h^2 B_0 \end{aligned}$$

and similarly for B and B$'$. Substituting this back into equation (4-29) we get

$$\begin{aligned} &\frac{2K^2}{K'^2+K^2}A_1 + \frac{2K'^2}{K'^2+K^2}A_2 + \frac{2K'^2}{K'^2+K^2}A_3 + \frac{2K^2}{K'^2+K^2}A_4 - 4A_0 - \frac{2K^2K'^2}{K'^2+K^2}h^2B_0 = 0 \\ &\frac{2K^2}{K'^2+K^2}B_1 + \frac{2K'^2}{K'^2+K^2}B_2 + \frac{2K'^2}{K'^2+K^2}B_3 + \frac{2K^2}{K'^2+K^2}B_4 - 4B_0 + \frac{2K^2K'^2}{K'^2+K^2}h^2A_0 = 0 \end{aligned} \tag{4-30}$$

These operators are shown in fig. 4-11. At the adjacent nodes 1, 2, 3 and 4 , the regular operators will have also to be modified in a

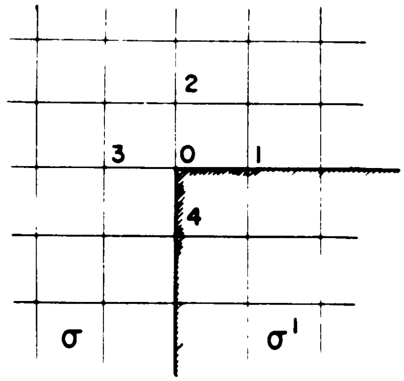

RIGHT ANGLE WEDGE BOUNDARY

FIG. 4-10

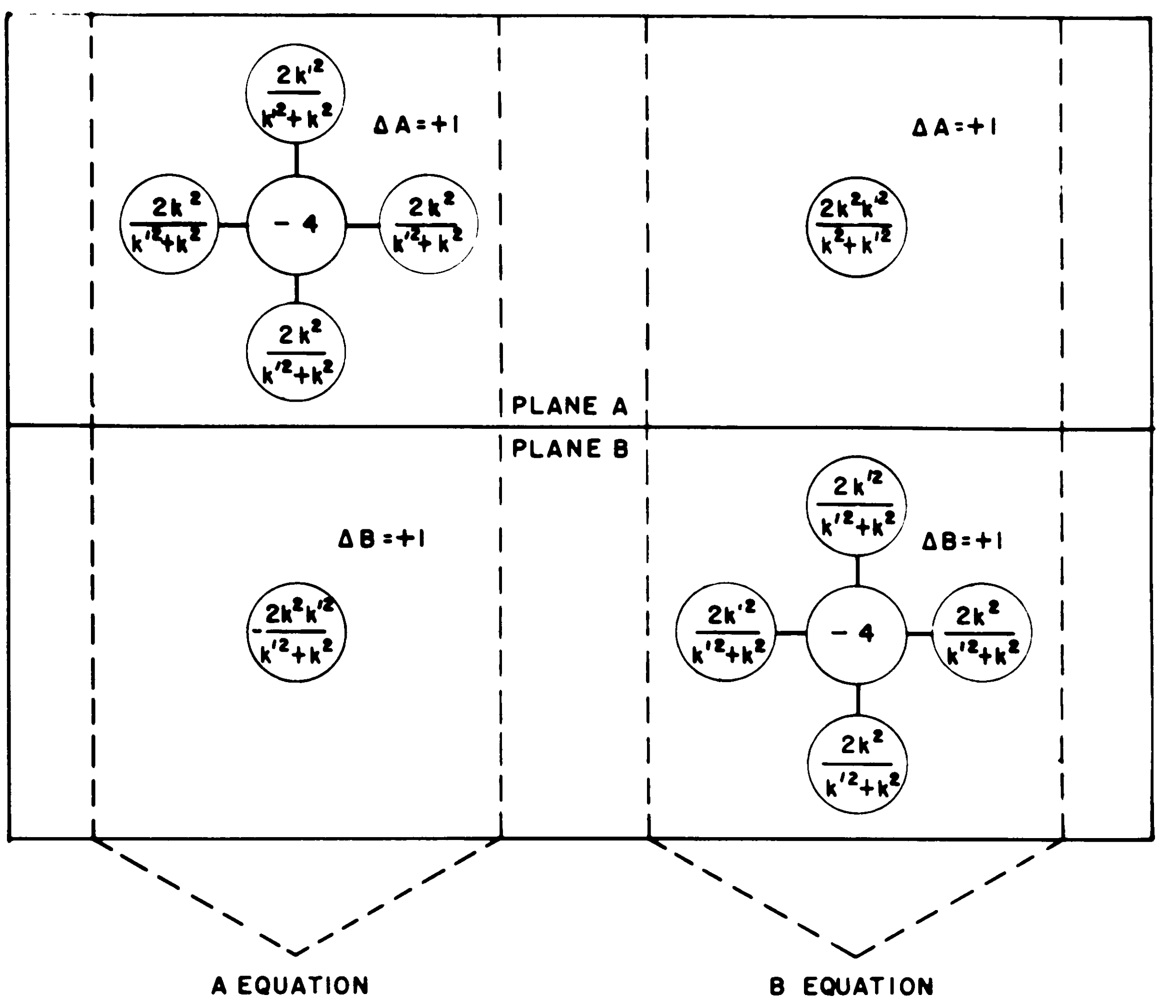

RELAXATION OPERATOR AT CORNER POINT

FIG. 4-11

manner similar to that illustrated by equations (4-27) and (4-28) in the case of straight boundaries.

4.3.4 Graded nets

The problem in which we are interested will commonly deal with two regions between which there will be a sharp contrast in electrical properties. As a result, in one of the media, or even in part of one and the whole region of the other we may have to describe the field by closer nets in order to obtain a sufficiently accurate solution. A way of making the transition from a coarser to a finer net is by the use of the so-called graded net technique (Southwell 98, 1946; Allen 69, 1954)

We will make the transition usually away from the effect of boundary operators and in the media where the solution is more accurate (by reason of the finer net size). In this manner we will minimize the inaccuracies due to finite difference approximation.

The manner in which the change in spacing is accomplished is illustrated in fig. 4-12; for the coarse grid the finite difference equations are known to be

$$\begin{aligned} HA - k^2h^2B_o &= 0 \\ HB + k^2h^2A_o &= 0 \end{aligned} \qquad (4\text{-}31)$$

where H denotes the Laplacian operator. For the finer grid the above equations are altered to the extent that instead of h we have h/2. Consequently in the region with smaller grid spacing, we have

$$HA - \frac{k^2h^2}{4} B_o = 0 \qquad (4\text{-}32)$$

$$HB + \frac{k^2h^2}{4} A_o = 0$$

Equations (4-31) and (4-32) refer then to the nodes marked □ and ● respectively. To write the equations for the intermediate nodes, we invoke the property of invariance of the operator ∇^2 with respect to a rotation of the axes of coordinates. Since at these intermediate nodes (denoted by O in fig. 4-12) the spacing is $h/\sqrt{2}$, their finite difference equations are

$$HA - \frac{k^2h^2}{2} B_o = 0 \qquad (4\text{-}33)$$

$$HB + \frac{k^2h^2}{2} A_o = 0$$

Although the above equations would correspond to the solutions of the Helmoltz equation in homogeneous regions composed exclusively of nodes like □ , ● and O, the fact that we are dealing with a transition region introduces nodes where careful application of the above operators is necessary. We have to keep in mind that the unit operator at a given node will be affected by all other nodes in the calculation of which residuals it enters. Consider for example, the node called A in fig. 4-12. Equations (4-31), (4-32) and (4-33) show that this node enters in the calculation of residuals at nodes B and C. Accordingly, the relaxation operator at A will contain points B and C as shown in fig. 4-13. The same applies for nodes like B, C, D, E and F which have the relaxation operators shown in figs. 4-15 to 4-18. All other nodes will

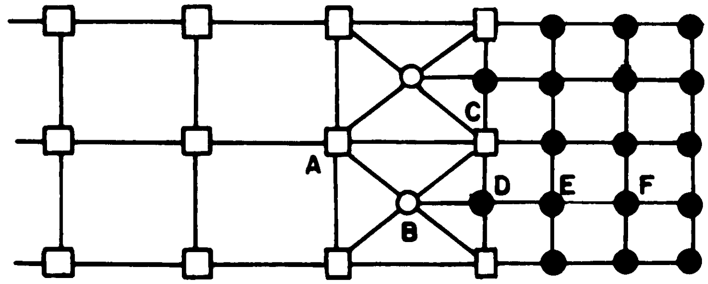

GRADED NET.

FIG. 4-12

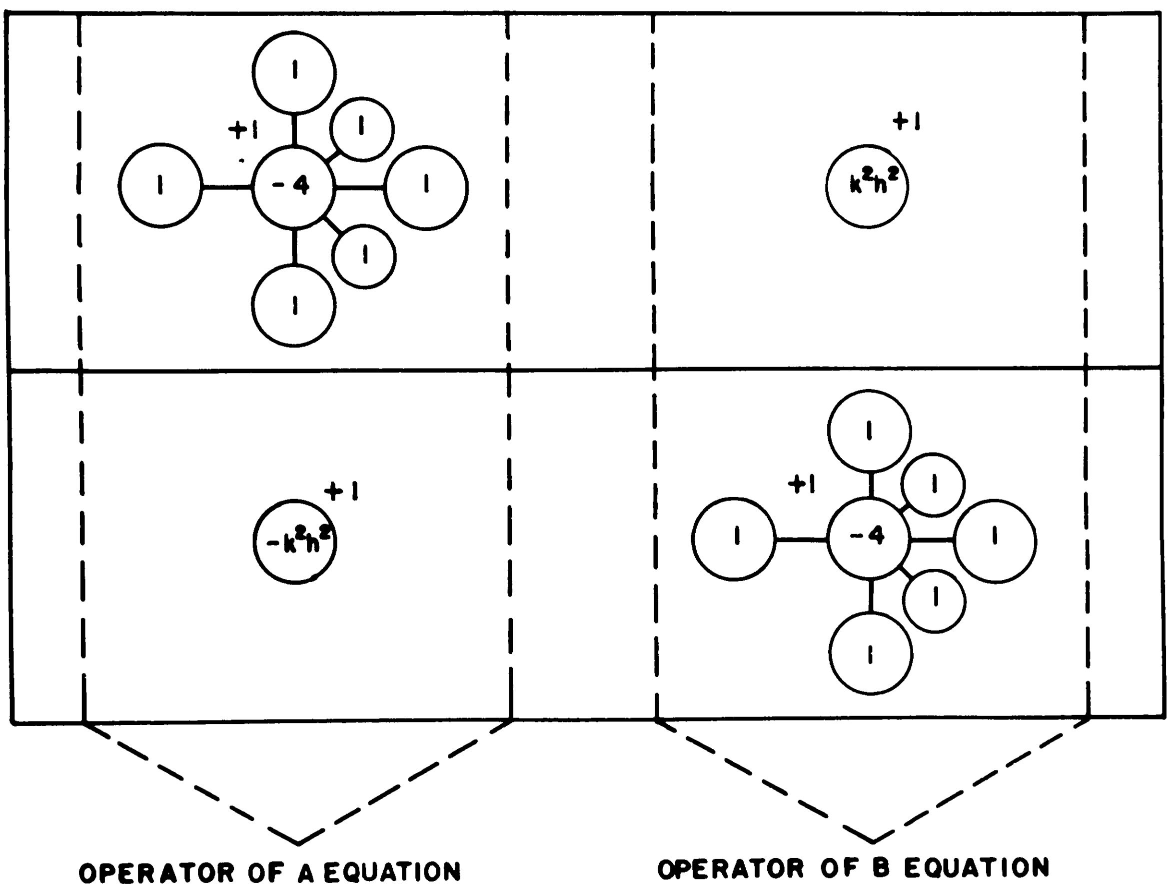

RELAXATION OPERATORS AT NODE A

FIG. 4-13

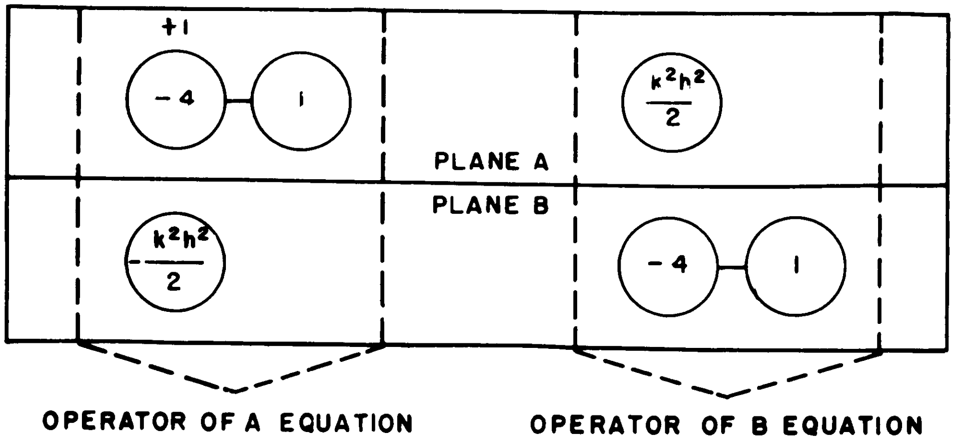

RELAXATION OPERATOR AT NODE B

FIG 4-14

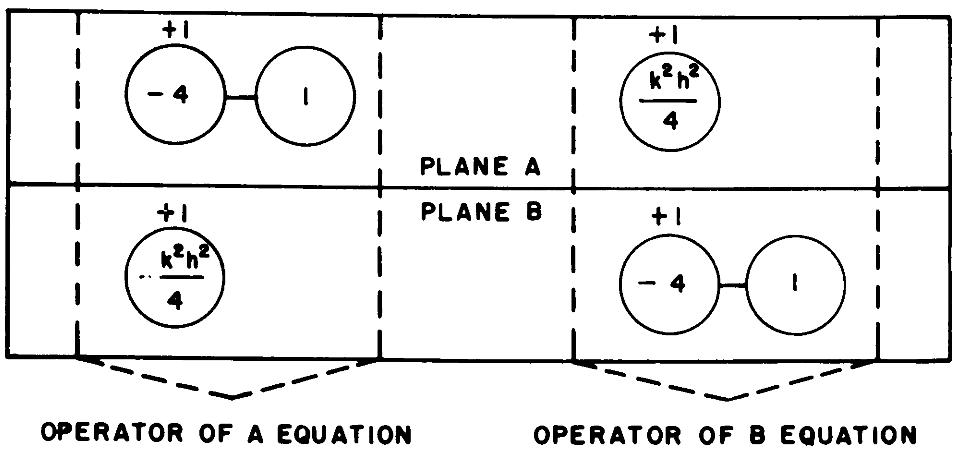

RELAXATION OPERATOR AT NODE D

FIG 4-15

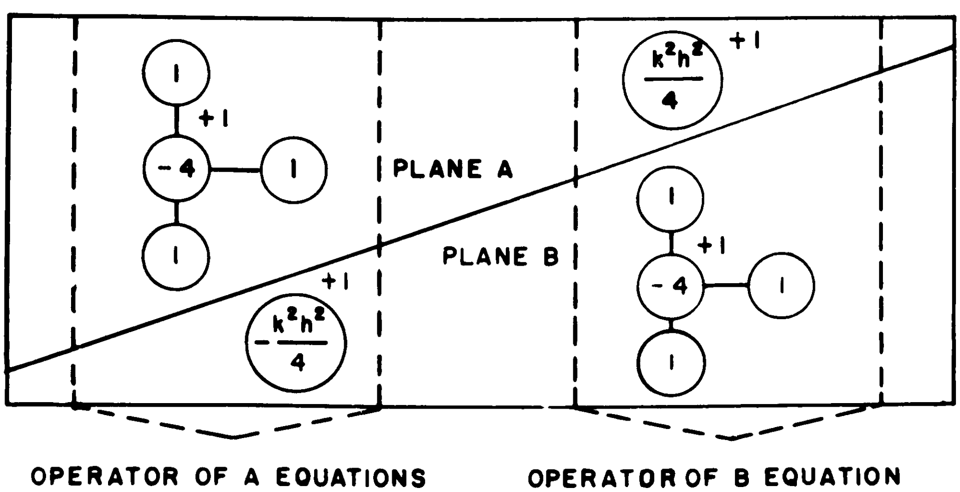

RELAXATION OPERATOR AT NODE E

FIG 4-16

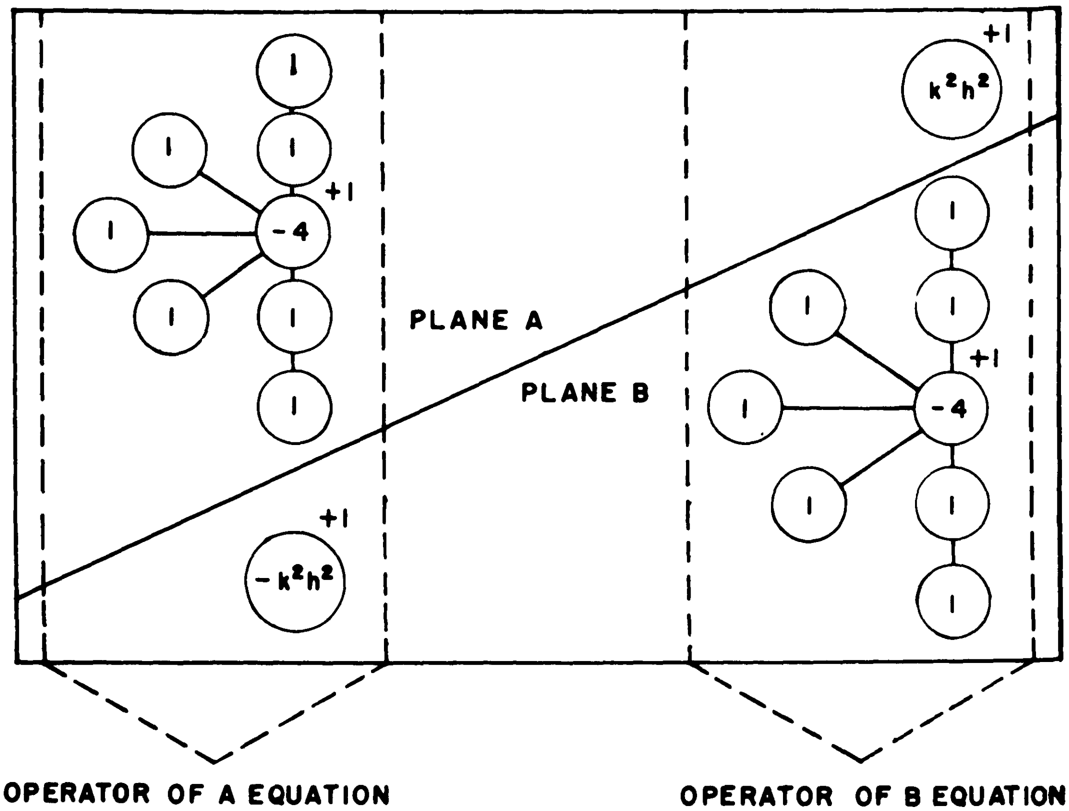

RELAXATION OPERATOR AT NODE C

FIG. 4-17

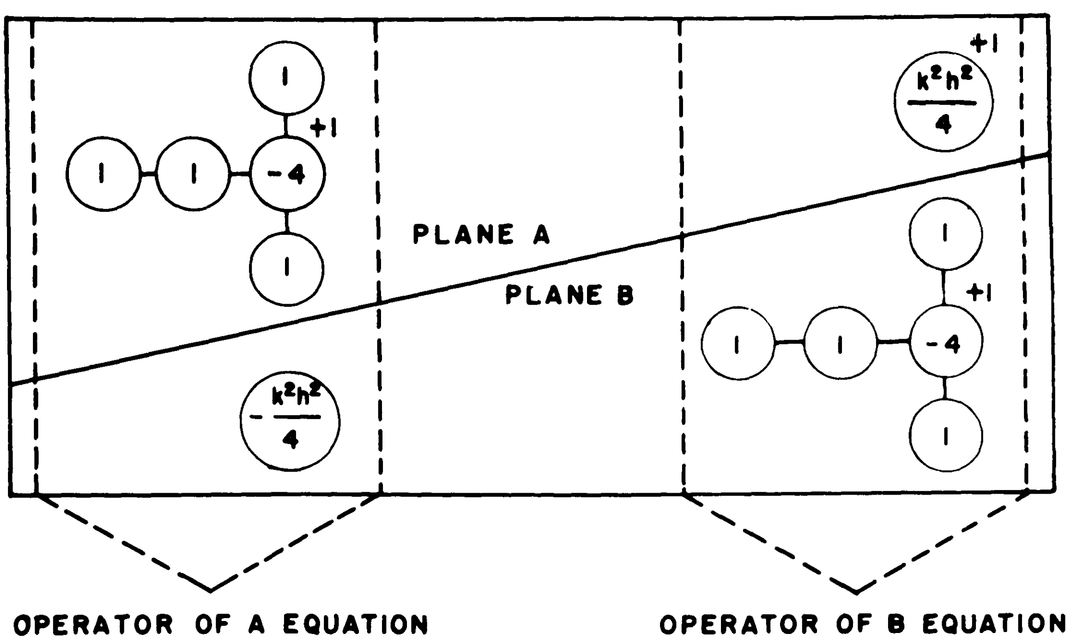

RELAXATION OPERATOR AT NODE F

FIG. 4-18

have either the coarse net operator of equation 4-31 or the finer net operator of equation (4-32)

The technique illustrated here for a change of net size starting at a straight vertical line of nodes can be easily adapted to horizontal line of nodes or extended to a two dimensional change of net size, i.e. when the transition line is a right angle corner.

4.3.5 Propagation constant and node separation

In problems of potential theory, which are the most commonly solved by finite differences, one gets used to have the node separation solely dependent on h. In problems involving the electromagnetic low frequency Helmoltz equation, the size of a finite difference net is tied down to the propagation constant as well as to the quantity h. Abbreviating the Laplacian operator by

$$Hu = \sum_{i=1}^{4} u_i - 4u_0$$

We write the Helmoltz equation as

$$HA - k^2h^2 B_0 = 0$$

$$HB + k^2h^2 A_0 = 0$$

It is of course the dimensionless quantity $k^2 h^2$, which is analogous to the differential $(kx)^2$ or $(kr)^2$, that dictates the node separation. As we have seen previously, the Helmoltz equation assumes the above form for equidimensional x and y separations. If, for example $k^2 h^2 = 2$, solving for h we have $h = \sqrt{2}/k$, which is the expression for the skin depth (see equation 2-5). The node separation in this case is equal to the skin depth or slightly less than a sixth of the wavelength. It is interesting to note how the finite difference formulation brings out the importance of the quantity kh. This is very closely related to the ideas of electrodynamic similitude discussed in next section.

4.4 Generality of the finite difference solution.

In obtaining finite difference solutions, which are on the form of contour maps of the function being investigated, one is interested in knowing how general a given solution is. Does it hold for all frequencies and inductivities? How do we convert from one conductivity to the other? What restrictions must be obeyed? And so on. Clearly this can be studied by the use of the concepts of electrodynamic similitude (Stratton, 488, 1941; Cagniard, 1953; Sinclair, 1948)

In general a given solution is valid for all similar geometries provided certain relationships are upheld in going from structure to structure. These can be easily deduced if we consider two structures, which are geometrically similar; then an electromagnetic field in one of the structures is described by

$$\nabla^2 \overline{\Pi} + K^2 \overline{\Pi} = 0 \tag{4-34}$$

whereas in the other structure we will have

$$\nabla^2 \overline{\Pi}' + K'^2 \overline{\Pi}' = 0 \tag{4-35}$$

Π being the Hertz vector. One aim is to investigate how the quantities involved can be changed in one of the structures while keeping $\overline{\Pi}$ and $\overline{\Pi}'$ at corresponding points of both structures invariant.

Equations (4-34) and (4-35) contain three variable quantities namely time, length and conductivity. (We are assuming the magnetic permeability, μ constant.) Let us suppose that they are related from one structure to the other by the constants of proportionality K_T, K_L, K_σ that is

$$L' = K_L L$$
$$\sigma' = K_\sigma \sigma$$
$$T' = K_T T$$

where L is the length dimension, σ the conductivity dimension and T the time dimension. Substituting these relationships into (4-35) we get

$$\nabla^2 \overline{\Pi}' + \left(\frac{K_L^2 K_\sigma}{K_T}\right) K^2 \overline{\Pi}' = 0$$

So that, in order to preserve invariance of $\overline{\Pi}$ and $\overline{\Pi}'$ we need to keep

$$K_T = K_L^2 K_\sigma$$

This fundamental relationship for electrodynamic similitude when displacement currents are negligible, also tells us that if we are dealing with a geometry having components of different conductivities, the ratios of the conductivities in one of the structures have to be equal to the ratio of conductivities in the other structure; only in this way invariance can be preserved.

Therefore, in the general case, we can transform a given finite difference solution to a different size, conductivity or frequency by applying equation (4-36); if the problem concerns a structure having regions of different conductivities, the conductivity contrasts have to be kept during the transformation.

However, in geometries without finite dimensions, the finite difference solution is much more general. Such geometries are of great importance in geology because they comprehend faults and dipping beds, a rather common feature. In effect, since these geologic features, from the analytic standpoint, do not have finite boundaries, only semi-infinite ones, from a dimensional point of view, there is no way of fixing the length scale without bringing the electromagnetic wave for comparison. In other words, in a semi-infinite structure, the conductivity of the medium and the frequency of the wave fix our length dimension. As a result in this class of problems the only parameters to be varied are the inclination of the layers and the conductivity contrasts. For a given conductivity contrast and dip we could, for example, obtain the complete frequency response of the structure from one map only. Referring to equation (4-36) it can be seen that this could be done simply by changing isotropically the scale of the map.

In geometries having finite dimensions the finite difference solution becomes much less general. The length dimension is not arbitrary any more and as such the frequency response of a structure cannot be obtained from one single solution. The fundamental similitude relationship loses its previous freedom and becomes completely constrained. If we change the scale we actually change the structure and we obtain the response of a scaled up or down (but different) structure at either another frequency or conductivity, or both. Because of this lack of generality in the solution, no computation of fields over such structures will be carried in this work. The need to compute the magneto-telluric field at different frequencies plus the combinations of size necessary to give an idea of the trends, would become prohibitive for desk calculator calculation. We may have to wait for the adaptation of the method to digital computers.

4.5 The method of approximation and the Helmoltz equation

Up to now we have been developping the technique of finite difference solution of plane electromagnetic problems without reference to the errors and inaccuracies inherent to the finite difference approach. In this section, we will pay attention to this aspect of the problem.

Four types of approximation have been included in the previous discussion. First, we should consider the truncation errors, that is, the errors introduced by representing a differential equation by a finite difference equation. Second, during the solution of the various boundary value problems, the residuals will never become completely zero; this is another source of error. Third, when we constrain the Helmoltz equation to become zero at a given depth, we must choose this depth so that the error is negligible. And fourth, since the non-polarized surface field is obtained through a numerical differentiation, it is convenient to study the accuracy of this operation.

Graphical and numerical presentation of the behavior of the one dimensional Helmoltz equation can be found at the end of section 4.5.3.

4.5.1 The finite difference approximation

Let us assume that a and b are the solution to the differential equations

$$\nabla^2 a - K^2 b = 0$$
$$\nabla^2 b + K^2 a = 0 \tag{4-36}$$

Call the finite difference Laplacian operator H and the finite difference solutions A and B

$$HA - K^2 h^2 B_o = 0$$
$$HB + K^2 h^2 A_o = 0 \tag{4-37}$$

Recalling the way in which the second derivative expression in finite differences was developped (see equation (4-8) and (4-9)) we see that the main term of the truncation error is

$$T_x = \frac{1}{12} h^4 \frac{\partial^4 A}{\partial x^4} \qquad T_y = \frac{1}{12} h^4 \frac{\partial^4 A}{\partial y^4}$$

and similarly for B. We have then that

$$\left| HA - h^2 \nabla^2 a \right| \leq \frac{h^4}{12} \left[\frac{\partial^4 A}{\partial x^4} + \frac{\partial^4 A}{\partial y^4} \right]$$

Subtracting (4-36) from (4-37) we find the finite difference error to be

$$\left| a - A \right| \leq \frac{h^2}{K^2} \left[\frac{\partial^4 A}{\partial x^4} + \frac{\partial^4 A}{\partial y^4} \right]$$

$$\left| b - B \right| \leq \frac{h^2}{K^2} \left[\frac{\partial^4 B}{\partial x^4} + \frac{\partial^4 B}{\partial y^4} \right].$$

These results show that for net sizes corresponding to one skin depth the solution will be in error by less than 16%, while for separations equal to half the skin depth the finite difference error should not exceed 0.2%. The first estimate is too high for most of the region under consideration (computed values are usually within 10% for the one dimensional equation) while the second is too low, because of course, it is based on the assumption that the relaxation is carried to complete liquidation of residuals. By carrying sufficient significant figures and spending enough time, this accuracy could be approached. In our case relaxation will be taken to within 0.5% to 2.5% of the differential solution in most cases.

4.5.2 The relaxation approximation

In practice, the relaxation process is never led to the point where all residuals are zero. Therefore, if the exact solution of the difference equations is

$$HA - \kappa^2 h^2 B = 0$$
$$HB + \kappa^2 h^2 A = 0$$

where H is the Laplacian operator, then the solution obtained by relaxation methods would be

$$HA' - \kappa^2 h^2 B' = r$$
$$HB' + \kappa^2 h^2 A' = s$$

and the error introduced at the node and surrounding points would have to satisfy

$$H\epsilon_s - \kappa^2 h^2 \epsilon_r \leq r$$
$$H\epsilon_r + \kappa^2 h^2 \epsilon_s \leq s$$

where $\epsilon_s = A' - A$ and $\epsilon_r = B' - B$. We may obtain a conservative estimate of the error involved if we assume that the errors in the points around the node add up to zero, so that all the error is concentrated in the node. In this case, solution of the equations for ϵ_s and ϵ_r give

$$\epsilon_r \leq -\frac{s + \frac{r}{4} k^2 h^2}{4 - \left(\frac{k^2 h^2}{2}\right)^2}$$

$$\epsilon_s \leq \frac{\frac{s}{4} k^2 h^2 - r}{4 + \left(\frac{k^2 h^2}{2}\right)^2}$$

If the residuals r and s are of the same magnitude, say m, the above equations become

$$\epsilon_r \leq -\frac{m\left(1 + \frac{k^2 h^2}{4}\right)}{4 - \left(\frac{k^2 h^2}{2}\right)^2}$$

$$\epsilon_s \leq -\frac{m\left(\frac{k^2 h^2}{4} - 1\right)}{4 + \left(\frac{k^2 h^2}{2}\right)^2}$$

4.5.3 Zero cut-off at depth approximation

The finite difference solution of the electromagnetic problems related to the magneto-telluric field depends on the ability to transform infinite boundary problems into finite boundary problems. This was accomplished by considering the field to become zero beyond the depth where its magnitude became smaller than the significant figures carried in the calculation. From a physical point of view constraining the field to go to zero at a given depth is equivalent to placing an infinitely conducting layer at that depth. In order to see how the depth at which

COMPARISON BETWEEN DIFFERENTIAL AND FINITE DIFFERENCE SOLUTIONS OF THE ONE DIMENSIONAL HELMOLTZ EQUATION IN A DISSIPATIVE MEDIUM

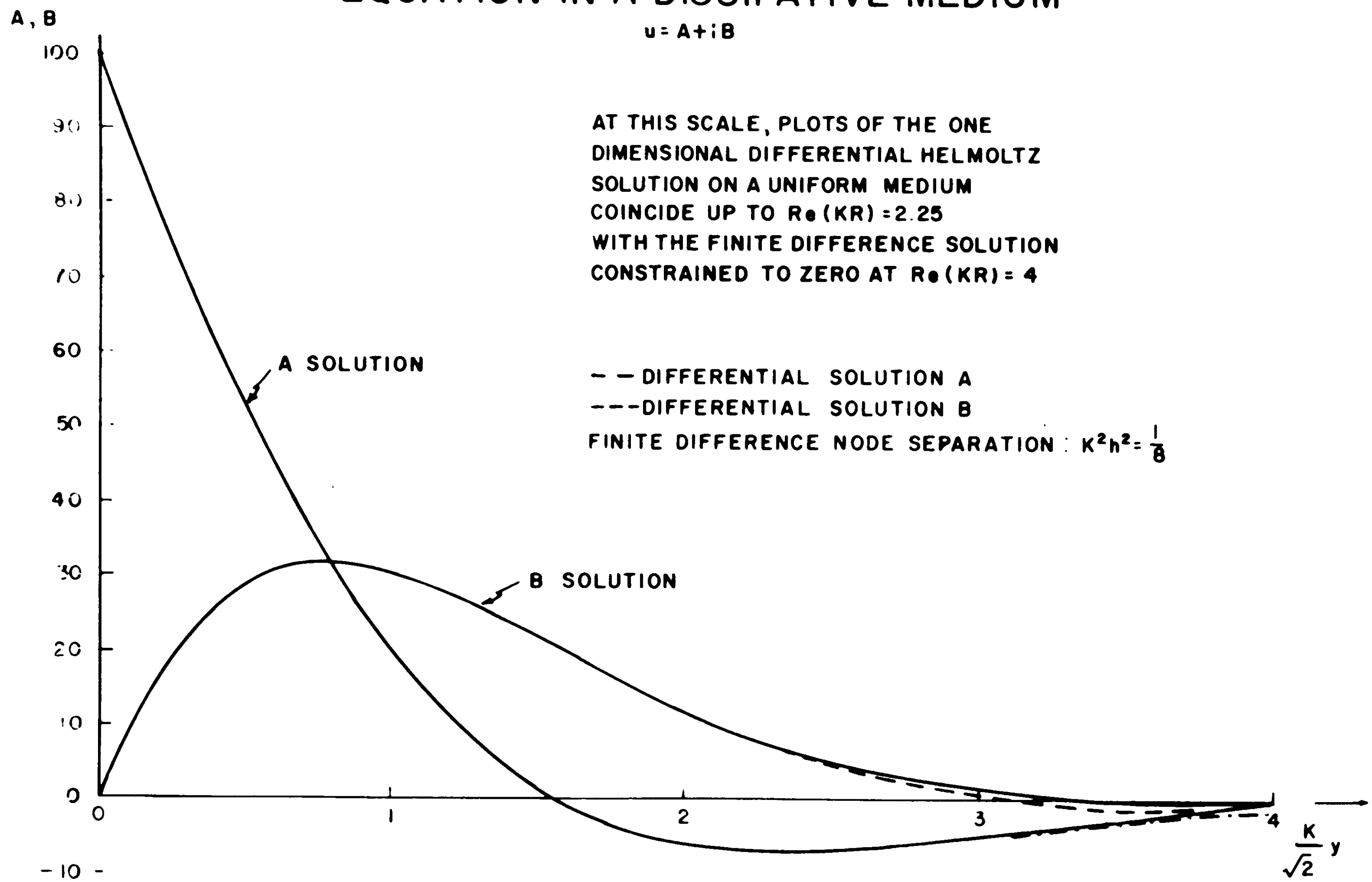

the layer is, affects the surface field, we may set up the boundary value problem

$$u = Ae^{iky} + Be^{-iky}$$

$u = h$ at $y = 0$

$u = 0$ at $y = a$

which is easily seen to yield

$$u = -h \frac{\sin k(y-a)}{\sin ka}$$

where $k^2 = i\mu\omega\sigma$. Now the field at the surface of a uniform earth is

$$u = he^{iky}$$

and a magneto-telluric measurement would be characterized by

$$\frac{E_z}{H_x} = \frac{k}{\mu\omega}$$

Similarly, the magneto-telluric measurement over a two layered earth (with the bottom layer being infinitely conducting) yields

$$\frac{E_z}{H_x} = -\frac{k}{i\mu\omega} \tan k(y-a)$$

and at the surface

$$\left.\frac{E_z}{H_x}\right|_{y=0} = \frac{k}{i\mu\omega} \tan ka$$

defining $p = \sqrt{\mu\omega\sigma/2}$

$$\left.\frac{E_z}{H_x}\right|_{y=0} = \frac{k}{i\mu\omega} \tan pa(1+i) = \frac{k}{\mu\omega} \frac{\tan pa + i \tanh pa}{\tan pa \tanh pa + i}$$

The above equation clearly becomes identical to that of the magneto-telluric field over a uniform earth if $\tanh pa = 1$. If we attend at the behavior of $\tanh pa$ we have

pa	tanh pa
3	0.99505
4	0.99933
5	0.99991
6	0.99999
6.5	1.00000

Thus we see that if we force the solution to zero at depths for which the surface field will be negligibly affected. If on the other hand we were actually interested in studying the wave fields inside the earth, we would have to choose the cut-off point at a greater depth, say, at depths for which $pa > 6$. We may note that $pa = \sqrt{\frac{\mu\omega\sigma}{2}}\, a = 1$ corresponds to the skin depth.

The following tables and graphs present some finite difference solutions for different sizes of net as well as some comparisons with the differential solutions.

4.5.4. Finite difference derivatives

Our ultimate aim is calculation of the magneto-telluric field over arbitrary geometries. Since the polarized field is constant, the surface non-polarized field is the quantity we are most interested in obtaining. However, all problems are solved in terms of the polarized

TABLE I

NUMERICAL SOLUTION OF THE ONE DIMENSIONAL HELMOLTZ EQUATION

$u = A + iB$

$\frac{K}{\sqrt{2}} y$ (rad.)	A	B	$\frac{K}{\sqrt{2}} y$ (rad.)	A	B
0	100.00	0	3.75	-1.93	-1.34
0.25	75.46	19.27	4.00	-1.20	-1.38
0.5	53.23	29.08	4.00	-1.20	-1.38
0.75	34.56	32.20	4.25	-0.64	-1.28
1.00	19.88	30.96	4.50	-0.23	-1.08
1.25	9.03	27.19	4.75	0.03	-0.86
1.50	1.58	22.25	5.00	0.19	-0.64
1.75	-3.10	17.10	5.25	0.27	-0.44
2.00	-5.63	12.30	5.50	0.29	-0.29
2.25	-5.95	7.37	5.75	0.27	-0.16
2.50	-6.58	4.91	6.00	0.24	-0.07
2.75	-5.90	2.44	6.25	0.19	-0.06
3.00	-4.93	0.70	6.50	0.15	0.03
3.25	-3.23	-0.42	6.75	0.11	0.05
3.50	-2.83	-1.06	7.00	0.07	0.06

TABLE II

COMPARISON BETWEEN SOLUTIONS $u = A + iB$ OF THE DIFFERENTIAL AND DIFFERENCE EQUATIONS VANISHING AT A DEPTH $Y = 4\sqrt{2}/K$

	differential solution		difference solution					
			$k^2 h^2 = 2$		$k^2 h^2 = 1/2$		$k^2 h^2 = 1/8$	
$Ky/\sqrt{2}$	A	B	A	B	A	B	A	B
0	100.000	0	100.000	0.000	100.000	0.000	100.000	0.000
0.25	74.46	19.27					75.3	19.2
0.50	53.23	29.08			53.004	28.201	53.1	29.0
0.75	34.56						34.55	32.1
1.00	19.88	30.96	21.32	27.2 0	20.097	29.908	19.9	30.8
1.25	9.03	27.19					9.05	27.0
1.50	1.43	22.23			2.132	21.565	1.5	22.0
1.75	-3.29	17.60					-3.25	16.8
2.00	-5.87	12.37	-2.941	11.76	-5.035	12.175	-5.75	12.0
2.25	-6.22	7.50					-6.85	8.2
2.50	-6.87	5.20			-6.20	5.320	-6.7	5.4
2.75	-6.17	2.88					-5.9	3.35
3.00	-5.12	1.34	-3.675	0.009	-4.695	1.58	-4.8	1.8
3.25	-3.26	0.44					-3.5	0.8
3.50	-2.60	0.02			-2.40	0.19	-2.2	0.2
3.75	-1.29	0.06					-1.1	0
4.00	0	0	0	0	0	0	0	0

vector component, so that the other electromagnetic vector, which is needed to define a magneto-telluric measurement, has to be obtained through Maxwell's curl equations. This involves finding the derivative of the polarized field at the point where we want to know the non-polarized field. In particular, since the magneto-telluric method is characterized by the ratio of tangential E and H at the earth's surface, we have to calculate the normal derivative of the polarized field at the earth's surface (see section 3.2)

In section 4.2.1 we presented a two point derivative based on central differences. Although useful for boundary conditions, this type of derivative is not appropriate to the earth's surface where we want a derivative in terms of forward differences. From the expression for the Taylor expansion about a point (equation (4-8)) we may easily deduce the three point derivative

$$\left.\frac{\partial f}{\partial y}\right|_{y=0} = \frac{1}{2h}\left[-3 f(0) + 4 f(h) - f(2h)\right]$$

which has a truncation error

$$T_\eta \leq 4 h^3 f'''(0)$$

The error in the derivative depends primarily on the spacing of the finite difference nodes, not so much from the error introduced by large spacing on the finite difference solution, as actually from the difficulty of trying to fit a low degree polynormal to a high degree one. Therefore, when we go from regions of low conductivity to another of high conductivity, keeping the same size of net (which is a practical necessity), we will get less accurate results on the more conductive

TABLE III

COMPARISON BETWEEN THE FINITE DIFFERENCE SOLUTION AND DERIVATIVE WITH $k^2 h^2 = 1/8$ AND THE SOLUTION AND DERIVATIVES WITH $k^2 h^2 = 2$ INTERPOLATED TO $k^2 h^2 = 1/2$ AND $k^2 h^2 = 1/8$

	$k^2 h^2 = 1/8$		$k^2 h^2 = 2$		$k^2 h^2 = 2$		$k^2 h^2 = 2$	
$Ky/\sqrt{2}$	A	B	A	B	A	B	A	B
0	100.00	0.00	100.00	0.00	100.00	0.00	100.00	0.00
0.25	75.30	19.2					75.93	18.44
0.50	53.10	29.0			53.35	29.24	54.2	27.36
0.75	34.55	32.1					35.89	29.53
1.00	19.90	30.8	21.32	27.2	21.32	27.20	21.32	27.2
$\left.\frac{\partial u}{\partial y}\right\|_{y=0}$	49.7		43.5		52.3		51.6	

region. We have seen in 4.3.5 how the conductivity of the medium is intimately connected with node separation. Thus in treating the error introduced by the finite difference derivative, we have to discuss them with respect to the parameter $k^2 h^2$.

Let us consider a uniform earth for which Re $(k) = 0.5$. In the differential solution the normal derivative of the polarized field at the surface will have a magnitude 0.5. The corresponding finite difference solution will have a node separation equal to half the skin depth or $k^2 h^2 = 1/2$. Using the above expression for the truncation error, we find that for such spacing the derivatives will be in error by less than 10%. Actual computation shows that they are in error by 4%. If instead, we decrease the net size by half, making $k^2 h^2 = 1/8$, we get from the truncation formula an estimated error of less than 3%; the actual error is 0.6%.

From these calculations, we see that 3 point derivatives taken with separations of $k^2 h^2 = 1/8$ are excellent for our purposes. However in many occasions, the time available will compel one to use larger separations (a typical vertical layer problem with a separation of $k^2 h^2 = 1/2$ may need 80 points; with a separation of $k^2 h^2 = 1/8$ the number of nodes will increase to 320. Graded nets are an alternative, but in most cases they also will increase sharply the computation load) which yield sufficiently accurate solutions, but which may be too large for the derivatives. In this case we may improve the derivatives by interpolation. That is, we may interpolate one or more points between the surface node and the next sub-surface node, by making the interpolated points satisfy the Helmoltz equation and coincide with the two nodes in question. Of course, the ideal procedure would be to solve all the problem in a fine net. However, by interpolating, we increase our accuracy without a prohibitive amount of computation. Supposing that we are solving a uniform earth problem on a $k^2 h^2 = 2$ net, we know from a previous discussion that the error at the points near the surface will be less than 18%. By interpolating one point we reduce the error by less than half and by interpolating more points, we reduce further the finite difference error. At the same time we improve the derivative, so that the process produces a much more accurate result. This is illustrated by table 4. The 3 point derivative of the one dimensional Helmoltz equation for a spacing $k^2 h^2 = 2$ is in error by 13%. By interpolating one point we reduce the error to 4.6% and by interpolating 3 points we reduce the error further to 3.2%. The error in the derivative by solving the whole problem in a finer net (equivalent to the 3 point interpolation) is 0.6%.

4.6 The magneto-telluric field in specific structures

4.6.1 Apparent conductivity patterns in inclined layers

As referred in 4.4, the finite difference solution of inclined layer problems is characterized by a degree of generality not found on finite boundary geometries. For this reason, we have chosen to illustrate the use of the finite difference method developped here with the calculation of the magneto-telluric field over a group of inclined layer structures, from which we can draw certain general conclusions on the behavior of the field over such structures.

Before going into the specific cases, we will point out that by using the "semi-quantitative transform" concept discussed in section 2.5, the apparent resistivity patterns in inclined layer geometries will have definite identifying characteristics. We may recall that the "semi-quantitative transform " was obtained by plotting the apparent resistivities at a given station at a depth equal to the skin depth in the mediu. As a result, all the lines of equal apparent resistivity will go through the strike of the fault. Thus the transform accomplishes the identification of the type of geometry involved. The only parameter lacking will be the dip of the bed. In order to do this, once we know that we are dealing with an inclined bed geometry, it is a simple procedure to obtain the frequency response of the structure. From this point on, it is a question of synthesis, which can usually be accomplished by curve matching. However, the synthesis problem is unique because it depends on one only variable, the angle of dip.

4.6.2 Sea coast effects

One of the most striking instances of lateral changes in conductivity is that associated with sea-land contacts. Its importance derives as much from its widespread occurrence as from the conductivity contrasts involved, which are on the order of 1000 or more. The magnitude of the contrast introduces effects on the apparent conductivities measured inland, to an extent that they may give an erroneous picture of the sub-surface structure if proper care is not exercised.

An incident plane wave will penetrate between 10 to 1000 times deeper on the continent than in the sea. For example, at 1 cycle per second, on a shield type area, an electromagnetic wave would be attenuated as much at a depth of about 80 kilometers as at a depth of 500 meters under the sea. This means that as we approach the sea, the telluric currents in the crust have to move upward. Once they get to the sea they become concentrated near the surface, by comparison with their distribution with depth in the continent.

In order to make a quantitative study of the behavior of the magneto-telluric field near the sea, we may set up an inclined layer model where one of the media has an infinite conductivity. Physically this is equivalent to a zero skin depth in the sea; in other words, it is the same as having the telluric currents in the sea concentrated entirely at the sea surface. This is certainly a valid approximation when we consider the ratio of about 1/100 and more between the distributions of the current with depth at sea to that inland. A problem of this type was solved by finite differences and the reader is referred to fig. 4-22 for the results.

According to our solution, as we approach the sea, the upward movement of telluric currents only becomes noticeable at a distance equivalent to $kr = 2.5$. At 1 cycle per second, for an earth with a resistivity of 10^3 ohm-meters, this would mean 40 kilometers from the coast; at 0.01 cycles per second it would be 400 kilometers. The following region, comprised between $kr = 2.5$ and $kr = 1.5$, is consequently characterized by apparent resistivities which are slightly higher than the actual resistivity of the medium (this would be a region 16 kms. long at 1 cycle or 160 kms long at 0.01 cycles per second, for the same resistivity as above). Finally, from $kr = 1.5$ on, towards the sea, the apparent resistivity falls off sharply; at $kr = 0.5$ (8 km at 1 cps; 80 at 0.01 cps) it has decreased to about 60% and by $kr = 0.25$ it has been reduced to about 40% of the actual resistivity.

The above description of the expected behavior of the magneto-telluric field near the sea assumes, of course, movable locations at a fixed frequency. Let us see now what it means in terms of a spectrum of frequencies at a fixed position. In this case the "kr" of the station is changed at every new frequency and for each one a response as described previously would follow. Therefore, under the assumption of the possibility of measuring a very broad band spectrum, at the highest frequency, we would get an apparent resistivity equal to the real resistivity under the station. Then, as we lowered the frequencies and went through the range which made the "kr" of the station about 2, we would get slightly higher apparent resistivities. Finally, as we keep lowering the frequency, we would run into the frequency region where the apparent resistivities begin to fall very rapidly. The curious fact is that this type of response has the same general features of the frequency response of a two layered earth, where the bottom layer is more conductive than the top layer. And, one is tempted to suspect that the profusion of papers dealing with two layered earths with infinitely conducting substrata has its origin in the mistaken identification of sea coast effects. However, we must add that with good data, that is, with a fairly large range of frequency response of apparent resistivities and phase angles no confusion should occur. Yet one must remember that practical matters of all kinds dictate the amount of data collected. Wide frequency response, simultaneous recording of magnitudes and phases of the angles require an amount of instrumentation not easily available.

In order to illustrate the above comments more concretely, let us take an example. By now, it must be fairly evident that the curves of fig. 4-22, giving the characteristics of the magneto-telluric field in function of the distance from the sea can also be used as the frequency response of the magneto-telluric field at a given station. This is, of course, because from previous considerations of electrodynamic similitude, by changing the frequency we change what we may call the electromagnetic distances involved; in other words the position of the station changes with respect to the wave length of the electromagnetic wave.

Now in fig. 4-22 values of the field are given at distance intervals equivalent to $kr = 0.5$. A given station or observatory will be at a distance r from the sea; since the k of the solution is actually the real part of the propagation constant as it is usually defined, it is given by $k = \sqrt{\mu\omega\sigma/2}$, where ω is the radian frequency and σ

the conductivity of the medium. The medium under the station will have a conductivity σ ; therefore, by changing the frequency ω the product kr assumes different values. In this manner the coordinate showing the distance from the sea in fig. 4-22 can be transformed into a frequency coordinate.

Let us for example consider an observatory 40 kms from the sea, in a medium of resistivity 10^3 ohm-meters. The frequency response of the apparent resistivity due to sea coast effect would be approximately

period (seconds)	apparent resistivity
1.0	10^3
2.8	0.85×10^3
16.6	0.6×10^{-3}
100.0	0.4×10^{-3}

To the observer unaware of the nature of sea coast effects, this data may seem to point to a layer of higher conductivity at depth. In fact, using the usual interpretational techniques of curve fitting, we would see that these measurements fit very closely the curve for a two layer earth with a top layer of resistivity 10^3 ohm-meters and a bottom layer of resistivity 0.5×10^3 ohm-meters at a depth of 20 kms.

However, if simultaneous recording of the phase angles were made, we would immediately detect the error of ascribing the response obtained to a layered structure. While for the layered structure the phase angle should start at 45° and go up with lower frequencies, for the sea coast effect the phase angle starts at 45° but decreases with lower frequencies. The reader is referred to Cagniard's paper (1953) for a set of standard interpretation curves in the case of a two layer earth.

We may conclude therefore by emphasizing the similarities between the apparent resistivity response of the sea coast and of a two layered earth, at a given station. The farther inland the station is, the the deeper the conductive lower layer appears to be. This is illustrated by the apparent resistivity map in fig. 4-22. Besides the effects mentioned above, we also must be aware that these lower resistivities at depth may mask the other sub-surface structure. It should also be pointed out that the way to avoid the pitfalls of interpretation is by taking as complete a set of data as possible. Geographic coverage is necessary. When it is impossible, apparent resistivities and phase angles throughout a wide spectrum of frequencies are a must. With simultaneous measurements of magnitude and phase no confusion between sea coast eff cts and layered media should arise. However, the only way to detect unambiguously the sub-surface structure is by geographical coverage.

4.6.3 Inclined layers

In this section, we will discuss some results concerning inclined layers when both media have finite conductivities. These results were obtained through the finite difference method that we have been describing. Following the treatment of previous sections, we will examine the magneto-telluric field for electric and magnetic polarization separately. For electric polarization, the E vector is parallel to the strike of the structure, and the current in the earth runs parallel to the strike; for magnetic polarization, it is the magnetic vector that aligns itself along the strike and the current in turn runs normal to the strike.

In the following discussion, in order to achieve a certain degree of generality, we will speak of distances in terms of kr's away from the strike. Thus when we write "at a distance $kr = 2$ in the resistive side" we mean a distance from the strike at which $kr = 2$. By using kr for the dimensions, we take in account conductivity, wave length, and the actual length dimension at once.

a. Electric polarization.

In dealing with this type of polarization, the current flow lines actually never cut across boundaries separating regions of different conductivities. Further, the boundary conditions require continuity of the electric field and its normal first derivative. These characteristics would lead one to expect a rather smooth and gradual change in the magnetic field at the surface, across the region of changing conductivity. Three examples of the magneto-telluric field

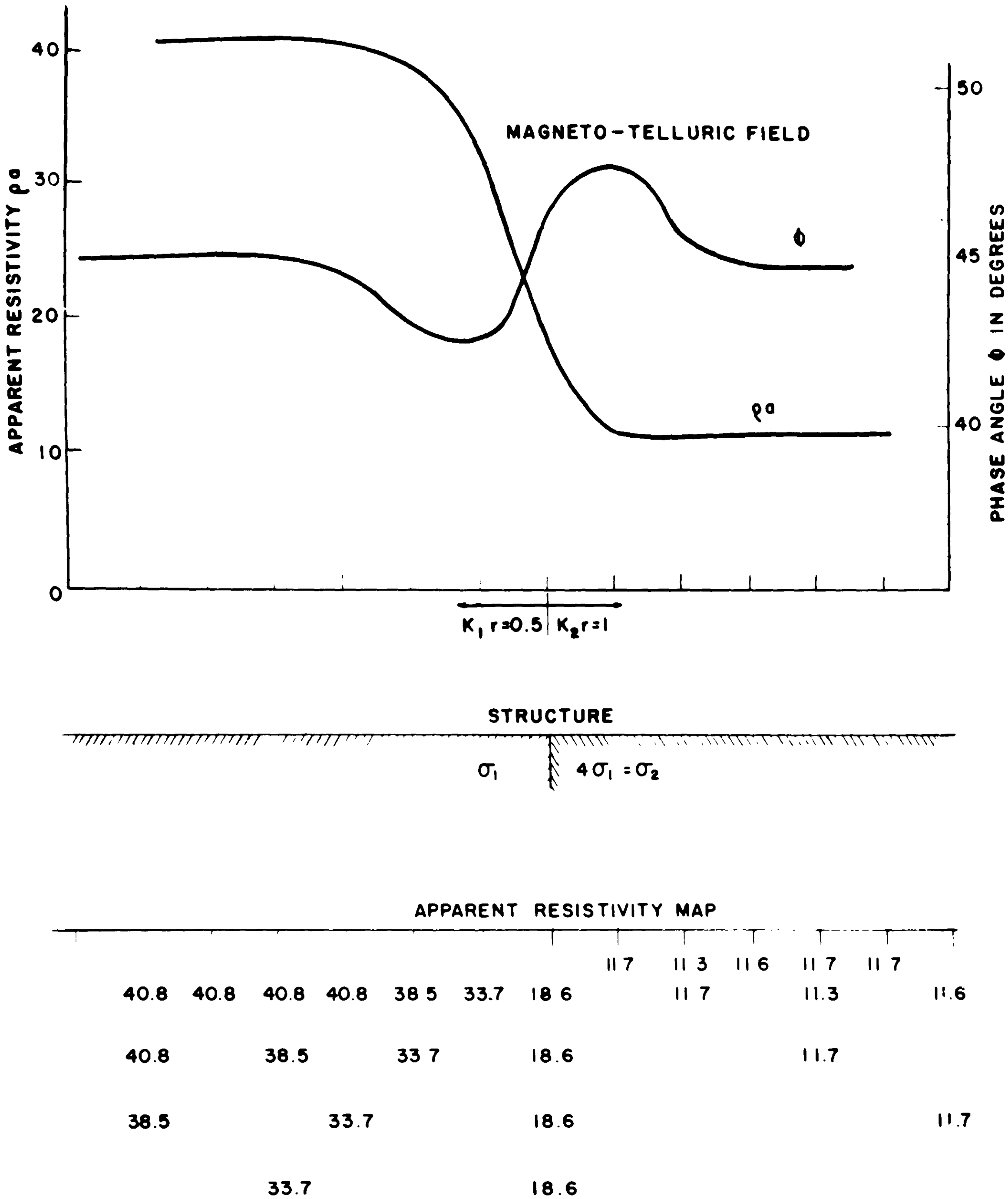

(VERTICAL SCALE OF MAP HAS BEEN HALVED)

MAGNETO-TELLURIC FIELD FOR A VERTICAL LAYER
ELECTRIC POLARIZATION
FIG.4-20

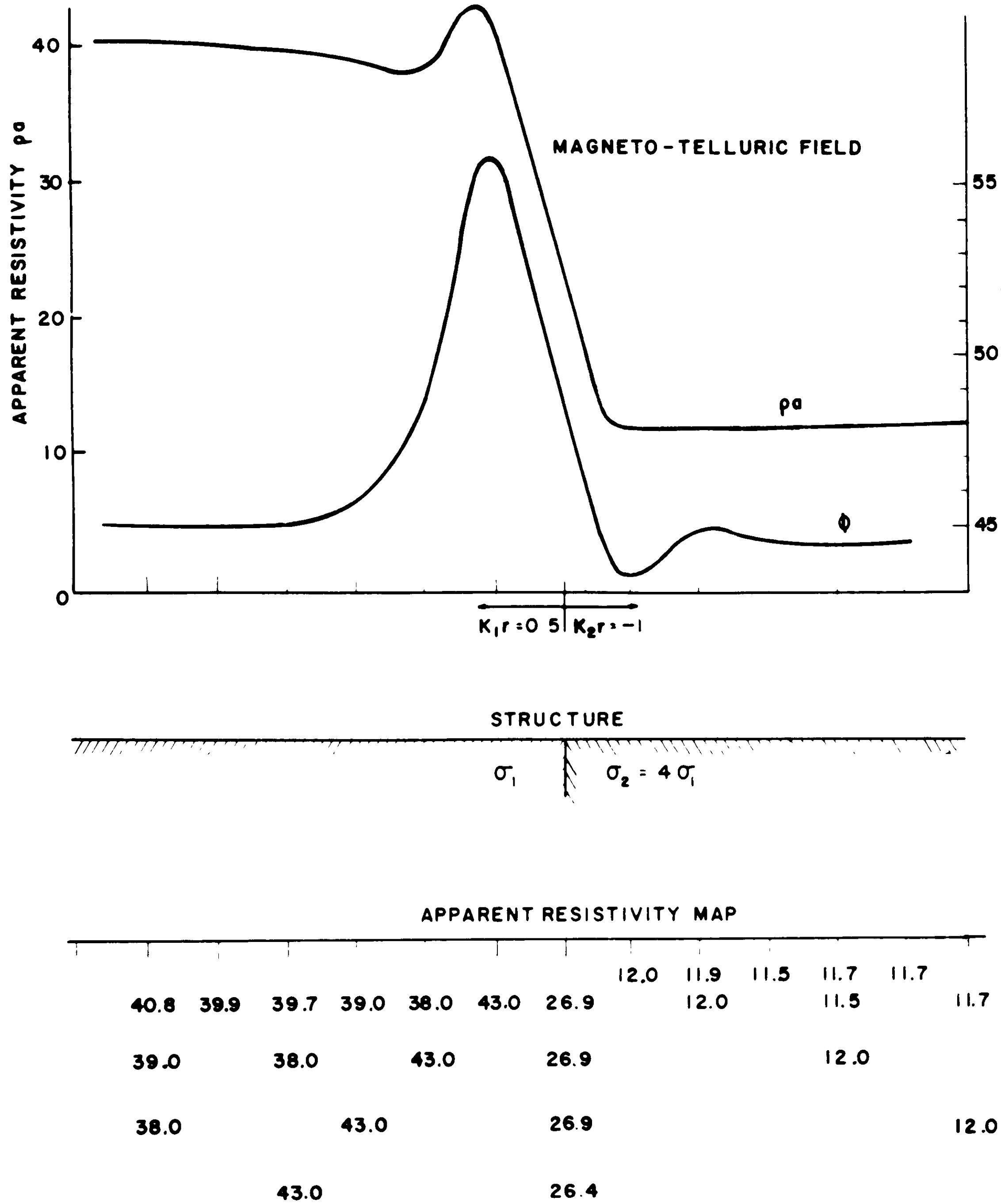

(VERTICAL SCALE OF MAP HALVED)

MAGNETO-TELLURIC FIELD FOR A VERTICAL LAYER
MAGNETIC POLARIZATION
FIG 4-21

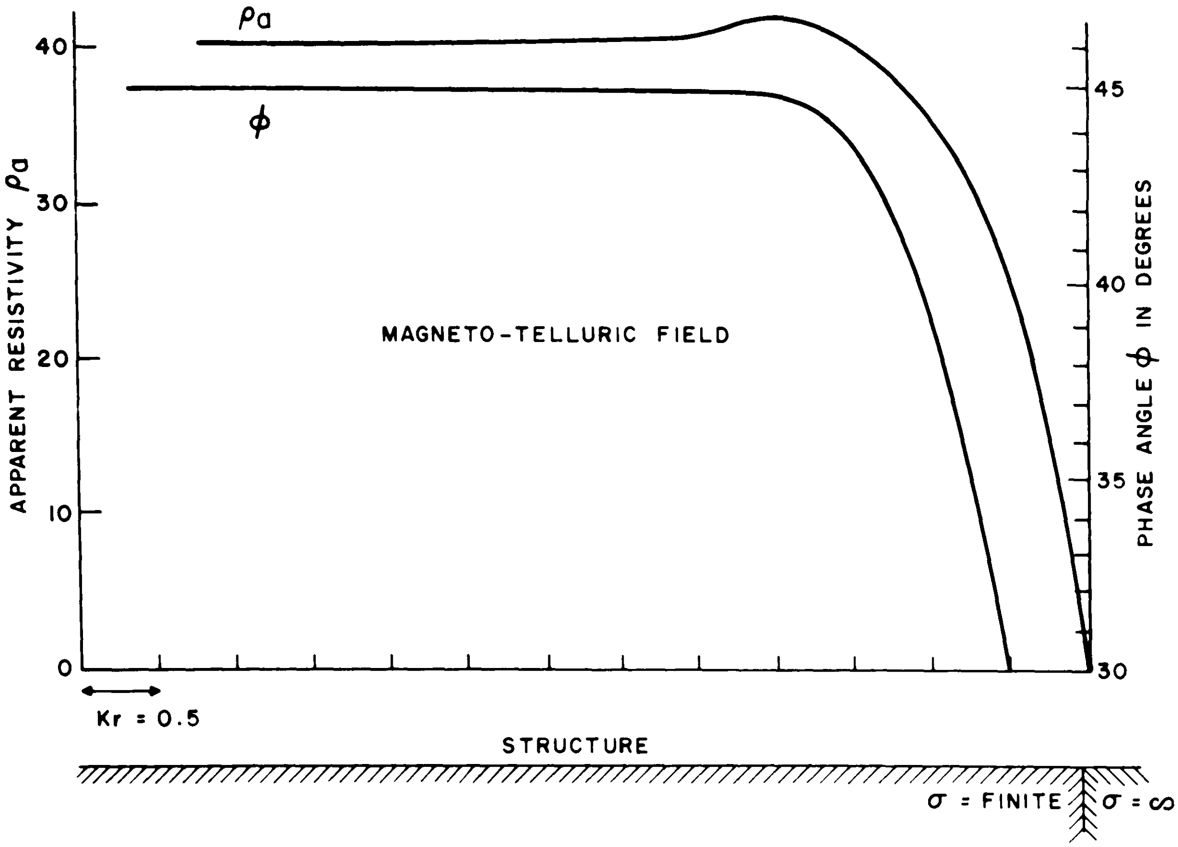

APPARENT RESISTIVITY MAP

40.8 40.8 40.8 40.8 40.8 40.8 40.8 40.8 41.7 40.2 36.7 25.7 0

40.8 40.8 41.7 40.2 36.7 25.7 0

40.2 36.7 25.7 0

40.2 36.7 25.7 0

(VERTICAL SCALE OF THE MAP HALVED)

MAGNETO-TELLURIC FIELD FOR A VERTICAL LAYER
WITH INFINITE CONTRAST
FIG.4-22

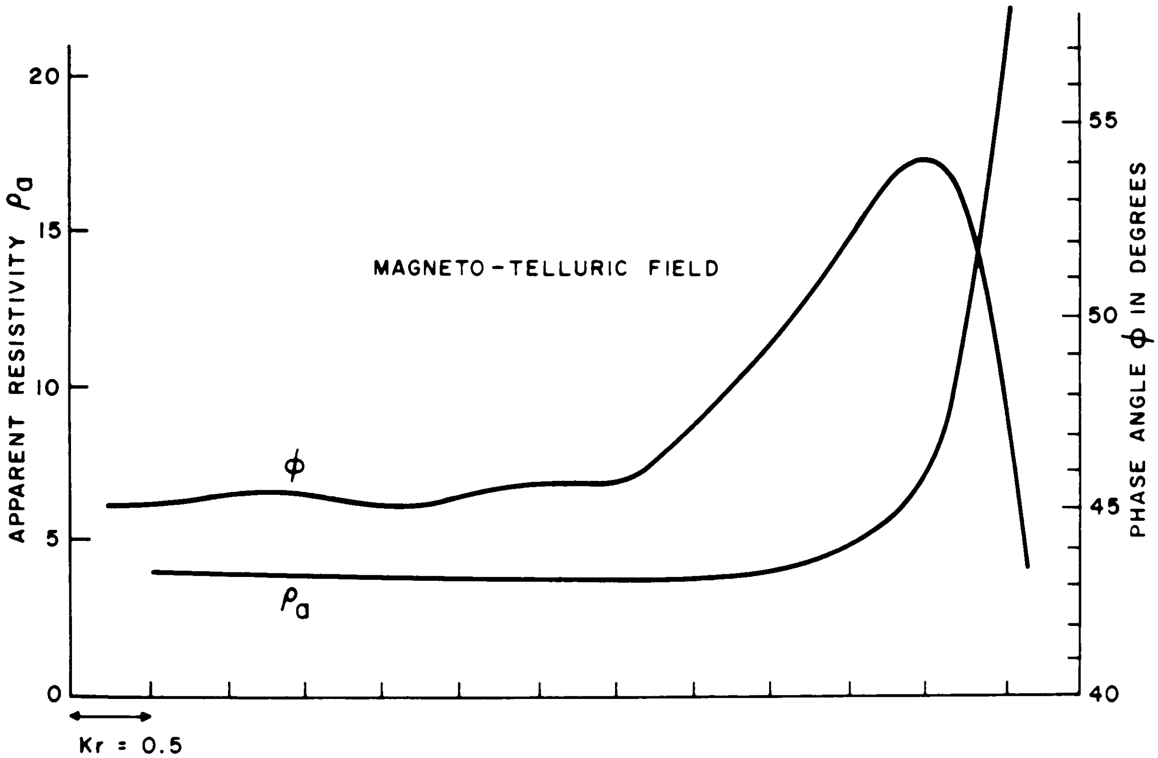

STRUCTURE

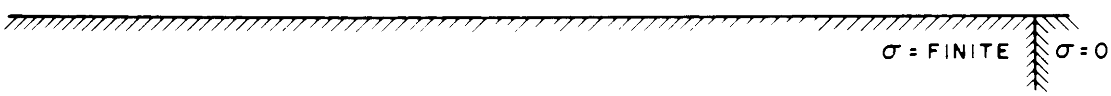

APPARENT RESISTIVITY MAP

4.1	4.1	4.0	4.0	4.0	3.8	3.8	3.8	4.0	4.9	7.1	20.7	∞
3.8	3.8	3.8	3.9	4.0		4.9		7.1		20.7		∞
4.0			4.9			7.1			20.7			∞
4.9				7.1				20.1				∞

(VERTICAL SCALE OF MAP HAS BEEN HALVED)

MAGNETO-TELLURIC FIELD FOR A VERTICAL LAYER
IN CONTACT WITH A NONCONDUCTING MEDIUM
FIG. 4-23

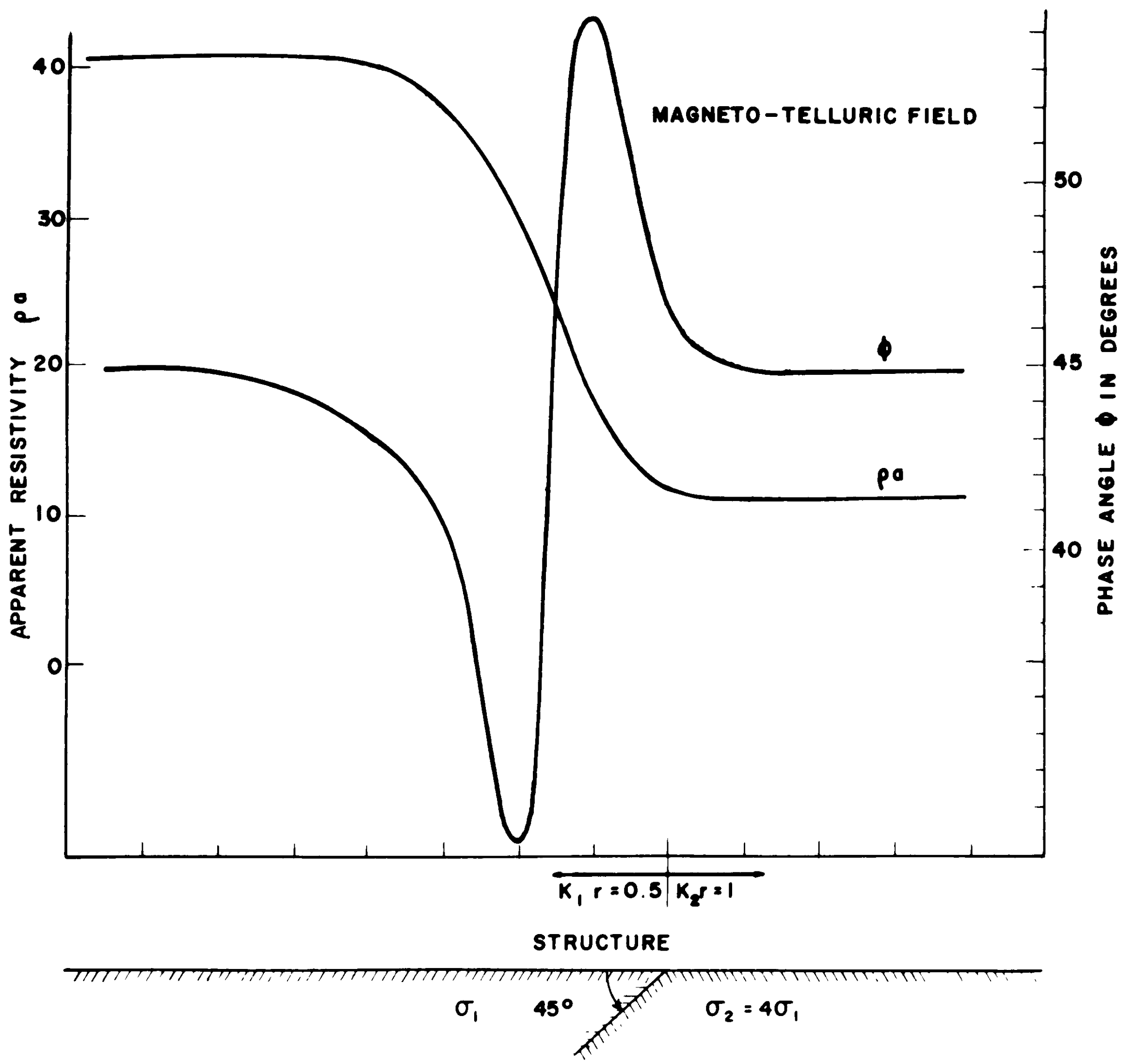

APPARENT RESISTIVITY MAP

							12.1	11.7	11.7	11.7	11.7
40.8	41.2	41.6	40.4	37.2	30.2	17.7	12.1		11.7		11.7
	37.2		30.2		17.7		12.1				11 7

(VERTICAL SCALE OF MAP HAS BEEN HALVED)

MAGNETO-TELLURIC FIELD FOR AN INCLINED LAYER
ELECTRIC POLARIZATION
FIG. 4-24

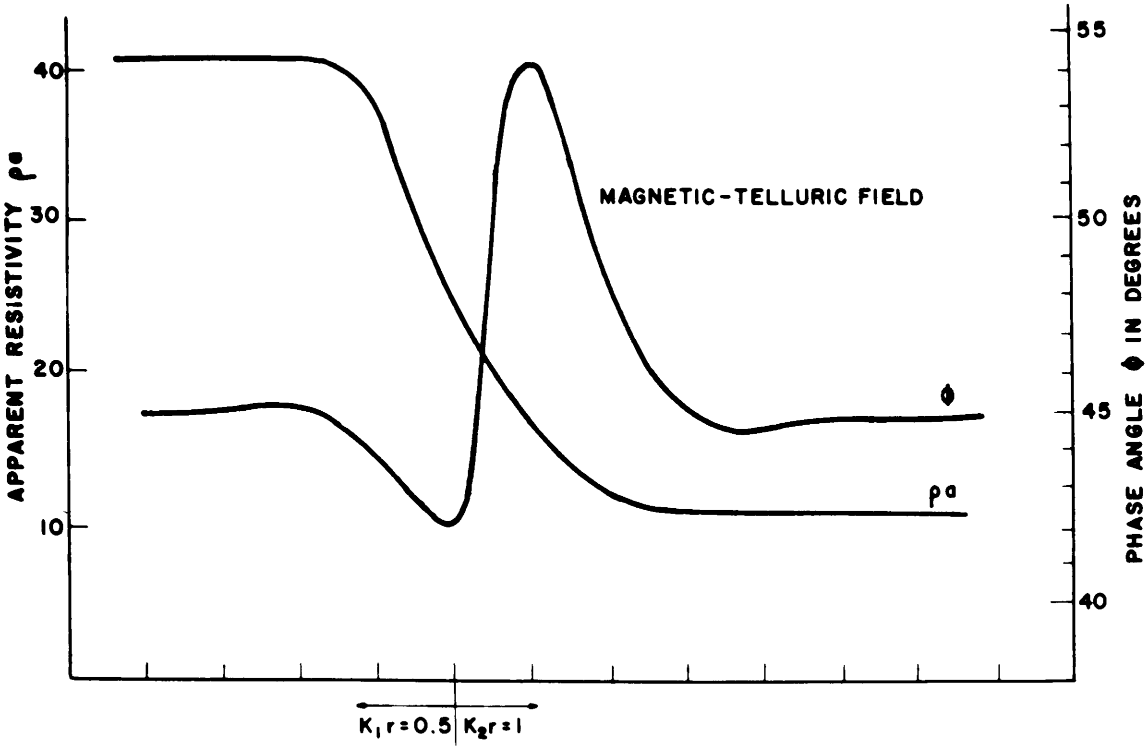

STRUCTURE

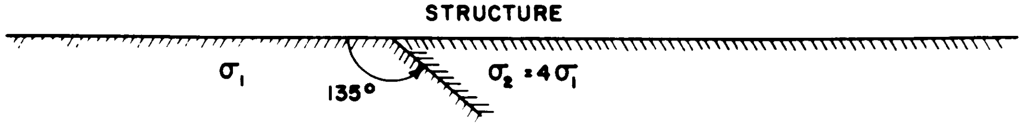

APPARENT RESISTIVITY MAP

				23.7	16.4	11.7	11.2	11.4	11.4	11.7	11.7	
40.8	40.8	40.8	37.6	23.7		16.4		11.7		11.2		
40.8		37.6		23.7			16.4					11.7

(VERTICAL SCALE OF MAP HAS BEEN HALVED)

MAGNETO-TELLURIC FIELD FOR AN INCLINED LAYER
ELECTRIC POLARIZATION
FIG. 4-25

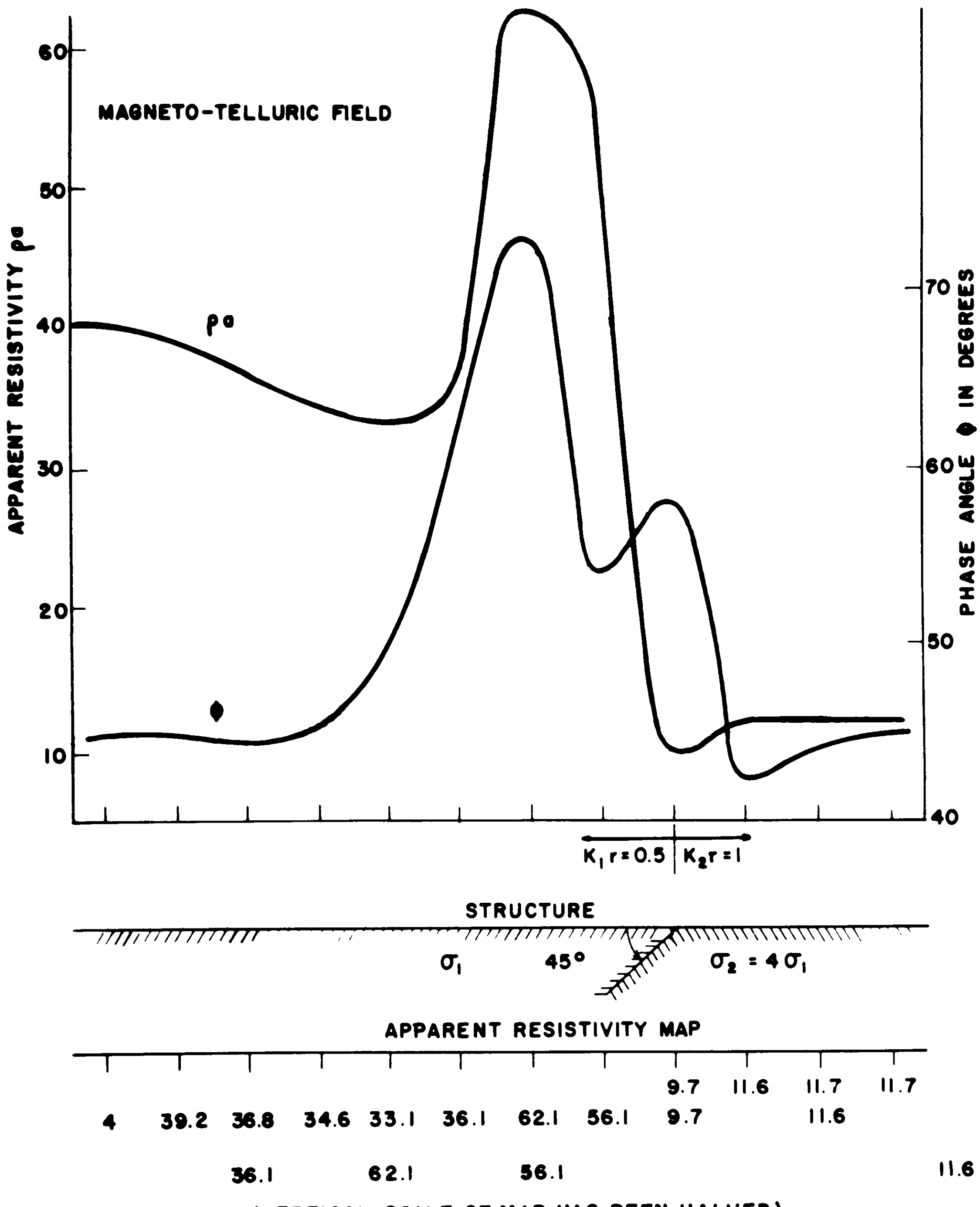

(VERTICAL SCALE OF MAP HAS BEEN HALVED)

MAGNETO-TELLURIC FIELD FOR AN INCLINED LAYER

MAGNETIC POLARIZATION

FIG. 4-26

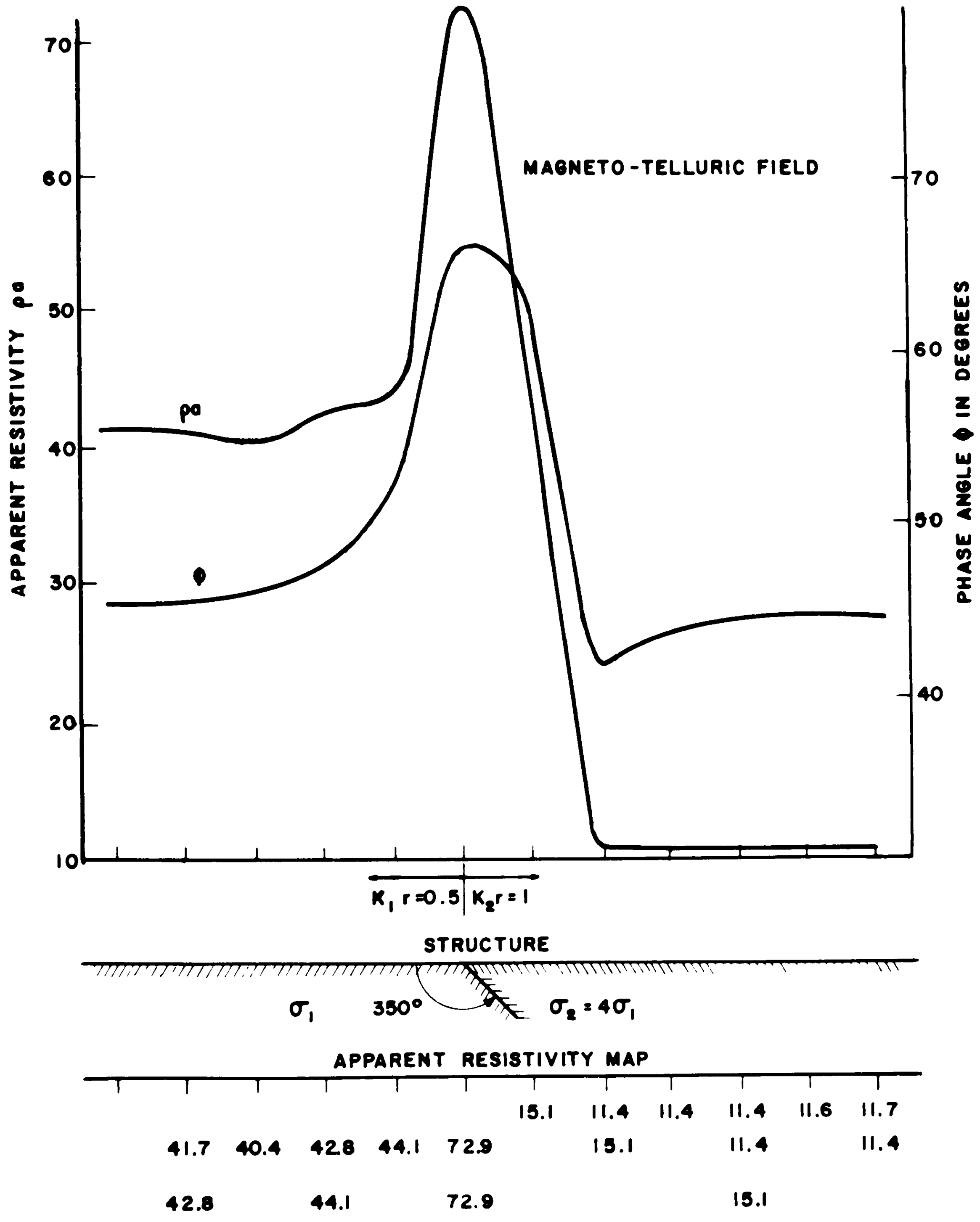

MAGNETO-TELLURIC FIELD FOR AN INCLINED LAYER
MAGNETIC POLARIZATION
FIG. 4-27

for electric polarization are given in fig. 4-20, 4-24, and 4-25, and they justify our expectations. These examples concern inclined layers with conductivity contrasts of 4 and angles of dip of 45° 90° and 135° . In all of them the apparent conductivity just takes intermediate values as we go from the more resistive to the more conductive side.

For the vertical layer case (90° angle of dip) as we approach the strike from the resistive side we begin to feel the influence of the boundary at $kr = 1.5$. For ease of exposition, let us call the difference between the resistivities of both media 100%. Then, as we get to $kr = 1$ in the resistive side, the apparent resistivity has already dropped about 5%. At $kr = 0.5$ the apparent resistivity has decreased by nearly 20%. When we reach the strike, the apparent resistivity is reduced to 30%. As we proceed into the more conductive medium, the apparent resistivities keep dropping; at a $kr = 0.5$ in the conductive side they are down to 14% and finally by $kr = 1$ the apparent resistivity equals the resistivity. Between $kr = 1$ and $kr = 3$ our solution showed a region of slightly lower apparent resistivities. These effects were on the order of 3% of the actual resistivity and it looked like some sort of recovery effect. Although we can be sure of its existence since it appears in other vertical layer and 135° layer examples more accurately solved, we cannot decisively say that in this case it disappears at a $kr = 3$. Probably it ceases to exist anywhere between $kr = 1$ and $kr = 3$, but since 3% effects are at the limits of our accuracy on the more conductive side, its impossible to state exactly where.

The values assumed by the phase angle as we cross over the vertical layer show a high degree of symmetry about the strike. This symmetry is in terms of actual distances not of kr's. At a $kr = 1.5$ in the more resistive medium, the phase angle is half a degree lower than in an uniform medium . The minimum phase angle occurs at $kr = 0.5$ and it is about $42°$, From here towards the fault the phase angle increases and the maximum occurs at a $kr = 1$ in the conductive side; its value is $48°$ and we may note that both the maximum and minimum are equally deviated from the $45°$ characteristic of an uniform medium. At a $kr = 3$ in the conductive side, the boundary ceases to affect the phase angle.

Let us see how these characteristics are modified when the angle of dip is changed from $90°$ to $45°$. A $45°$ degree dip means that actually we have a conductive layer sloping downward underneath the resistive medium. Therefore, as it would be expected, the apparent resistivities on the resistive side are affected farther away from the strike than in the vertical layer case. Actually, there is an added feature: in the resistive side, between $kr = 3$ and $kr = 2$ there is a region of slightly higher apparent resistivities ($\sim 2\%$). From $kr = 2$ on, towards the more resistive side, the apparent resistivities fall in a gradual fashion and as we get to the strike they are reduced to about 3% of the difference of the actual resistivities of both media. By $kr = 1$ on the conductive side no boundary effects are detectable.

As to the phase angle, the lateral effects begin at $kr = 2.5$ on the resistive side with a steady decrease from $45°$. The previous symmetry about the strike disappears. A very abrupt change occurs, still on the resistive medium, in the short space between $kr = 1$ and the strike line; here the angle goes from a minimum of 32° to a maximum of 54°. We may note the greater deviation of the angle on the side nearer to the dipping contact; the same will be seen to happen for 135°. At a $kr = 1.5$ in the conductive side, the geometry no longer affects the phase angle.

Finally, we may look into the response of an inclined bed at 135°. Here the fact that the resistive bed slopes under the conductive one keeps the apparent resistivities on the resistive medium unaffected until about $kr = 0.5$ from the strike. The usual pattern of gradually falling apparent resistivities follows and as we reach the strike, the apparent resistivity is the average of the resistivities of both media. At a $kr = 2$ on the conductive side, we get real resistivities, but then for about 2 kr's follows a region exhibiting the same slightly lower apparent resistivities as in the case of vertical layers.

The phase angle shows the same general pattern as before except for the fact that the minimum and maximum occur now respectively over the strike and at $kr = 1$ on the conductive side. Also, as pointed out previously, the maximum (which is in the side nearer to the inclined layer) represents a greater deviation from the uniform earth phase angle than the minimum.

The knowledge of the response of dipping beds is useful either to detect and define dipping beds or to avoid their effects. We may summarize our results for a contrast of 4 (and certainly generally applicable within a certain range of 4) by stating that the detection of inclined beds in the resistive side begins at:

$kr = 3$ for 45° dip

$kr = 1.5$ for 90° dip

$kr = 0.5$ for 135° dip

The corresponding distances in the conductive side are

$kr = 1$ for 45° dip

$kr = 3$ for 90° dip

$kr = 0.5$ for 135° dip

having in mind that beyond $kr \simeq 0.5$, $kr = 1$ and $kr = 2$, respectively, the effect is a very small one.

All the discussion up to now has been based on the rather low conductivity contrast of 4. In order to estimate how the contrast affects the distances at which the effects are felt, we solved 2 vertical layer problems dealing with limiting cases of extreme conductivity contrast. In one, a finitely conductive medium was assumed to be in contact with an infinitely conducting one; this is an approximation to the case of very large contrast as seen from the more resistive medium. In the other, the finitely conductive medium was assumed to be in contact with a nonconducting medium; this is, of course, the approximation to the case of very large contrast as seen from the less resistive medium. The data obtained is given in fig. 4-22 and 4-23.

These results are very interesting because they show that for vertical layers the region where the changes in apparent resistivity take place are the same either for a contrast of 4 or for a contrast of infinity; this is, $kr = 1.5$ on the resistive side and $kr = 3.5$ on the conductive side. Besides, these results also show the small recovery effects described previously. On the resistive side they occur between $kr = 2.5$ and $kr = 1.5$ and amount to 2% of the actual resistivity; on the conductive they occur between $kr = 2$ and $kr = 3.5$ and are on the order of 5% of the actual resistivity. In face of these results, we may conclude that the general features of the results for a contrast of 4 can be used to estimate the response for higher contrasts.

In a manner identical to that described in the preceding section, we may use the magnitude and phase curves which we have been discussing, to study the frequency response at a given station near an inclined layer. At the highest frequencies the values would be those of an uniform earth (provided the kr were large enough i.e. $kr = 3$) and at the lowest frequencies the apparent resistivity would tend to that of the strike. Again, we see that for a fixed location we would obtain curves similar to those of a two layered earth. On the resistive side the substratum would appear more conductive, on the conductive side the substratum would appear more resistive. However, any confusion would be dispelled by the phase angles which consistently go in the direction opposite to that expected of the two layered earths described above.

We may note that the point directly over the strike of an inclined layer has the interesting property of constant apparent resistivity throughout the range of frequencies. Therefore, a magneto-telluric on the strike would seem to show an uniform earth of resistivity different from that of either medium in question. For inclined layers, the phase angle deviation from 45° would show the erroneous interpretation. But for a vertical layer, even the phase angle is nearly 45°. Here is then one more instance calling for geographical coverage.

b. Magnetic polarization

The fact that in magnetic polarization current flow lines run across boundaries separating regions of changing conductivity and that although the polarized field is continuous at the boundary its normal derivative is not, might lead one to expect a less smooth behavior for magnetic polarization than for electric polarization. This turns out to be true. The reader is referred to figs. 4-21, 4-26, and 4-27, which give results for inclined layers with dips of 45°, 90° and 135°, respectively, in the case of magnetic polarization.

The general behavior of the magneto-telluric field for several inclinations of the layers is very similar. As we approach the strike from the resistive side, the first effect is a downward flow of current which produces lower resistivities. This occurs generally around $kr = 3$ from the boundary. The minima on the apparent resistivities comes in at $kr = 2$, $kr = 1$, and $kr = 1.5$ for 45°, 90°, and 135°, respectively. As it might be expected, while for the 45° inclined layer the effect is rather strong (20% of the difference in conductivities of both media) at 90° it is reduced to about 4%, and at 135° is little more than 1%. After this minimum, we run into a region where the current is rushing to the surface and consequently produces high apparent resistivities. This maximum occurs at a $kr = 1$, $kr = 0.5$ and over the strike, for the 45°, 90° and 135° inclined layers.

Such behavior can be explained in terms of the current flow trying trying to force its way into the nearest region of higher conductivity. In the resistive side the current at depth attempts to reach the surface. For dip angles of less than 90°, the surface current near the contact tries to go down; for dip angles of more than 90° the currents at depth have to climb at a much steeper angle than for smaller dips. The result is that we get more pronounced resistivity maxima for inclined than for vertical layers. For the 45° fault, we get apparent resistivities which are twice as large as the resistivity of the less conducting medium; for 135° fault they are one and a half times larger. In comparison, the vertical fault produces a small effect, on the order of 5% of the resistivity of the less conducting medium.

In all three cases the current is moving down as we cross into the more conductive side. An exception is the 135° fault where the surface current moves down from both sides of the strike and crosses the contact essentially horizontally . Immediatly following the strike, on the conductive side, we usually run into a region with apparent resistivities smaller than the actual resistivity of the conducting medium. This effect is small for angles larger than 90° (about 1%) but for 45° it reaches 8% of the true resistivity of the conducting medium. By $kr = 1.5$, $kr = 2$ and $kr = 3$, for 45°, 90°, and 135° , respectively, the boundary effects cease to be detectable.

The above results are partially confirmed by modelling work. A model involving a vertical bed over a nonconducting substratum (fig. A-3) showed the same sequence of apparent resistivities from the resistive to the conductive medium, namely, the minimum followed by the maximum and decreasing values as we went across the contact. Another scale model, that of a buried cylinder near the surface (fig. 2-6) again showed the minimum in the apparent resistivity at a kr between 3 and 2 from the cylinder, followed by the maximum close to the cylinder boundary.

Let us turn our inquiry from the geographic response, to the frequency response of the magneto-telluric field in a given locality. The previous results show that in the resistive side, the inclined layer will produce changes in the apparent resistivity resembling those due to a three layer earth (or even a four layer earth, if the minimum is pronounced); such a layered earth will in general appear to have a very conductive bottom layer and a very resistive middle layer. On the conductive side, as the angle of dip goes beyond 90°, a response like that of a three layered earth, of small conductivity contrast and with a resistive bottom layer and a conductive middle layer, will be obtained; for smaller inclinations of the beds the number of layers will appear to be two, with a conductive bottom layer(correspondingly in the resistive side it will look like a 4 layer earth). In all these cases, however, the phase angles will show that the layered earth interpretation is wrong.

Finally, we may add that if the location is on the strike, the apparent resistivities will be unchanged throughout the frequency spectrum. This response might be taken for that of a uniform earth, if it were not for the values assumed by the phase angles.

APPENDIX I

A SCALED DOWN MODEL FOR THE MAGNETO-TELLURIC FIELD

1.1 An analogue model for the magneto-telluric field

At the beginning of this investigation, it was thought that much information regarding the behavior of the magneto-telluric field could be obtained from a scaled down model. Unforeseen difficulties restricted the value of the model and reliable results were obtained for only two geometries. However, this data is well worth reporting on account of the complete lack of results regarding plane waves in two dimensional geometries. It provides confirmation of the field behavior predicted by the finite difference methods of chapter IV as well as an inquiry into the possibilities of model work.

The first question to be taken is the manner by which the magneto-telluric field was simulated in the laboratory. The problem consisted in producing a field analogous to that associated with incident plane waves in the earth. As discussed in section 2.3 this field is characterized by horizontal and uniform current flow in a homogeneous earth. The idea of transmitting antennas or other methods involving electromagnetic coupling between sender and ground, was ruled out on the basis of the resulting low level signal, interference from objects in the laboratory and restrictions on the distance at which the antennas could be placed. Instead, a system relying on conductive coupling was adopted. This

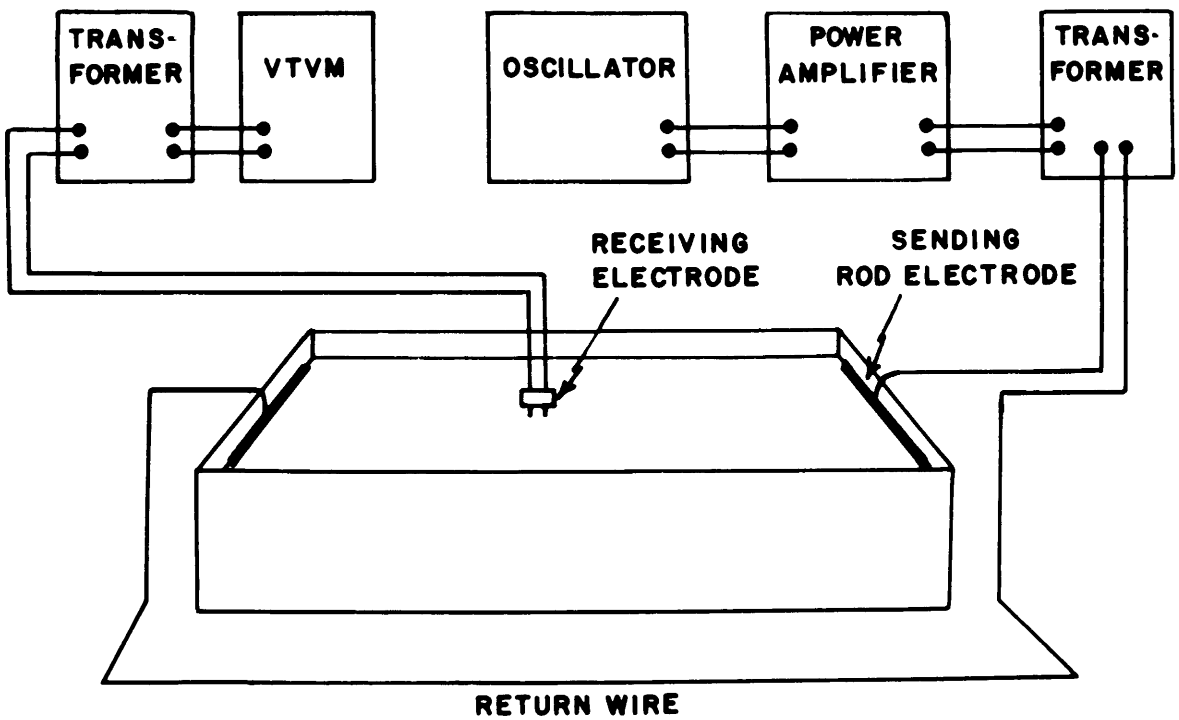

SCALED DOWN MODEL FOR THE
MAGNETO-TELLURIC FIELD

FIG.A-1

consisted of two horizontally lying rod electrodes, parallel to each other, located at each end of the model tank and buried just beneath the surface (fig. A-1).

The sending electrodes were 2 feet apart and the model measurements were carried along a one foot center strip, running perpendicular to the rod electrodes. There was provision for checking the lateral uniformity of the field through 2 parallel lateral strips, 4 inches to each side of the central strip.

The receiver was a dipole with a one centimeter separation between electrodes. High frequency coaxial wire was used in the receiving system as well as everywhere possible, but the need for a return wire between sending electrodes posed serious electromagnetic coupling problems. In speaking of these coupling difficulties, we must bear in mind that the voltages measured were extremely small, on the order of tenths of millivolts. Thus a very small amount of electromagnetic coupling was enough to spoil the measurements. Whenever using metallic model materials, we were restricted to frequencies below 250 kylocycles; even at lower frequencies care had to be exercised in the layout of wires and some of the larger decoupling transformers could not be used due to induction in their highly permeable cores. With more resistive materials, such as sand with a saturated NaCl solution, electromagnetic coupling became less of a problem.

With appropriate precautions, percentage changes in the field for a homogeneous half space of the order of 10% from a point at the center of the tank to the point nearest to the rod sender, were achieved. This deviation from uniformity posessed always a trend towards higher apparent resistivity at the outer ends of the measuring strip. Such behavior could be thought to be connected with the gradual adaptation of the current coming out of the rod electrodes to horizontal flow. However, the fact that the percentage change in the apparent resistivities from the center to the ends went also up with frequency seems rather to point to electromagnetic coupling effects.

As referred above, the frequency response of the half space, within the measuring strip, agreed with expected behavior of a plane wave field up to frequencies of 250 kylocycles whenever very conductive material was used, which was most of the time. Above this frequency, the ever present electromagnetic coupling masked completely the plane wave field.

It should be mentioned that the intrumentation of fig. A-1 was done by T. R. Madden, D. A. Fahlquist, and the author, for the model research connected with the A. E. C. contract AT(05-1)-718

1.2 The size of model

In obtaining a scaled down model of the earth, the electrodynamic similitude relationships of section 4.4 must be upheld. These relationships state the need to keep certain ratios between the dimensions of length, frequency and conductivity. In our case, practical considerations dictated the first restriction, a restriction on the length dimension. The problems of interest were the large scale geologic features (such as inclined layers) for which the existing large tank was unsuitable; the possibility of building a self supporting surface of contact between two different electrolytes, with dimensions 5' x 6',

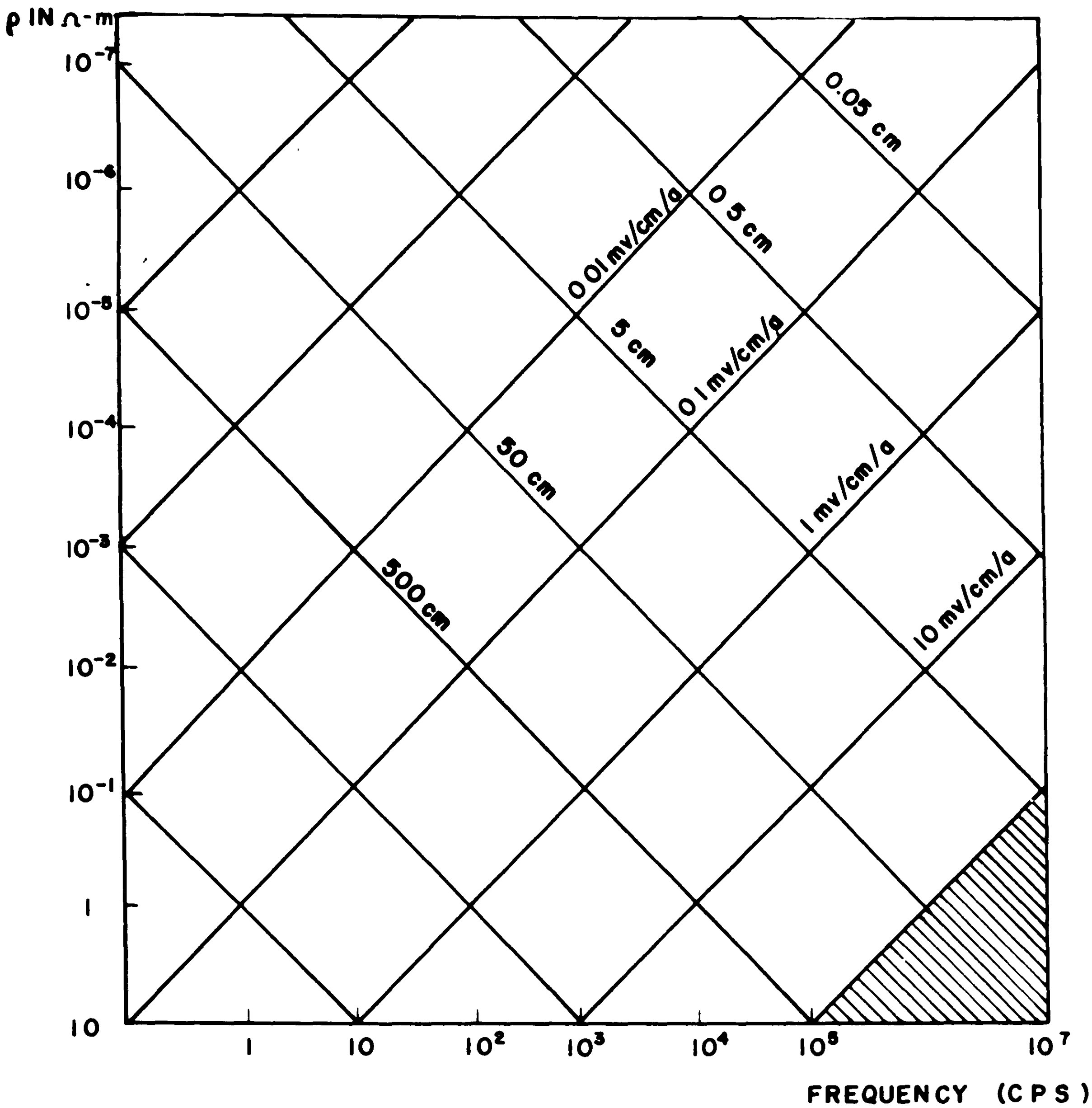

DISPLACEMENT CURRENTS LARGER THAN 0.5% OF CONDUCTION CURRENTS.

mv/cm/a = MILLIVOLT/CENTIMETER/AMPERE

SKIN DEPTH IN CENTIMETERS

SKIN DEPTHS AND SIGNAL LEVEL IN FUNCTION OF RESISTIVITY AND FREQUENCY

FIG. A-2

without introducing extraneous electrical properties at the contact appeared very dim indeed. In this manner, we were led to the consideration of a small model. Here a few calculations show us that the choice is rather restricted. The reader is now referred to fig. A-2 in which the parameters of importance are presented graphically. One of the restrictions is of course how small a voltage one can measure. Without going into extremely complex instrumentation, we cannot expect to measure below 0.1 mv. At the same time currents of a few amperes, 2 or 3 should be considered the maximum, on account of heating and contact problems. Since the wanted receiving electrode separation should be on the order of centimeters, we see that we will have to work in the region below the line 0.1 mv/cm/a in fig. A-2. From the lines for skin depth, we get our model size. The amount of material needed as well as the "structural" problems just mentioned lead us to choose a size corresponding to skin depths of about 5 cm. Electromagnetic coupling effects, the relaxation time of electrolytes (important at about 10^9 cps) and displacement currents force us to use frequencies of less than 10^6 cps. We see therefore that we are thus restricted to a region calling for conductivities on the range of 10^2 to 10^4 and frequencies between 5×10^4 and 10^6. These requirements, plus those connected with allowance for wall effects were satisfied by a 2' x 1'x 1/2' model tank which had been built for the A. E. C. project previously mentioned and which we were kindly permitted to use.

1.3 Model materials

We have just seen how we were confined to work with materials on the 10^{-2} to 10^{-4} ohm-mater range. In looking for natural occurring substances having these electrical properties, we find that these consist largely of sulfides (table V). Unfortunately, sulfides do not come in large homogeneous blocks, one foot by one foot by a half. The alternative was then to achieve such conductivities by the use of mixtures of metals and appropriate fillers. An extensive investigation aimed at developping a workable mixture was carried by the M. I. T. group and most results have been reported in the annual progress report (T. R. Madden et al, 1957). The results were not completely satisfactory. Brass filings, in saturated NaCl solution to provide better contacts and more homogeneous distribution of current, had about the right conductivity and the best frequency response characteristics, but these were far from ideal. The following measurements illustrate the main difficulty with brass fillings. Just after they were laid down:

frequency	100	1kc	10kc	100kc	200kc	400kc	600kc
$(\Omega\text{-m})\times 10^{-3}$	2.2	2.2	2.2	2.1	2.1	2.1	2.1

One day later:

$(\Omega\text{-m})\times 10^{-3}$	0.76	0.76	0.75	0.762	0.78	0.83	0.93

T. R. Madden has suggested that as the material settles and becomes more conductive, an inductive component of its impedance becomes noticeable. Such an inductive component could be produced by the self-inductance of the brass fillings resulting from the fact that the current paths are not

TABLE IV

HIGH CONDUCTIVITY

Substance	Resistivity (r-m)
copper	1.73×10^{-8}
aluminum	$3.66 - 5.8 \times 10^{-8}$
brass	$6.4 \times 8.4 \times 10^{-8}$
nickel	9.6×10^{-8}
iron	1.2×10^{-7}
Dow metal	1.83×10^{-7}
lead	2.27×10^{-7}
monel	4.55×10^{-7}
stainless steel	7.1×10^{-7}
graphite	1.4×10^{-5}

MEDIUM CONDUCTIVITY

magnetite	3.6×10^{-4}
pyrite	2.4×10^{-4}
galena	2×10^{-3}
specularite	$3 - 7 \times 10^{-3}$
marcasite	1×10^{-1}

TABLE IV (cont.)

LOW CONDUCTIVITY

Substance	Resistivity (r-m)
5N NaCl	5×10^{-2}
6N KCl	2×10^{-2}
3N $MgSO_4$	2×10^{-1}
Salt water	2×10^{-1}
Tap water	50

straight. Simple calculations on the basis of a model of loosely wound parallel coils predicts frequency response difficulties for current flow paths of 1 cm radius, one turn for each 4 cm length, and materials of resistivity smaller than 10^{-3} in the 100,000 to 500,000 cps range (T. R. Madden et al, 73, 1953)

Other effects that had to be taken into account were induced polarization and heating. The former, arising from the conversion from ionic to electronic current flow, became conspicuous whenever large surface contacts between electrolyte and metal existed. The latter derived from the necessity of using high currents to obtain readable voltages and produced a rather steady drift with time of the volt-ampere ratios.

Finally reference should be made to the relative size of the brass filings, which ranged between 1/5 to 1/10 of the electrode separation. The resulting many possible arrangements of ohmic paths between electrodes introduced a scatter on the measured apparent resistivity. In extreme cases this scatter reached 10% of the volt-ampere ratio being measured. Since the resistivity is proportional to the square of the volt-ampere ration, one can see how difficult it would be to detect small frequency effects.

Until great improvements are made on the materials, models of the type desired for our purposes will only yield results in cases where spectacular effects are present. This is true of the model structures described in the next section.

1.4 The magneto-telluric field in specific model structures

1.4.1 Vertical layer geometry

All the model work was done with magnetic polarization, that is, with the current running normal to the strike of the structures. In the vertical layer model, brass in a saturated solution of NaCl was used for the more conductive quarter space and sand with the same NaCl solution for the adjoint less conductive side of the vertical layer geometry. The conductivity contrast was about 200.

The results of fig. A-3, show us the behavior of the current flow as it is forced to come nearer to the surface in the more conductive quarter space. This behavior is not totally expected but agrees with that predicted by the finite difference solution. Rather than just rushing nearer to the surface as it approaches the boundary of the more conductive medium, the current actually dips down a short distance before the boundary. This produces a minimum in the apparent resistivity with values lower than the actual resistivity of the less conducting medium. Only very close to the vertical layer does the current concentrate near the surface causing a maximum in the apparent resistivity. In our particular case the minimum was on the order of 65% of the actual resistivity while the maximum was only about 15% above the resistivity of the medium. Just before crossing the boundary from the resistive to the conductive medium, the surface current is moving downward again; apparently, in adapting itself to the more conductive region, the current initially concentrates nearer to the surface than it would on a homogeneous medium of equal conductivity. Thinking in terms of wave

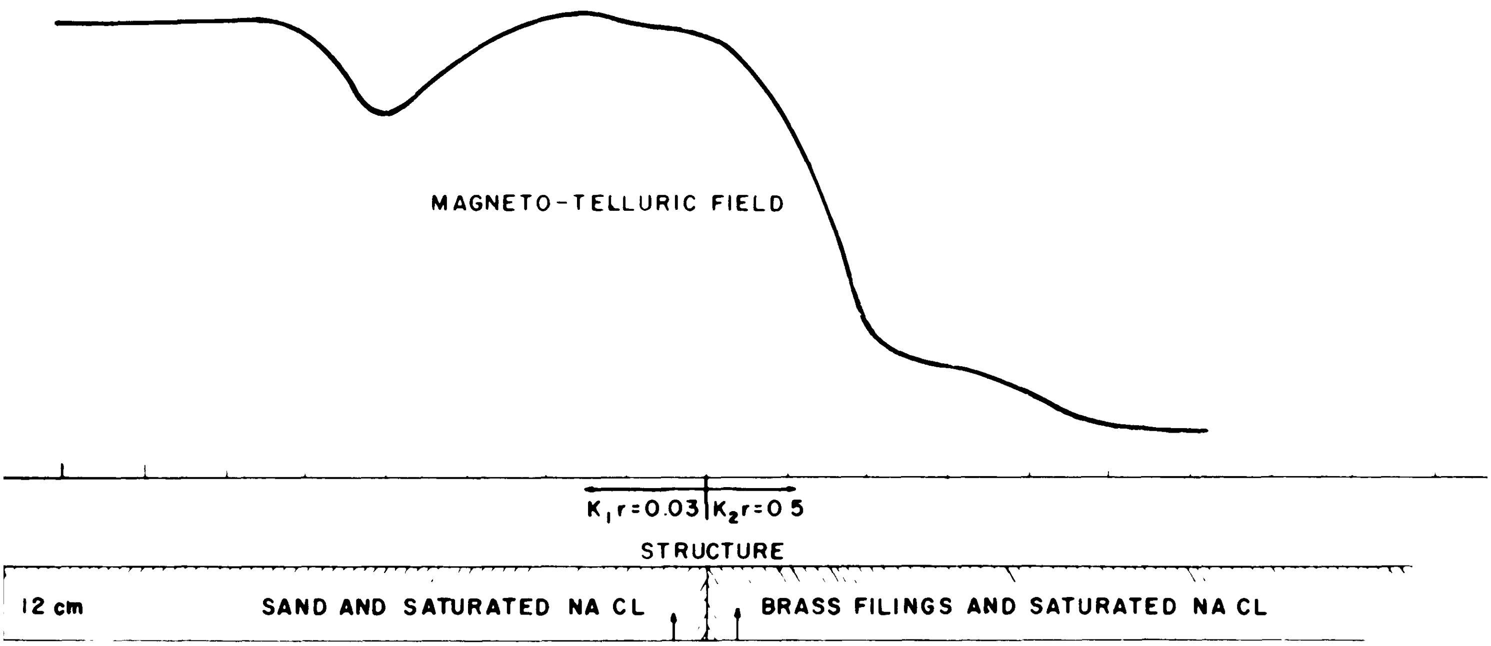

LISTING OF APPARENT RESISTIVITIES VS. FREQUENCIES

1 cm

																	FRE
57	55		52.4	33	46	62	51	49								0 163	6
90	85	90	78	490	675	928	79	71	9								4
115	110	115	104	658	917	116	98	95	12							0 164	3
165	160	165	147	955	132	167	142	142	185	1.5	0.82	0.48	0.23	0.26		0 172	2
253	250	268	235	156	227	280	238	245	40	2.5	0.92	0.47	0.20	0.23	0.27	0.15	1
310	310	310	284	206	298	360	470	482	90	5.2	1.3	0.60	0.19	0.21	0.22	0.16	[illegible]
									194	14.4	3.4	1.44	0 32	0.28	0 28	0 24	[illegible]

VERTICAL LAYER OVER A NONCONDUCTING SUBSTRATUM (SCALE MODEL) ρa IN 10^{-3}

FIG-A-3

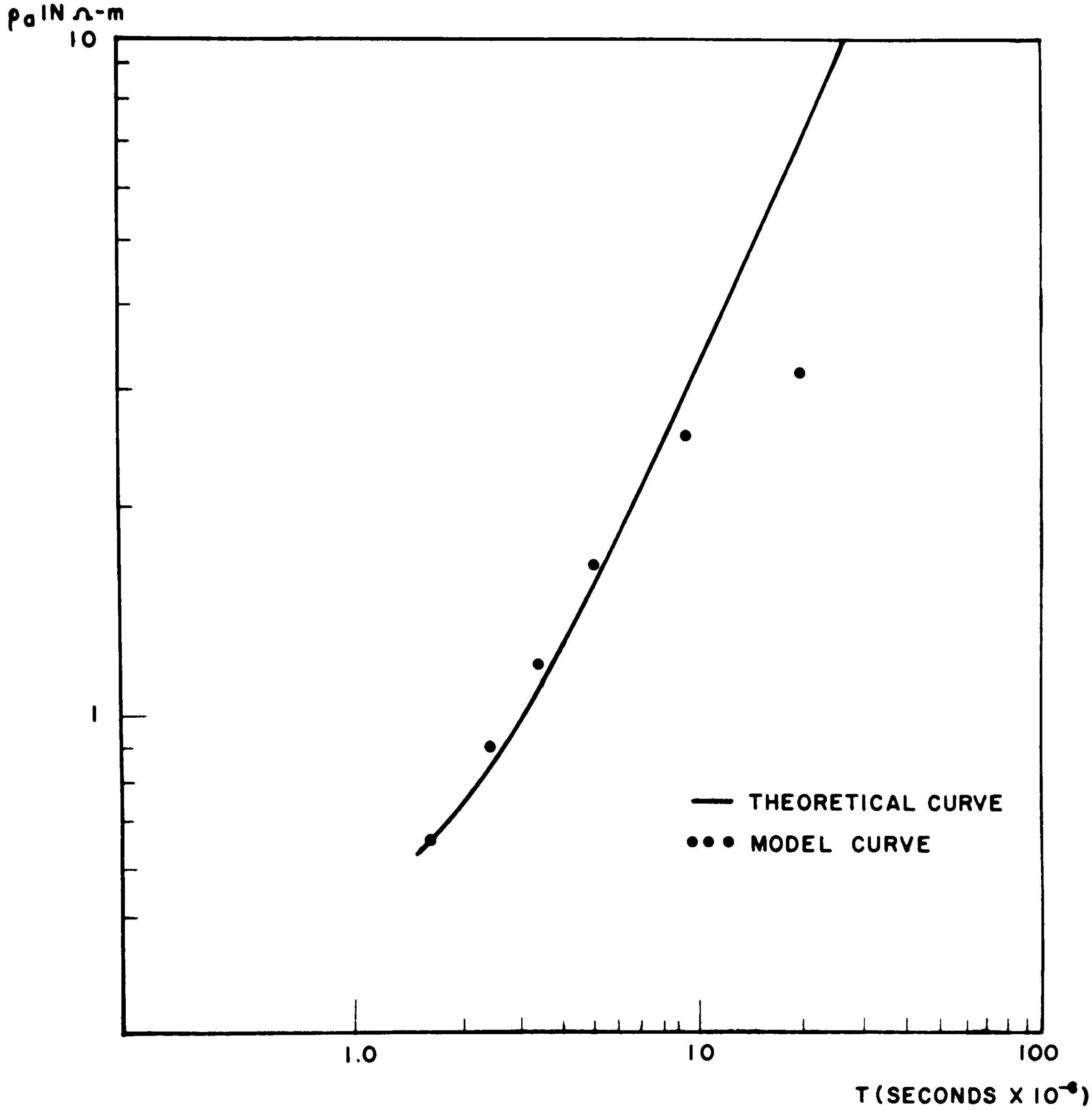

THEORETICAL RESPONSE OF A TWO LAYER EARTH WITH A NONCONDUCTIVE BOTTOM LAYER AND A 12 cm TOP LAYER COMPARED WITH THE RESPONSE OF THE MORE RESISTIVE SIDE OF THE VERTICAL LAYER MODEL OF FIG. A-3

FIG. A-4

propagation, we recognize in this the familiar "source" effect characteristic of corners. Finally at a distance corresponding to a kr of about 3 (away from the fault, in the conductive side) the current flows like in a homogeneous earth, without being affected at all by the vertical layer. We have seen therefore that the field behaves in a distinct fashion from one medium to the other. Approaching the vertical layer from the conductive side the surface current just moves upward; approaching from the resistive side, the surface current goes through a complete cycle in the direction that it takes. We may note again that this confirms the relaxation results.

A point we have not discussed is the frequency dependence of the apparent resistivities in the less conductive side of the model of fig A-3. A consideration of the frequency and conductivities involved leads one immediately to suspect that the frequency dependence arises from reflections from the bottom of the model tank; on the more conductive side, where skin depths are a fraction of the depth of the depth of the tank, these effects are not found. A comparison between the theoretical response of a layer with the depth and conductivity of the resistive quarter space, overlaying a non-conductive bottom layer, fits very closely the model results (fig. A-4). Therefore it might be more appropriate to label the model in question a vertical layer overlying a non-conductive horizontal bottom layer.

1.4.2 Buried cylinder geometry

This model was prepared partly to show the interpretative possibilities of the magneto-telluric method. For a map of results the reader is referred to fig. 2-6.

Probably the most important result from this model is a further confirmation of the nature of current flow when it runs into horizontal changes in conductivity. Again, as we approach the more conductive body from the less conductive one, we go through a minimum in the apparent resistivity, followed by a maximum just before reaching the boundary. It is rather interesting to notice that the minimum occurs at a distance from the cylinder for which kr is between 3 and 2, a result that agrees with that of the finite difference solution for a vertical layer with infinite contrast.

APPENDIX II

WAVE FIELDS WITHIN THE EARTH

2.1 Relaxation maps.

This section contains all the complete solutions of the electromagnetic field within the earth. It was from these solutions that the examples of section 4.6 were obtained.

We are including the complete solutions on the appendix for various reasons. They may be used as starting points for finer nets and more accurate solutions. As they are, the maps show the degree of accuracy to which the relaxation process was taken in the different regions. Further, from them, one can find the general patterns of the electromagnetic field within the earth. Of course one must be aware of the existence of a certain amount of distortion, arising from reflections from the boundary at which the solution was constrained to zero. All these are points of interest not only regarding the present work, but also, as far as future investigations may be concerned.

It may be added that in plotting the maps, the top number refers to solution A and the bottom one to solution B; the total solution, as before, is $u = A + iB$. The dimensions are indicated in the map, but it should be kept in mind that equidimensional horizontal and vertical separations are being used. The station numbers are indicated at the top of the map.

2.2 Vertical layer: electric polarization

1	2	3	4	5	6	7	8	9	10
100 0	100 0	100 0	100 0	100 0	100 0	100 0	100 0	100 0	100 0
53.0 28.2	52.9 27.6	52.8 26.7	51.4 25.7	47.0 25.5	34.5 29.5	23.3 29.9	21.2 28.0	21.1 27.3	21.3 27.2
20.1 29.7	20.3 28.9	20.4 27.5	19.1 25.7	14.8 23.0	4.3 20.3	-3.0 14.9	-3.7 12.3	-3.14 11.8	-2.94 11.8
2.13 21.3	2.53 20.7	2.8 19.3	2.7 17.2	0.6 14.0	-4.0 8.9	-5.8 3.8	-4.9 1.9	-4.17 1.8	-3.67 2.2
-5.03 12.2	-4.74 11.8	-4.2 10.9	-3.6 9.17	-3.5 6.8	-4.2 3.0	-3.3 -0.1	-2.2 -0.7	-1.4 -0.4	0 0
-6.2 5.32	-5.9 4.32	-5.3 4.67	-4.4 3.7	-3.5 2.5	-2.9 1.3	-1.7 -0.2	-0.7 -0.5	0 0	
-4.69 1.58	-4.5 1.58	-3.8 1.5	-3.0 1.0	-2.1 0.5	-1.4 0	-0.6 -0.2	0 0		
-2.4 0.19	-2.2 0.19	-1.9 0.19	-1.4 -0.3	-0.8 -0.4	-0.4 -0.3	0 0			
0 0	0 0	0 0	0 0	0 0	0 0	0 0			

$\longleftarrow k_1 r = 1$ | contact | $k_2 r = 1 \longrightarrow$

2.3 Vertical Layer: magnetic polarization

1	2	3	4	5	6	7	8	9	10	11	12
100 0	100 0	100 0	100 0	100 0	100 0	100 0	100 0	100 0	100 0	100 0	100 0
53.0 28.2	52.7 28.2	52.4 28.2	52.1 28.8	51.8 31.1	55.1 37.7	44.8 34.2	22.2 24.3	21.8 27.3	21.5 27.2	21.3 27.2	21.3 27.2
20.1 29.9	19.5 29.9	19.0 29.8	18.1 30.2	16.87 32.2	15.8 37.6	9.67 31.0	-1.2 12.4	-2.5 12.5	-2.7 11.9	-2.94 11.8	-2.94 11.8
2.13 21.6	1.53 21.6	0.9 21.2	-0.1 21.1	-1.9 21.5	-5.06 23.7	-5.99 17.8	-4.1 3.2	-4.0 2.15	-3.9 1.7	-3.97 1.9	-3.67 2.2
-5.04 12.2	-5.43 12.18	-6.19 11.5	-6.9 10.8	-8.25 10.4	-10.9 9.95	-9.6 6.3	-2.5 -0.4	-1.6 -0.7	-1.5 -0.6	-1.04 -0.2	0 0
-6.2 5.32	-6.5 5.32	-7.1 4.7	-7.56 3.9	-8.6 2.8	-10 1.4	-8.1 -0.1	-0.9 -0.9	0 -0.7	0 -0.5	0 0	
-4.69 1.58	-4.69 1.58	-4.9 1.2	-5.3 0.4	-5.8 -0.6	-6.8 -1.8	-5.0 -2.2	-0.5 -0.9	0 -0.6	0 0		
-2.4 0.19	-2.4 0.19	-2.3 -0.05	-2.6 -0.5	-2.8 -1.1	-3.2 -1.6	-2.3 -1.6	-0.1 -0.5	0 0			
0 0	0 0	0 0	0 0	0 0	0 0	0 0	0 0				

$k_1\ r = 1$ contact $k_2\ r = 1$

2.4 Vertical layer: infinite contrast

8	7	6	5	4	3	2	1
100 0	100 0	100 0	100 0	100 0	100 0	100 0	100 0
53.0 28.2	53.0 28.2	53.0 27.7	53.2 27.1	52.8 25.5	50.1 21.5	40.3 16.4	0 0
20.1 29.9	20.1 29.9	20.2 29.4	20.6 28.5	20.5 26.5	19.1 21.8	13.8 12.9	0 0
2.13 21.6	2.13 21.6	2.3 21.5	2.9 21.0	2.7 19.9	4.0 15.3	3.3 8.69	0 0
-5.03 12.2	-5.03 12.2	-4.4 12.2	-3.5 12.1	-2.8 11.2	-1.3 8.6	-0.1 5.0	0 0
-6.2 5.3	-5.9 5.3	-5.2 5.6	-4.4 5.7	-3.6 4.9	-2.4 4.1	-1.0 2.3	0 0
-4.69 1.58	-4.39 1.58	-3.5 1.9	-3.2 2.2	-2.7 2.1	-1.9 1.5	-0.7 0.8	0 0
-2.4 0.19	-2.4 0.19	-2.0 0.45	-1.6 0.6	-1.3 0.5	-0.9 0.5	-0.4 0.3	0 0
0 0	0 0	0 0	0 0	0 0	0 0	0 0	0 0

$\leftarrow$ Kr = 1 contact

2.5 Vertical layer in contact with a non-conducting medium

1	2	3	4	5	6	7	8	9	10	11	12	13
100	100	100	100	100	100	100	100	100	100	100	100	100
0	0	0	0	0	0	0	0	0	0	0	0	0
53.0	53.0	52.8	52.5	52.3	51.9	51.6	51.8	52.9	56.9	64.8	79.0	
28.2	28.2	28.2	28.2	28.0	28.3	29.0	30.2	32.1	33.8	34.2	27.1	
20.1	20.1	19.8	19.3	18.8	18.0	17.6	17.8	19.9	26.6	40.5		
29.9	29.9	29.9	29.6	29.6	30.1	31.3	33.6	37.0	41.1	42.8		
2.13	2.13	1.73	1.13	0.43	-0.5	-1.2	-1.1	1.35	9.3			
21.6	21.6	21.3	20.9	21.1	21.8	23.4	26.5	28.6	37.4			
-5.03	-5.04	-5.33	-6.23	-7.24	-8.3	-9.2	-9.2	-6.9				
12.2	12.0	11.6	11.4	11.5	12.2	14.1	17.8	23.7				
-6.2	-6.5	-7.0	-7.6	-8.6	-9.6	-10.8	-11.3					
5.32	5.12	4.62	4.02	4.12	4.92	6.5	10.8					
-4.69	-4.99	-5.69	-6.39	-7.5	-8.59	-10.9						
1.58	1.18	0.48	-0.22	-0.52	-0.12	2.08						
-2.70	-3.3	-3.4	-4.9	-6.0	-7.3							
0.19	-0.21	-1.0	-1.7	-1.9	-2.0							
0	-1.8	-2.5	-3.5	-4.6								
0	-0.4	-1.1	-1.8	-1.7								
	0	-1.2	-2.9									
	0	-0.8	-1.6									
		0										
		0										

k r = 1

contact

2.6 Inclined layer 45°: electric polarization

1	2	3	4	5	6	7	8	9	10	11	
100 0	100 0	100 0	100 0	100 0	100 0	100 0	100 0	100 0	100 0	100 0	100 0
53.0 28.2	53.0 28.2	53.2 27.9	53.2 27.0	52.6 25.8	50.5 24.1	45.1 23.6	33.7 27.8	23.7 29.0	21.5 27.8	21.3 27.4	21.3 27.2
20.1 29.9	20.1 29.9	20.6 29.1	20.7 27.5	20.0 25.3	16.7 22.3	8.5 20.0	1.0 16.4	-2.3 13.1	-3.14 12.16	-2.94 11.8	-2.94 11.8
2.13 21.6	2.13 21.6	2.53 20.3	3.2 18.3	2.3 15.2	-0.8 11.5	-3.5 7.0	-4.3 4.0	-3.87 2.3	-4.18 2.2	-4.08 2.2	3.68 2.2
-5.03 12.2	-5.03 12.2	-4.2 10.7	-3.5 8.4	-3.9 5.1	-3.6 2.3	-2.8 0.2	-2.2 -0.7	-1.6 -0.8	-1.4 -0.4	0 0	0 0
-6.2 5.32	-6.0 5.0	-5.0 3.7	-3.1 1.4	-2.8 -0.3	-1.7 -0.9	-0.9 -0.8	-1.0 -1.0	-0.4 -0.8	0 0	0 0	
-4.7 1.58	-4.0 1.2	-3.0 0	-1.7 0	-1.1 -0.8	-0.5 -0.7	0 -0.4	0 0	0 0	0 0		
-2.4 0.19	-1.7 -0.3	-1.0 0.7	-0.5 -0.5	-0.4 -0.4	-1.1 -0.8	0 0	0 0	0 0	0		
0 0	0 0	0 0	0 0	0 0	0 0	0 0	0 0				

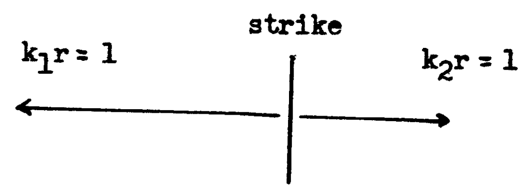

2.7 Inclined layer 135°: electric polarization

1	2	3	4	5	6	7	8	9	10	11	12
100	100	100	100	100	100	100	100	100	100	100	100
0	0	0	0	0	0	0	0	0	0	0	0
53.0	52.5	51.0	46.9	35.0	23.2	20.9	21.1	21.3	21.3	21.3	21.3
28.2	27.7	27.0	26.8	31.3	31.2	28.2	27.2	27.4	27.2	27.2	27.2
20.1	19.6	18.1	15.1	8.7	-0.4	-4.1	-3.6	-3.0	-2.94	-2.94	-2.94
29.9	29.1	27.7	25.9	23.7	19.3	13.6	11.5	11.2	11.6	11.8	11.8
2.13	2.13	1.23	-0.2	-2.67	-5.2	-6.3	-4.9	-4.1	-3.8	-3.68	-3.68
21.6	20.6	19.4	17.4	14.3	9.6	4.2	1.2	1.1	1.4	1.8	2.2
-5.03	-5.03	-5.3	-5.5	-5.9	-5.9	-5.2	-3.3	-1.8	-1.3	-1.0	0
12.2	11.5	10.4	9.1	6.9	3.9	0.8	-1.4	-1.4	-1.0	-0.5	0
-6.2	-6.2	-6.2	-6.2	-5.7	-4.8	-3.9	-2.5	-1.1	-0.1	0	0
5.32	5.32	4.32	3.52	2.52	0.8	-0.2	-1.0	-1.3	-0.5	0	0
-4.7	-4.7	-4.7	-4.7	-4.2	-3.6	-2.7	-1.5	-0.5	0	0	0
1.58	1.58	1.58	1.1	0.3	-0.3	-0.1	-0.45	-0.5	0	0	0
-2.4	-2.4	-2.4	-2.4	-2.4	-2.4	-2.0	-0.9	0	0	0	0
0.19	0.19	0.19	0.19	0.19	-0.3	0.15	0.1	0	0	0	0
0	0	0	0	0	0	0	0	0	0	0	0
0	0	0	0	0	0	0	0	0	0	0	0

strike

contact

$k_1 r = 1$ ← | → $k_2 r = 1$

2.8 Inclined layer 45°: magnetic polarization

1	2	3	4	5	6	7	8	9	10	11	12	13	14
100	100	100	100	100	100	100	100	100	100	100	100	100	100
0	0	0	0	0	0	0	0	0	0	0	0	0	0
53	52.5	51.8	50.7	49.3	48.5	51.1	63.2	59.4	11.8	20.8	21.6	21.3	21.3
28	27.7	27.4	27.7	29.2	33.5	41.4	51.8	35.4	17.5	23.9	26.4	27.2	27.2
20.1	19.3	17.9	15.8	12.7	10.3	13.3	20.4	0.5	-2.9	-2.5	-2.54	-2.94	-2.94
29.4	28.6	28.2	28.7	31.6	39.7	55	48.5	11.3	8.5	10.1	11.3	11.8	11.8
2.13	1.132	-1.17	-4.3	-8.9	-13.3	-7.8	-2.9	-3.5	-3.7	-3.68	-3.68	-3.68	-3.68
20.8	19.5	18.8	19.4	23.3	33.8	34.5	7.4	3.0	1.5	1.5	1.9	2.2	2.2
-5.03	-6.34	-8.9	-13.1	-19.4	-16.3	-4.8	-2.9	-1.9	-1.5	-1.5	-1.5	-1	0
12.2	9.68	8.3	8.3	12,3	15.2	2	0.6	-0.5	-0.5	-0.5	-0.2	0	0
-6.2	-7.8	-11.2	-16.1	14.7	-3.3	-1.8	-0.5	0.1	0	-0.3	0	0	
4.12	2.12	0.12	-1.2	0.5	-0.5	-1	-0.8	-0.5	-0.3	-0.2	0	0	
-4.70	-4.7	-6.195	-9.7	-9.8	-1.5	-0.5	0	0	0	0	0		
1.58	0.38	-1.22	-4.7	-4.2	-1.8	-1.1	-0.4	0	0	0	0		
-2.4	-2.4	-3.7	-4.5	-0.7	0	0	0	0	0	0			
0.19	-0.81	-2.59	-4.4	-1.3	-0.8	-0.5	0	0	0	0			
0	0	0	0	0	0	0	0	0	0				
0	0	0	0	0	0	0	0	0	0				

contact

strike

$\xleftarrow{k_1 r = 1}$ | $\xrightarrow{k_2 r = 1}$

2.9 Inclined layer 45°: magnetic polarization

1	2	3	4	5	6	7	8	9	10	11	12	
100 0	100 0	100 0	100 0	100 0	100 0	100 0	100 0	100 0	100 0	100 0	100 0	
53 28.2	53 28.8	53.2 30.3	55.4 34.3	65.7 45	32 45.4	20.5 24.4	21.4 26.4	21.2 27	21.3 27.2	21.3 27.2	21.3 27.2	
20.1 29.9	20.1 30.5	19.5 31.7	19 33.5	17.6 39.3	6.5 45.7	-7.3 27.5	-3.5 11.4	-3.62 12	-2.94 11.8	-2.94 11.8	-2.94 11.8	
2.13 21.6	2.13 21.9	1.33 22.4	0.33 22.9	-2.1 24.2	-8 23.1	-14.8 17.8	-12.7 5.1	-5 1.6	-4 1.96	-3.68 2.2	-3.68 2.2	
-5.03 12.2	-5.03 12.2	-5.5 12.4	-6.23 12.48	-7.73 12.48	-10 9.4	-11.8 2.6	-12.8 2.2	-7 -5.7	-1.6 -1.5	-1.6 -0.8	-1.2 0	
-6.2 5.32			-6.2 5.32	-6.6 4.52	-7.2 2.72	-7.8 -1.2	-7.1 -4.4	-5.6 -8.1	-2.3 -5.6	-0.2 -0.9	0 -0.4	
-4.7 1.58			-4.7 1.58	-4.7 1.08	-4.7 0.38	-4.7 -1.72	-4 -3.5	-2.9 -6.5	-1.7 -5.6	-0.4 -3.1	0 -0.4	
2.4 0.19			2.4 0.19	2.4 0.19	-2.4 -0.31	-2.4 -1.2	-1.9 -1.81	-1.5 -2.2	-0.8 -2.4	-0.4 -2.4	0 -1	contact
0 0	0 0	0 0	0 0	0 0	0 0	0 0	0 0	0 0	0 0	0 0	0 0	

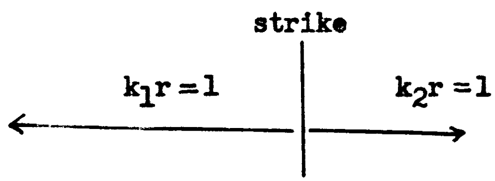

SUGGESTIONS FOR FURTHER WORK

The sequel to any investigation is the appearance of new problems related to those studied. Two of the more evident topics are:

1. The adaptation of the finite difference method of chapter IV to a high speed computer. Only then we can solve the host of geometries that will give us a sure feeling for the behavior of the magneto-telluric field.

2. The integration of the formal solutions for the inclined layer problems.

BIBLIOGRAPHY

ALLEN, D.N., 1954, RELAXATION METHODS, McGraw Hill Bk. Co., N.Y.

ALPERT, Ia. L., GINZBURG, V.L., FEINBERG, E.L., 1953, Field over an inhomogeneous plane earth. Part I: Theory of radiowave propagation along the earth's surface. Gosudarstvennoe Izdatel' stvo Teniko-Teoreticheskoi Literatury, Moscow.

BEAUFILS, Y., 1952, Repartition spectrale des variations rapides dans les courants telluriques. Ann. de Geoph., tome 8, 100-104.

BONDARENKO, A.P., 1953, Correlation between telluric currents and geomagnetic variations (in Russian). Akad. Nauk S.S.S.R. Doklady, tom 89, no.3, 443-445.

__________, 1953, Electric field induced by vertical component of geomagnetic variations. Akad. Nauk S.S.S.R. Doklady, tom 90 no.3, 367-370.

BOWKAMP, C.F., 1954, Diffraction theory. Rep. on Progress in Physics (The Physical Society of London) 17, 35-100.

BREMMER, H., 1954, The extension of Sommerfeld's formula for the propagation of radio waves over a flat earth to different conductivities of the soil, Physica XX, no.8,441-572.

BURKHART, K. 1951, Earth current investigation at the Furstenfeld-bruck Magnetic Observatory (in German) Geofisica Pura e Appl. 19, no.1-2, 19-38,

CARDUS, J.O. 1950, Sobre la ley de las fases en las corrientes teluricas. Rev. Geofisica, 9, no. 35, 215-233.

CAGNIARD, L. 1956, "Electricite tellurique" Handbuch der Geophysik vol. 17, 407-468, Verlag Julius Spenger

CLEMMOW & BOOKER, 1950, Sommerfeld theory and straight edge diffraction theory. Proc I.E.E., 97, partIII 21.

__________,1950, The concept of angular spectrum of plane waves and its relation to that of polar diagram and aperture distribution. Proc. I.E.E., 97, part III, 11,

CLEMMOW, P.C., 1951, A method for the exact solution of a class of 2-dimensional diffraction problems. Proc. Royal Society of London, A 205, 286.

_________, 1953, Radio propagation over a flat earth across a boundary separating two different media. Phil. Trans. Royal Soc., A 246, 1-55.

_________, 1950, The diffraction of a cylindrical wave by a perfectly conducting half plane. Quart. J. of Mech. and Appl. Math. 3, 377.

_________, 1950, Some extensions to the method of integration by steepest descents. Quart. J. of Mech and Appl. Math 3, 241.

CUNNINGHAM, J., 1957, Instrumentation for the magneto-telluric method. B. Sc. thesis, Dept. Geol. and Geoph., M. I. T.

DOUGALL, J., 1899-1900, The determination of Green's functions by means of spherical harmonics. Proc. of Edinburgh Math. Soc. XVIII, 33-84.

DURAND, E., 1953, ELECTROSTATIQUE ET MAGNETOSTATIQUE, Masson et Cie., Paris.

DUPOUY, G., 1950, Perturbation du champ magnetique terrestre et des courants telluriques par les chemins de fer electrifies. Ann. de Geoph. tome 6, 18-50.

ERDELYI, MAGNUS et al., 1953, HIGHER TRANSCENDENTAL FUNCTIONS, McGraw Hill Bk. Co., N.Y.

_________, 1953, TABLES OF INTEGRAL TRANSFORMS, McGraw Hill Bk. Co.

GIBAULT, G., 1952, Variations rapide du champ magnetique terrestre Ann. de Geoph., 8, 258.

GORN, S., 1953, Series expansions of rays in isotropic non-homogeneous media. Quart. Appl. Math, 11, 355-60.

GRANNEMAN, W.W. and WATSON, R.B., 1955, Diffraction of electromagnetic waves by a metallic wedge of acute diehal angle. J. Appl. Physics 26, 4.

GRAY, A.; MATHEWS, G.; MACROBERT, T.M., 1922, A TREATISE ON BESSEL FUNCTIONS, MacMillan and Co., London.

GRINBERG, G.A., 1948, Diffraction from a perfectly conducting wedge. Part IV: Wave fields 471-485. Izdatel'stvo Akad. Nauk. S.S.S.R. Moscow, Leningrad.

GUNBERG, G., 1943, Suggestions for the theory of coastal refraction. Physical Review, 63, 5 and 6

HALLOF, P., 1957, The interpretation of resistivity and induced polarization measurements. Ph.D. thesis, Dept. Geol. and Geoph. M.I.T.

IVANOV, A.G., 1951, Impulsive perturbations of telluric currents Akad. Nauk S.S.S.R. Doklady, tom 81, no.5, 807-810.

JONES, D.S., 1952, Diffraction by an edge and by a corner. Quart. J. Mech. Appl. Math. 5, 363-378.

_________, 1952, Removal of an inconsistency in the theory of diffraction. Proc. of the Cambr. Philos. Soc. 48, 737-74.

KATO, YOSHIO, and KIKUCHI, TAKEHIKO, 1950, On the phase difference of earth currents induced by the changes of the earth's magnetic field. Tohoku Univ. Sc. Rep. 5th ser. Geophysics V 2, no. 2, pt. 1, p 138-141; pt. 2, p 142-145.

KARP, S. and SOLFREY, 1950, Diffraction by a dielectic wedge. New York Uni., Math. Res. Report No. EM-23.

KONTOROVICH, M.J. and LEBEDEV, N.N., 1939, On a method of solution of some problems of diffraction theory. Acad. of Sc. U.S.S.R. Journal of Physics I, 3, 229.

KUNETZ, G., 1954, Enregistrement des courants telluriques a l'occasion de l'eclipse de soleil du 25 Febrier, 1952. Anal. Geoph. 10, 262.

_________, 1953, Correlation et recurrence des variations des courants telluriques et du champ magnetique. Actes du Congres de Lux. 72eme Ses. de l'Association pour l'Advancement des Sciences.

_________, and DE GERY, J.C., 1956, Potential and resistivity over dipping beds. Geophysics, XXI, 3, 780

LEBEDEV, N.N., 1946, Sur une formula d'inversion. C. R. Doklady Acad. Sc. U.R.S.S. (N.S.) 52, 655-658.

_________, 1947, On the representation of an arbitrary function by an integral involving Macdonald functions of complex order. Akad. Nauk S.S.S.R. Doklady (N.S.)

_________, 1949, The analogue of Parseval theorem for a certain integral transform. Akad. Nauk S.S.S.R. Doklady (N.S.) 68 653-656.

_________, 1949, On the representation of an arbitrary function by integrals involving cylinder functions of imaginary index and argument. Akad. Nauk S.S.S.R. Doklady (N.S.), Prikl. Mat. Meh. 13, 465-476.

LIPSKAYA, N.V., 1953, Some correlations between harmonics of periodic variations of terrestrial electromagnetic fields. Akad. Nauk. S.S.S.R. Izv. Serv-Geofix. 1, 41-47.

LOWAN, A.N., 1941, On the problem of wave motion for the wedge of an angle. Philos. Magaz. 7, 31, 373-381.

MADDEN, T.R., 1956, Inverse boundary value problems in Geophysics. M.I. T. Geol & Geoph. Dept., Geophysics Seminar.

_________, MARSHALL, D.; FAHLQUIST, D.; NEVES, A., 1957, Background effects in the induced polarization method of geophysical exploration. Ann. Progress Report, A.E.C. Contract At (05.1) 718, Dept. Geol & Geoph., M.I.T.

MAEDA, K., 1955, Apparent resistivity over dipping beds. Geophysics XX, 1, 123.

MIGAUX, L., 1950, Quelques exemples d'application de la methode tellurique. Int. Geol. Cong., Great Britain, 18th Session, 1948, Rept. pt. V, Proc. Sec. D, 85-95.

MILES, J.W., 1952, On the diffraction of an electromagnetic pulse by a wedge. Proc. Roy. Soc. A, 212, 547-551.

_________, 1952, On the diffraction of an acoustic pulse by a wedge. Proc. Roy. Soc. A, 212, 543-547.

MILNE, W.E., 1953, NUMERICAL SOLUTION OF DIFFERENTIAL EQUATIONS, John Wiley and Sons, N.Y.

MONTEATH, G., 1951, Application of the compensation theorem to certain radiation problems. I.E.E. Proc. pt IV, 98.

NOMURA, Y., 1951, On the diffraction of electric waves by a perfectly reflecting wedge. Sc. Rep. Res. Inst. Tohoku Univ. B 1-2, 1-23.

OBERHETTINGER, F., 1954, Diffraction of waves by a wedge. Communications on pure and applied mathematics, 7, 551-563.

RIKITAKE, T., 1951, Changes in earth currents and their relation to the electrical state of the earth's crust. Tokyo Univ. Earthquake Research Inst. Bull. 29, pt. 2, 27-275.

SCHELKUNOFF, S.A., 1943, ELECTROMAGNETIC WAVES. Van Nostrand Co., Inc., N.Y.

SCHLUMBERGER, M. et KUNETZ, G., 1948, Observations sur les variations rapides des courants telluriques. Dorel, Paris.

SENIOR, T.B.A., 1953, The diffraction of a dipole field by a perfectly conducting half plane. Quart. J. Mech & Appl. Math 6, 101.

_________, 1952, Diffraction by a semi-infinite metallic (imperfectly conducting) sheet. Proc. Roy. Soc. London, A, 213, 436.

SHAW, F.S., 1953, RELAXATION METHODS, Dover Publications, N.Y.

SIEGEL, K.M. and al., 1955, Electromagnetic and acoustical scattering from a semi-infinite cone. J. Appl. Phys. 26, 3,

SINCLAIR, R., 1948, Theory of models of electromagnetic systems. Proc. Inst. Radio Eng. 1364-70.

SOLLFREY, W., 1953, Diffraction of pulses by conducting wedges and cones. N.Y.U, Rep. EM-45, Math Res. Group.

SOMMERFELD, A., 1896, Math Annalen 47, 317-374 also in DIFFERENTIAL-GLEICHUNGEN DER PHYSIK chapter 20, Edited by Frank and Von Mises 1927, 1934.

SOUTHWELL, R., 1946, RELAXATION METHODS IN THEORETICAL PHYSICS. Oxford Univ. Press.

STAKGOLD, I., 1954, Boundary values problems for $\nabla^2 u + k^2 u = 0$ Stanford Univ., Appl. Math & Statisti. Lab., Tech. Rep. 17.

STEVENSON, A.F., 1953, Solution of electromagnetic scattering problems as power series in ratio dimension scatterer/wave length. J. Appl. Physics, Vol. 24, 9, 1135.

_________, 1953, Electromagnetic scattering by an ellipsoid in the third approximation. J. Appl. Physics, 24, 9, 1143.

_________, 1954, Note on the existence and determination of a vector potential. Quart. of Appl. Math. XII, 2, 194.

STRATTON, J., 1941, ELECTROMAGNETIC THEORY, McGraw Hill Bk. Co., N.Y.

TIKHONOV, A.N., 1950, Determination of electrical properties of deep strata of earth's crust. Akad. Nauk S.S.S.R. Doklady 73, 295.

_________ and LIPSKAYA, N.V., 1952, On the variations of the terrestrial electric field. Akad. Nauk S.S.S.R. Doklady, tom 87, 4, 547-550

TRANTER, C.J., 1954, Dual integral equations. Proc Intern. Math Congress, Amsterdam 386-387.

_________, 1954, A further note on dual integral equations and an application to the diffraction of electromagnetic waves. Quart. J. Mech. & Appl Math 7, 317-325.

TROITSKAYA, V.A., 1953, Short period disturbances of electromagnetic field of the earth. Akad. Nauk. S.S.S.R. Doklady, tom 91, 2 241-244.

TURLYGIN, S. Ya. and KARELINA, N.A., 1952, The influence of dry land and sea on the distribution of telluric currents over the surface of the earth. Akad. Nauk. S.S.S.R. Izv. Ser. Geofiz. 4, 55-75.

VESHEV, A.V., SEMINOV, A.S., and NOVOZHILOVA, M.F., 1952, A new kind of natural electric field in the ground. Akad. Nauk. S.S.S.R. Doklady, tom 87, 6 939-941.

VOZOFF, K., 1956, The quantitative interpretation of resistivity data. Ph.D. thesis, Dept. Geol. and Geoph., M.I.T.

BIOGRAPHY

The author, Antonio Saldanha de Sousa Neves, was born in Lisbon, Portugal, on the 29th of May 1930. His parents moved shortly afterwards to Lourenco Marques, Mozambique. There he went to grade and high school. In June 1949, he graduated from Liceu Nacional Salazar (formerly 5 de Outubro) and in September, 1949, he arrived in the United States, enrolling in the Chauncy Hall School of Boston. He entered as a freshman in M. I. T. in September, 1950, and graduated with a B. Sc. in Geophysics in September 1953. In the same year he started working towards a M. S. in Geology, but in September, 1954, changed its registration to that of a Ph. D. candidate in Geophysics.